The MRE11 Complex and EXO1 Collaborate to Support Mammalian Development and the Cellular Responses to DNA Damage

Katrin Rein

Tesi Doctoral UPF 2015

Director

Travis H. Stracker, PhD

Institute for Research in Biomedicine, Barcelona

Genomic Instability and Cancer Laboratory

Experimental and Life Science Department

Acknowledgements

First and foremost I want to say a huge THANK YOU to my supervisor Travis for giving me the opportunity to do a PhD, and for the continuous support and encouragement during all these years. Many thanks to every member of the lab, it has been really nice to work with all of you! I would also like to thank the entire Symington lab for making me feel so welcome, it was a great experience to work with you. Thank you also for the Helleday lab for teaching me the tricky and interesting fibre assay that provided many good results.

During all the Barcelona years I spent a great deal of time with Suvi, Michela, Natalia and Hanna. Thank you for everything – for being good friends and flatmates, for being always there and encouraging me with everything. Special thanks to Manuel for the great friendship and for all these conversations, you taught me so much! Thank you Egle for your eternal smile and positivity, and Gonzalo for all the advice and help!

Tänan ka Katrinit, minu parimat korterikaaslast, kogu koosveedetud aja eest Barcelonas, Tallinnas, Philadelphias ja New Yorgis. Erilised tänud Kätlinile, Nellele, Annikale, Allanile, Martinile ja Vallutile, te aitasite mind selle töö valmimisel palju. Suured tänud ka kõigile Nuhelejatele, ilma teieta oleks elu väga igav!

Kõige rohkem tänan ma oma peret ja muid loomi kogu toetuse ja mõistmise eest.

Abstract

The maintenance of genome stability is crucial for homeostasis, development and suppression of diverse pathologies that include developmental disorders, premature aging and cancer. The DNA damage response coordinates the appropriate cellular responses following the detection of lesions to prevent genomic instability. The MRE11 complex is a sensor of DNA double strand breaks and plays key roles in multiple aspects of the DNA damage signaling, including the initiation of DNA end resection that is critical for the accurate break repair and the replication fork maintenance. Many studies have implicated the exonuclease EXO1 in DNA resection and shown that the MRE11 complex functions upstream, but the exact influence of EXO1 on double strand break responses remain unclear. In this thesis we examine the genetic relationship between the MRE11 complex and EXO1 during mammalian development and the cellular responses to DNA damage. Our work shows that the deletion of *Exo1* in mice expressing a hypomorphic allele of *Nbs1*, a member of the MRE11 complex, leads to severe developmental defects, embryonic death and chromosomal instability. While EXO1 deficiency does not strongly affect DNA replication, DNA repair or checkpoint signaling in normal cells, our results reveal a crucial role for EXO1 in these functions when the MRE11 complex is compromised.

Resumen

El mantenimiento de la estabilidad del genoma es esencial para la homeostasis y para la supresión de diversas patologías que incluyen trastornos del desarrollo, el envejecimiento prematuro y el cáncer. La adecuada respuesta al daño del ADN coordina las funciones celulares originadas por la detección de lesiones, para prevenir la acumulación de inestabilidad en el genoma. El complejo MRE11 es un sensor de roturas en el ADN de doble cadena y juega un papel clave en múltiples aspectos de la señalización del daño en el ADN; incluido el inicio de la resección del ADN terminal, que es a su vez fundamental para la reparación precisa de escisiones y el mantenimiento de la horquilla de replicación. La función del complejo MRE11 precede a las funciones de la exonucleasa EXO1, la cual está implicada en la resección del ADN y en las respuestas a los daños del ADN. En esta tesis examinamos la relación genética entre el complejo MRE11 y la proteína EXO1 durante el desarrollo de células de mamífero y las respuestas celulares al daño en el ADN. Nuestro trabajo muestra que la eliminación del gen *Exo1* en ratones que expresan un alelo hipomórfico de *Nbs1*, un miembro del complejo MRE11, conduce a un defecto severo del desarrollo embrionario, la muerte del embrión y la inestabilidad cromosómica. Aún cuando la eliminación de EXO1 no afecta significativamente la replicación o reparación del ADN ni el control de la señalización, en conjunto, nuestros resultados revelan un papel crucial de EXO1 en estas funciones cuando el complejo MRE11 está comprometido.

Preface

Damage to the DNA is a threat to organismal survival and the faithful transmission of the genetic material to the offspring. Eukaryotic cells have evolved strategies to rapidly respond to these threats, collectively termed the DNA damage response. The DNA damage response is an evolutionally conserved signal transduction network that senses DNA lesions and coordinates the appropriate cellular responses to prevent the accumulation of genomic instability. Genomic instability can contribute to diverse pathologies including developmental disorders, premature aging, infertility and cancer. Knowledge of the DNA damage response is applied in cancer therapeutics where tumor cell lethality is achieved by creating cytotoxic levels of DNA damage in tumor cells using radiotherapy and chemotherapeutic drugs. Despite the fact that these therapies are also toxic to normal tissues, they are often efficacious, as cancer cells are more sensitive due to high rates of proliferation and the acquisition of frequent mutations in DNA repair genes. A detailed understanding of the cellular responses to DNA damage is therefore essential to understand the diverse pathological outcomes that result from genomic instability and to improve cancer therapies. Of the various types of DNA lesions, DNA double strand breaks are considered the most cytotoxic form of DNA damage but also one of the most dangerous as they can result in oncogenic chromosome translocations if not faithfully repaired. Double strand breaks are recognized by the conserved MRE11 complex (MRE11, RAD50 and NBS1), which coordinates multiple cell fate decisions and DNA repair. All MRE11 complex members are essential for mammalian viability, at the cell and organismal level, and available data suggests that this is due to the function of MRE11 complex in suppressing replication associated DNA damage. The MRE11 complex initiates DNA resection that is necessary for both signal transduction and accurate repair of DNA damage and restart of stalled replication forks. Additional players in resection, which include several important nucleases and helicases, have only recently been identified due to a high level of functional redundancy. Therefore it has been challenging to study the molecular mechanisms of resection and available results are largely based on genetic analyses and biochemistry performed in yeast. The exonuclease EXO1 has a role in resection and yeast studies showed that deficiency in any of the Mre11 complex members led

to strong synthetic interactions when combined with Exo1 deficiency, even though the MRE11 complex is proposed to act upstream of EXO1. Studies in mammalian cells have led to conflicting evidence regarding the role of EXO1 in resection and the response to DNA breaks and have not revealed the extent of dependency between EXO1 and MRE11 complex. In this work we have focused on addressing the genetic and functional relationship of these factors in mammalian development and the responses to DNA damage using mice with a hypomorphic allele of *Nbs1* and an *Exo1* loss of function allele. Our results reveal a strong genetic and functional relationship between EXO1 and the MRE11 complex and indicate that EXO1 may play a key role in suppressing various pathological outcomes resulting from compromised MRE11 complex function, suggesting that *EXO1* may be a phenotypic modifier of human diseases resulting from MRE11 complex mutations. Moreover, MRE11 complex members are frequently mutated in human cancers and our results identify EXO1 as a strong modulator of the cellular sensitivities to various chemotherapeutic agents in cells with mutant NBS1. Therefore, knowing the status of both the MRE11 complex and EXO1 may be important for selecting chemotherapeutic drugs and developing small molecule inhibitors to EXO1 could benefit the treatment of cancer patients carrying MRE11 complex mutations.

Abbreviations

4N DNA content	G2 or mitotic DNA content
4-OHT	4-hydroxytamoxifen
53BP1	p53-binding protein 1
6-4 PPs	6-4 pyrimidine-pyrimidone photoproducts
9-1-1 complex	RAD9, RAD1 and HUS1 complex
A (amino acid)	alanine
A (nucleotide base)	adenine
ADP	adenosine diphosphate
A-T	ataxia telangiectasia
ATLD	ataxia telangiectasia-like disorder
ATM	ataxia telangiectasia mutated
ATMIN	ATM-interacting protein
ATP	adenosine triphosphate
ATR	ATM and Rad3-related
ATRIP	ATR-interacting protein
BAC	bacterial artificial chromosome
BER	base excision repair
BLM	Bloom's syndrome gene/protein
bp	base pair
BRCA1	breast cancer 1, early onset
BRCA2	breast cancer 2, early onset
BRCT	BRCA1 C-terminal domain
BrdU	5-bromo-2-deoxyuridine
C (nucleotide base)	cytosine
Cdc1	cell division cycle 1 (*S.pombe*)
CDC25	cell division cycle 25

CDK	cyclin-dependent kinase
CFS	common fragile site
CHK1	checkpoint kinase 1
CHK2	checkpoint kinase 2
CldU	5-chloro-2′-deoxyuridine
CMV	cytomegalovirus
CNS	central nervous system
CO	crossover
CPD	cyclobutane pyrimidine dimers
CPT	camptothecin
CS	Cockayne syndrome
CSR	class switch recombination
C-terminal	carboxy-terminal
CtIP	C-terminal binding protein (CtBP) interacting protein
D (amino acid)	aspartic acid
DAPI	4',6-diamidino-2-phenylindole
DDR	DNA damage response
dHJ	double Holliday junction
DNA-PK	DNA-dependent protein kinase
DNA-PKcs	catalytic subunit of DNA-dependent protein kinase
dNTP	deoxyribonucleotide
DSB	double strand break
dsDNA	double stranded DNA
E	embryonic day
E (amino acid)	glutamic acid
E. coli	*Escherichia coli*
ER	estrogen receptor
EXO1	exonuclease 1

FA	Fanconi anemia
FANC	Fanconi anemia complementation group
FHA	forkhead-associated
FITC	fluorescein isothiocyanate
G (amino acid)	glycine
G (nucleotide base)	guanosine
G1	gap phase 1
G2	gap phase 2
GFP	green fluorescent protein
Gy	gray, unit of ionizing radiation dose
H3S10	histone 3 serine 10
HDR	homology-directed repair
HER2	human epidermal growth factor receptor 2
HNPCC	hereditary nonpolyposis colorectal cancer
HRP	horseradish peroxidase
HU	hydroxyurea
IdU	5-iodo-2'-deoxyuridine
IR	ionizing radiation
IRIF	ionizing radiation induced nuclear foci
K (amino acid)	lysine
kb	kilo base
LOH	loss of heterozygosity
LTR	long terminal repeat
M (amino acid)	methionine
MAP	mitogen-activated protein
MDC1	DNA damage checkpoint protein 1
MEF	mouse embryonic fibroblast
MK2	MAP kinase-activated protein kinase 2

MLH1	MutL homolog 1
MMC	mitomycin C
MMEJ	microhomology-mediated end joining
MMR	mismatch repair
MMS	methyl methanesulfonate
M-phase	mitosis
MRE11	meiotic recombination 11
mRNA	messenger RNA
MSH2	MutS homolog 2
mtDNA	mitochondrial DNA
NBS	Nijmegen breakage syndrome
NBS1	Nijmegen breakage syndrome 1
NBSLD	Nijmegen breakage syndrome-like disorder
NCO	noncrossover
NER	nucleotide excision repair
NHEJ	non-homologous end joining
N-terminal	amino-terminal
p26	26 kDa product
p38MAPK	p38 mitogen-activated protein kinase
p70	70 kDa product
PAR	poly (ADP-ribose)
PARP	poly (ADP-ribose) polymerase
PCNA	proliferating cell nuclear antigen
PCR	polymerase chain reaction
PI	propidium iodide
PIKK	phosphatidylinositol 3-kinase-like protein kinase
R (amino acid)	arginine
Rad3	*S.pombe* orthologue of mammalian ATR

Rad53	*S.cerevisiae* orthologue of mammalian CHK2
Rb	retinoblastoma gene
RMI1	RecQ mediated genome instability 1
ROS	reactive oxygen species
RPA	replication protein A
S (amino acid)	serine
S. cerevisiae	*Saccharomyces cerevisiae*
S. pombe	*Schizosaccharomyces pombe*
Sae2	*S.cerevisiae* orthologue of mammalian CtIP
SA-βgal	senescence-associated β galactosidase
Sgs1	*S.cerevisiae* orthologue of mammalian BLM
SHM	somatic hypermutation
shRNA	short hairpin RNA
siRNA	small interfering RNA
SKP2	S-phase kinase-associated protein 2
SMC1	structural maintenance of chromosomes 1
S-phase	DNA synthesis phase
SSA	single-strand annealing
SSB	single strand break
ssDNA	single stranded DNA
SV40	simian virus 40
T (nucleotide base)	thymine
TAP	tandem affinity purification
TOP1	topoisomerase 1
TOP2	topoisomerase 2
TOP3α	topoisomerase 3α
TOPBP1	topoisomerase-binding protein 1
UTR	untranslated region

UV	ultraviolet
V(D)J	variable, diversity and joining
WRN	Werner
XP	Xeroderma Pigmentosum
XPG	Xeroderma pigmentosum group G
XRCC1	X-ray repair cross complementing protein 1
XRCC4	X-ray repair cross complementing protein 4
Xrs2	*S.cerevisiae* orthologue of mammalian NBS1
YKu70	yeast Ku70
γ-H2AX	phosphorylated H2AX histone variant

Table of Contents

INTRODUCTION

1. Genome integrity and genomic instability

The maintenance of genome integrity is essential for organism survival

Genomic integrity must be maintained in order to ensure the correct transmission of genetic information to subsequent generations. This is a challenging task as the DNA is constantly exposed to environmental DNA damaging agents and endogenous processes that involve DNA breakage or mutagenesis. In order to protect the DNA, cells have developed mechanisms, collectively termed the DNA damage response (DDR). Following the detection of DNA lesions, the DDR signals their presence, mediates DNA repair, and coordinates programs to remove damaged cells, such as apoptosis or senescence. These responses are highly regulated, as unrepaired or incorrectly repaired DNA lesions can lead to mutations that can be pathogenic for the whole cell or organism (Jackson & Bartek 2009).

The role of DNA damage response in normal development

In addition to repairing genotoxic DNA lesions, the DDR is also required for multiple biological processes during development and homeostasis. The DDR is essential for programmed genome alterations in developing B and T lymphocytes to generate immunoglobulin and T-cell receptor diversity. Different antigen receptors on B and T lymphocytes are generated by assembling variable, diversity and joining gene segments, termed V(D)J recombination. B cells undergo further genetic alterations to enhance their specificity, termed somatic hypermutation (SHM) and class switch recombination (CSR) (Dudley et al. 2005). In addition to immune system development, the DDR has an important role in creating genetic diversity via sexual reproduction during sister chromatid exchange in meiosis (Richardson et al. 2004). DDR components also function at telomeres in order to maintain telomere homeostasis and prevent premature aging or chromosomal instability (Verdun & Karlseder 2007).

Consequences of genomic instability

Mutations in some genes that encode DDR proteins result in the accumulation of DNA lesions that can eventually lead to genomic instability, a state defined as a reduction in the fidelity in transmitting genetic information from parental cells to daughter cells (Stracker et al. 2004). Genomic instability is a prominent hallmark of cancer cells (Hanahan & Weinberg 2011) and many DDR gene mutations that lead to hereditary cancer predisposition have been characterized. A defective DDR and genomic instability also characterize a variety of rare genomic instability syndromes that lead to severe pathologies including predisposition to cancer, infertility, progeria, immunodeficiency and neurodevelopmental abnormalities (Taylor, 2001).

Ataxia Telangiectasia and related disorders

Ataxia telangiectasia (A-T), first described in the 1920s, results from mutations in the A-T mutated (ATM) protein kinase, one of the main controllers of DNA damage induced signal transduction that will be discussed in more detail later. A-T is a multisystem disorder, characterized by progressive neurodegeneration, immunodeficiency and extreme sensitivity to ionizing radiation and cancer, especially lymphomas (McKinnon 2004). Mutations in another central controller of the DDR, the ATM and Rad3-related (ATR) kinase, results in Seckel syndrome, characterized by growth retardation, microcephaly and mental retardation (O'Driscoll et al. 2003). In addition to ATR, other defective genes have been identified that result in Seckel syndrome, such as C-terminal binding protein-interacting protein (CtIP), whose mutations cause impaired ATR activation (Qvist et al. 2011).

ATM associates with the MRE11 complex, which is composed of meiotic recombination 11 (MRE11), Nijmegen breakage syndrome 1 (NBS1) and RAD50, mutated in A-T-like disorder (ATLD), Nijmegen breakage syndrome (NBS) and NBS-like disorder (NBSLD), respectively. Patients with ATLD exhibit chromosomal instability, ionizing radiation sensitivity, and cerebellar degeneration, but they are not immunodeficient and only two cases have been

reported with cancer (Uchisaka et al. 2009; Taylor et al. 2004). NBS patients are immunodeficient, exhibit increased cancer incidence and mental retardation, but unlike A-T, do not exhibit ataxia. However, these patients present with microcephaly and mental retardation (van der Burgt et al. 1996), symptoms also reported with the few NBSLD patients that have been identified (Waltes et al. 2009).

Syndromes associated with RecQ DNA helicases

The human RecQ helicase family, often referred to as guardians of the genome, is involved in DNA recombination and repair. Three out of five members are tumor suppressor genes and mutated in genomic instability syndromes, all of which present with predisposition to cancers and premature aging. These are *BLM*, *WRN*, and *RECQ4*, the genes mutated in Bloom's syndrome, Werner's syndrome, and Rothmund-Thompson syndrome, respectively (Mohaghegh & Hickson 2002). Despite the similarity in disease presentation, these molecules play distinct roles in DNA replication and genome maintenance. WRN and BLM are both DNA-structure specific helicases that are able to unwind different DNA structures, such as DNA duplexes containing internal single stranded DNA (ssDNA), 4-way Holliday junction structures and G-quadruplex structures that can form at guanine-rich sequences and triple helix DNA. WRN is unique among the RecQ helicases as it also possesses 3'-5' exonuclease activity (Shen et al. 1998; Kamath-Loeb et al. 1998). Deficiencies in BLM or WRN result in a specific attenuation of p53-mediated apoptosis following DNA damage (Wang et al. 2001; Spillare et al. 1999). Several studies have shown that in addition, BLM promotes DNA double strand break (DSB) repair and affects DNA repair pathway choice (Gravel et al. 2008; Grabarz et al. 2013; Nimonkar et al. 2011), which will be described in more detail in this chapter. RECQ4, on the other hand, binds to replication origins and has a role in DNA replication initiation and replication fork progression (Thangavel et al. 2010).

Fanconi anemia

Fanconi anemia (FA) is characterized by congenital abnormalities, bone marrow failure, infertility and increased cancer susceptibility. Currently, sixteen Fanconi anemia complementation group (FANC) genes are associated with patient mutations (*FANCA-FANCQ*), all of them collaborating in the repair of DNA crosslinks (Walden & Deans 2014). The FA DNA repair pathway has been implicated in genome protection during development from the damage caused by endogenous aldehydes, which are byproducts of many metabolic pathways. Therefore, the bone marrow failure in FA is proposed to be driven by aldehyde-mediated genotoxicity in hematopoietic stem cells (Garaycoechea et al. 2012; Oberbeck et al. 2014).

Disorders of nucleotide excision repair

Nucleotide excision repair (NER), described in more detail later, is the main pathway responsible for repairing the damage resulting from exposure to ultraviolet (UV) light. Mutations in this pathway are responsible for multiple genetic disorders, such as Xeroderma Pigmentosum (XP) and Cockayne syndrome (CS). The main clinical symptoms of XP patients are photosensitivity and predisposition to skin cancer. CS, on the other hand, is mainly characterized by neurological and developmental phenotypes as well as premature aging (Cleaver et al. 2009). NER factors are also implicated in biological processes that are not directly associated with DDR, including mitochondrial function and redox homeostasis. Oxidative and energy metabolism are proposed to be the causative factors in the clinical heterogeneity of NER disease (Hosseini et al. 2014).

Cancer

As mentioned above, one of the most prominent hallmarks of many cancers is genomic instability. In hereditary cancers, mutations in several DDR genes have been shown to drive genomic instability and cancer formation. The most well-known examples include breast cancer susceptibility genes BRCA1 and BRCA2 or mutations in DNA mismatch repair (MMR) genes that cause hereditary

nonpolyposis colorectal cancer (HNPCC, also known as Lynch syndrome). In sporadic cancers it is not clear if defective DDR is the cause or the consequence of the cancer progression. It has been proposed that the order of the events could start from deregulation of growth-regulating genes. This can lead to chronic DNA replication stress and damage, which can selectively pressure the inactivation of tumor suppressor genes, thereby allowing cells with damaged DNA to escape from the cell death, resulting in genomic instability and cancer progression (Negrini et al. 2010). Cancer treatment also includes employing DDR to induce DNA damage in cancer cells, which will be discussed in detail later in this chapter.

Understanding the DNA damage response is necessary for many aspects of human health

In summary, DDR is an essential signaling pathway in response to DNA lesions to prevent genomic instability and for the normal development of organism. Knowledge of DDR is important to understand numerous human diseases and conditions, including cancer and aging (Figure 1). New insights of DDR are therefore essential for disease prevention, detection and management.

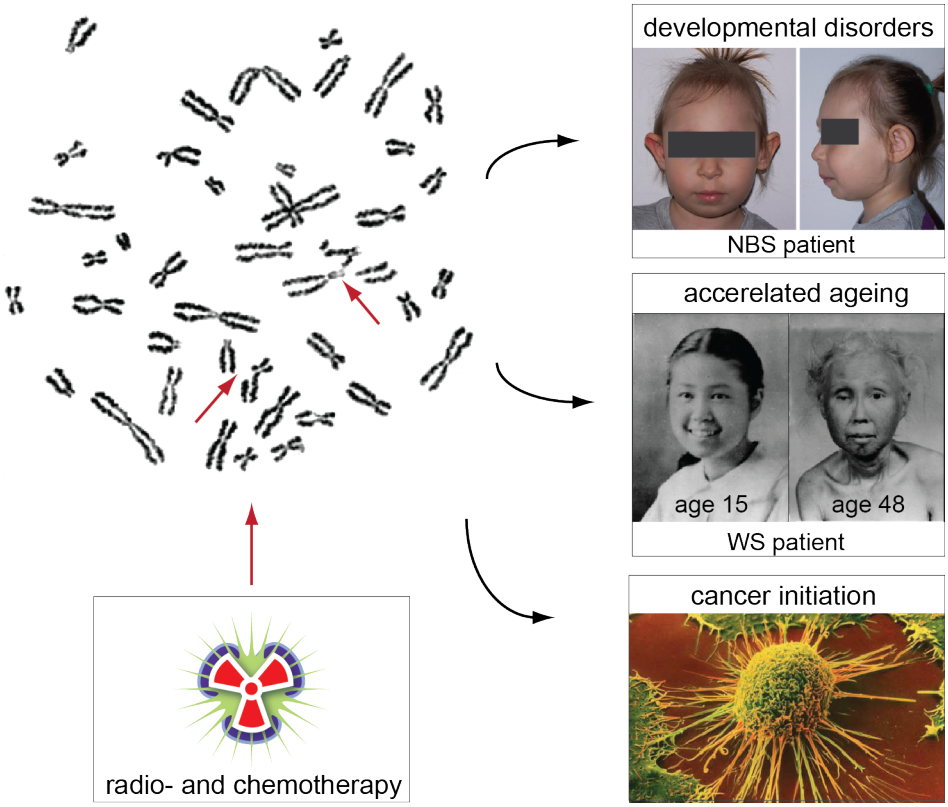

Figure 1. Understanding the DDR is applicable to various human pathologies. A defective DDR can lead to different genomic instability syndromes and cancer. Cancer treatment is also largely based on knowledge about the DDR.

2. The DNA damage response

DNA damaging agents, either endogenous or exogenous, can induce various DNA lesions; therefore multiple and distinct pathways have evolved to repair them. Despite responding to distinct lesions and using diverse repair pathways, responses are generally coordinated by a similar framework (Figure 2). The DDR, initiated upon recognition of a DNA lesion, amplifies the damage signal through rapid signal transduction and coordinates the recruitment of various mediators and effectors through a broad spectrum of posttranslational modifications. The DDR activates cell cycle checkpoints, resulting in arrested or slower cell-cycle progression, ensuring that DNA is repaired before cell division continues. If the damage cannot be repaired or occurs in particular cell types, DDR signaling induces cell death by apoptosis or permanent growth arrest through senescence. Collectively, this prevents unrepaired or incorrectly repaired lesions that can lead to mutations from resulting in diseases, that include cancer and aging (Ciccia & Elledge 2010; Jackson & Bartek 2009).

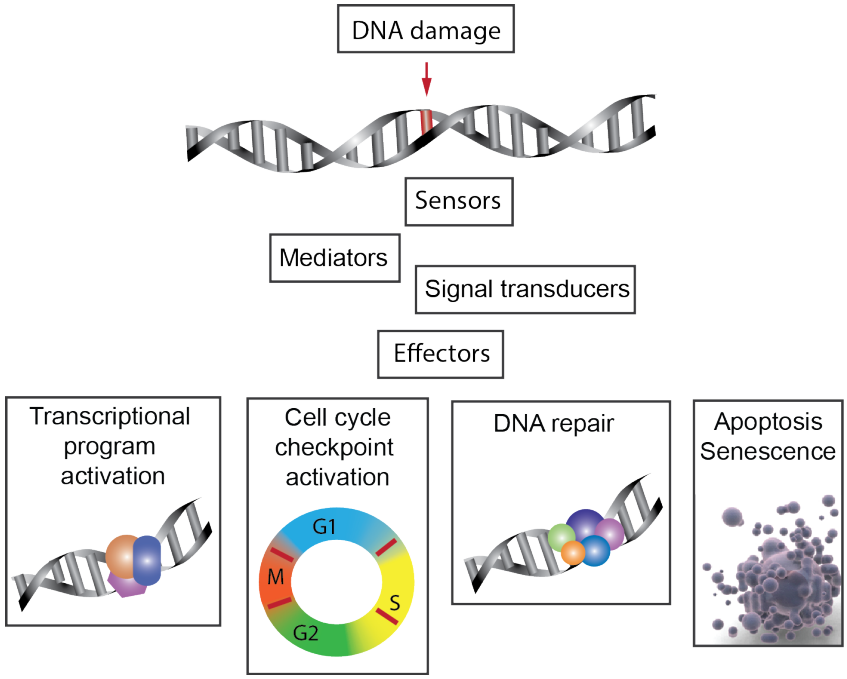

Figure 2. Overview of DNA damage response. The DDR coordinates the consequences of the damage by altering DNA metabolism, inducing cell-cycle arrest, organizing the repair and triggering cell death if necessary. A correct response to DNA damage is essential for preventing the accumulation of mutations that can lead to disease.

Endogenous DNA damage

It is estimated that in humans approximately 10^7 cells divide every second and that a third of them experience some form of endogenous damage (Marnett & Plastaras 2001). Natural DNA decay can lead to the loss of up to 10,000 bases per day by nonenzymatic hydrolytic cleavage of glycosyl bonds. During replication, spontaneous DNA mismatches can happen due to misincorporated deoxyribonucleotides (dNTPs). Topoisomerase 1 and 2 (TOP1 and TOP2, respectively) are enzymes that regulate DNA supercoiling by making cuts on DNA helix to relax and extend the coil. TOP1 binds to DNA and induces a single-stranded break to allow one strand rotation (Hsiang et al. 1989), and TOP2 induces a double strand break (Berger & Wang 1996). Therefore, abortive TOP1 or TOP2 activities result in DNA structural alterations or strand breaks (Ciccia & Elledge 2010). DNA is also constantly susceptible to damage caused by various reactive metabolites and coenzymes. Hydrolytic cytosine deamination, for example, causes interconversion between DNA bases. Non-enzymatic methylation by s-adenosylmethionine, which is a reactive methyl donor that is present in most cellular transmethylation reactions, modifies DNA bases. Moreover, DNA is vulnerable to various types of oxidative damage created by reactive oxygen species (ROS). These chemicals can lead to DNA replication fork stalling or collapse, which poses a serious threat to genome stability if not dealt with properly (Lindahl & Barnes 2000; Jackson & Bartek 2009).

Exogenous DNA damage

Environmental DNA damage is produced by numerous physical of chemical sources. The most prevalent physical genotoxic agents are UV light, which induces cyclobutane pyrimidine dimers (CPDs) and 6-4 pyrimidine-pyrimidone photoproducts (6-4 PPs), and ionizing radiation (IR) that originate from cosmic radiation, medical X-rays or radiotherapy, which generates oxidative damage and DNA single strand breaks (SSBs) and DSBs. Chemical DNA damaging agents are used in cancer chemotherapy, targeting the DNA of rapidly dividing

tumor cells. Alkylating agents, such as methyl methanesulfonate (MMS) add alkyl groups to DNA bases. Covalent links between DNA bases are induced by crosslinking agents, such as mitomycin C (MMC) and cisplatin. TOP1 and TOP2 inhibitors, such as camptothecin (CPT) and etoposide lead to abnormal DNA structures and breaks. Besides cancer therapy, many chemical DNA damaging agents can be found in cigarettes, causing adducts and oxidative damage in lungs and other tissues (Ciccia & Elledge 2010). Particulate air pollution and toxic industrial compounds can also induce DNA damage, many documented instances exist in which chemical exposure has caused cancers in humans (Robinson 2002).

Signaling of DNA breaks

Signaling cascade that follows the DNA damage requires the actions of various proteins, whose functions can be categorized as DNA damage sensors, transducers, mediators, and effectors. Sensor proteins directly recognize specific types of DNA lesions and activate a coordinated recruitment of factors to the damage site. In many cases, the recruitment to damage is dependent on various posttranslational modifications which are recognized by specific protein domains (Harper & Elledge 2007). Different types of DNA damage require different sensor proteins and these will be discussed in more detail later.

The main DDR transducers belong to the phosphatidylinositol 3-kinase-like protein kinase (PIKKs) family. These are the ATM, ATR, and DNA-dependent protein kinase (DNA-PK) (Ciccia & Elledge 2010). ATM and DNA-PK are mainly activated by DNA DSBs (Harper & Elledge 2007), while ATR and its partner, ATR-interacting protein (ATRIP), recognizes ssDNA that is coated by replication protein A (RPA), a structure generated by many different types of DNA damage and during replication stress (Cimprich & Cortez 2008). PIKKs phosphorylate the histone variant H2AX in megabase chromatin domains surrounding DSBs, leading to large regions of phosphorylated H2AX (known as γ-H2AX). These regions are thought to provide a platform for the recruitment of additional DDR factors and promote the proximity of DNA ends. In addition, they lead to the

generation of foci visible by fluorescent microscopy, termed IR-induced nuclear foci (IRIF) that have become an important diagnostic tool for measuring DNA damage and repair (Stucki & Jackson 2006; Chapman et al. 2012).

In addition to the PIKKs, many members of the poly (adenosine diphosphate(ADP)-ribose) polymerase (PARP) family are crucial for signal transduction. From the 17-member poly ADP ribose polymerase (PARP) superfamily, PARP1, PARP2 and PARP3 have been implicated in the DDR. They are activated by DNA strand interruptions and catalyze the addition of poly (ADP-ribose) (PAR) chains. Massive synthesis of PAR occurs very quickly after DNA damage and acts to amplify the signal and recruit additional DDR factors, and facilitate chromatin remodeling in response to DNA damage (Schreiber et al. 2006; Li & Yu 2014).

Mediator proteins act to fine-tune the damage signal. Many of them contain phospho-peptide recognition domains including forkhead-associated (FHA) domains and BRCA1 C-terminal domain (BRCT). One of them is the DNA damage checkpoint protein 1 (MDC1), which interacts with γ-H2AX, and this interaction is believed to be the first step for the damaged site of DNA to be prepared for repair (Falck et al. 2005). Other mediators include p53-binding protein 1 (53BP1), BRCA1 and topoisomerase-binding protein 1 (TOPBP1), which help the transducers to activate various effectors, including the cell cycle checkpoint kinases 1 and 2 (CHK1 and CHK2, respectively) which arrest cell cycle progression in response to damage (Polo & Jackson 2011).

Cell cycle and DNA damage-induced cell cycle checkpoints

Cell cycle

The stages of the cell cycle are G1 (stands for gap1), S (DNA synthesis), G2 (gap2) and M (mitosis). In G1 phase, the cell grows and prepares for DNA synthesis, during which the DNA replication occurs until all the chromosomes have been replicated. In G2 phase, cell continues to grow and gets ready for the mitotic division. In M phase, the cell divides, separating the replicated chromosomes into two daughter cells (Cooper & Hausman 2007). Cyclin-

dependent kinases (CDKs) function as central regulators of the cell cycle. CDKs are a family of serine/threonine kinases that form catalytically active complexes with cyclins. Cyclin E/CDK2 complex is required for the G1 to S phase transition, cyclin A/CDK1 for DNA replication, and cyclin B/CDK1 for the G2 to M transition and for initiation of mitosis. Cell division cycle 25 (CDC25) phosphatases act as activators of CDK complexes (Mailand et al. 2000; Liu & Kipreos 2000).

Cell cycle checkpoints

Term “cell-cycle checkpoint” refers to mechanisms by which the cell stops the progression through the cell cycle until the earlier process, such as DNA replication, is complete (Hartwell & Weinert 1989). To correctly repair the DNA damage and prevent additional chromosomal instability, it is essential that the cell cycle slows down or arrests until the damage is repaired. Initiation of ATM and ATR activities are one of the first steps in the activation of signal transduction that inhibits cell-cycle progression after DNA damage by targeting checkpoint mediators and the checkpoint kinases CHK1 and CHK2. These kinases reduce CDK activity, which slows down or stops cell cycle progression at the G1-S or intra-S checkpoints, both of which prevent inappropriate DNA replication, or G2-M checkpoint, which prevents cells with, damaged DNA from entering mitosis (Figure 3). The G2-M checkpoint is especially important for tumor suppression, as mutations in this pathway allow cells with damaged DNA to divide and thus amplify chromosomal aberrations (Kastan & Bartek 2004).

The G1-S checkpoint can be induced by the activation of p53 that is a target of both the ATM/ATR and CHK1/CHK2 kinases. Following DSBs, the phosphorylation of p53 by both ATM and CHK2 on different sites is important for its stabilization and activity (Canman et al. 1998; Takai et al. 2002). A key transcriptional target of p53 is the CDK inhibitor p21, which inhibits cyclin E/CDK2 complex activity, leading to G1 arrest. CHK1 and CHK2 can both target CDC25A, leading to its proteosomal degradation and inhibition of cyclin E (or cyclin A)/CDK2 complexes. This is implemented rapidly and delays the G1-S

transition only for few hours, while the p53-mediated mechanism prolongs G1 arrest (Kastan & Bartek 2004).

The intra-S phase checkpoint causes the inhibition of actively firing DNA replication origins and protects the integrity of stalled replication forks. It operates via two, at least partially independent, mechanisms (Falck et al. 2002). In response to IR, ATM is phosphorylating CHK2, which induces CDC25A degradation that ultimately leads to the inhibition of the cyclin E/CDK2 complex. In parallel, ATM initiates the second pathway through MRE11 complex, which phosphorylates structural maintenance of chromosomes 1 (SMC1) protein, resulting in silencing the replication origins in damaged region (Bartek et al. 2004).

The G2-M checkpoint prevents cells from initiating mitosis when they experience DNA damage during G2 or when they have some unrepaired damage from previous cell cycle phases. The target of this checkpoint is the cyclin B/CDK1 complex, whose activation is inhibited by ATM/ATR, CHK1/CHK2 or WEE1 kinase through the inhibition of the CDC25 phosphatases (Donzelli & Draetta 2003; Mir et al. 2010). Two biologically distinct G2-M checkpoints have been identified (Xu et al. 2002). The first one occurs rapidly and applies mostly on the cells that were in G2 phase during the damage. In contrast, several hours after the damage cells start to accumulate in G2-M phase which represents the population that that had been in earlier cell cycle phases during the damage and is p53 dependent. P53-deficient tumor cells depend on p38 mitogen-activated protein kinase (p38MAPK) – MAPK-activated protein kinase 2 (MK2) pathway to induce G2-M checkpoint (Reinhardt et al. 2007).

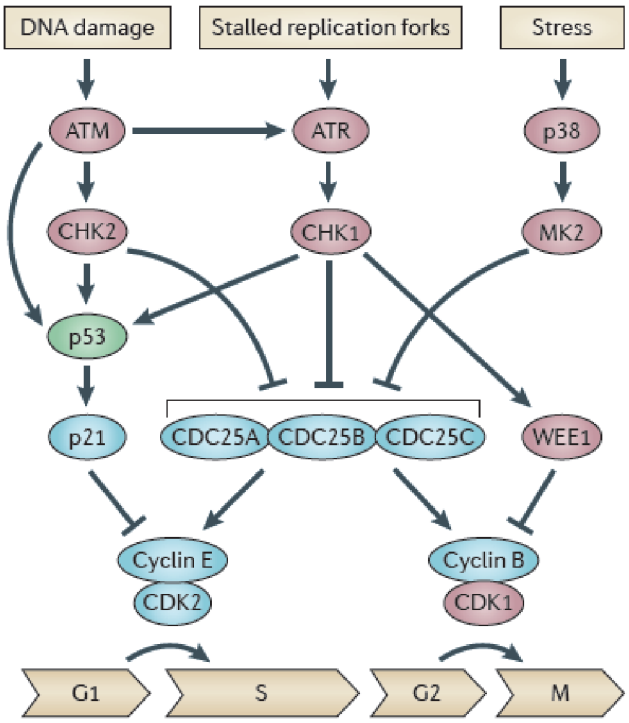

Figure 3. DNA damage-induced cell cycle checkpoints. ATM, CHK1 and CHK2 can all activate p53, resulting in G1-S checkpoint arrest. CHK1 is phosphorylated by ATR in response to replication stress or DNA damage. CHK1 and CHK2 both can arrest the cell cycle in intra-S or G2-M phases by inhibiting CDC25 phosphatases. Alternatively, CHK1 can activate WEE1 to induce G2-M checkpoint. P53 deficient tumor cells have been shown to rely on p38-MK2 mediated pathway for G2-M checkpoint induction. Figure from (Bouwman & Jonkers 2012).

DNA repair pathways

Nucleotide excision repair

NER pathway has the ability to eliminate a wide array of different helix-distorting lesions. These include the major lesions induced by UV radiation (CPDs and 6-4 PPs), different types of chemical adducts, intra- and interstrand crosslinks, caused by drugs such as cisplatin, and ROS-generated cyclopurines. NER operates via two sub-pathways that differ by the recognition of the lesion: global-genome NER, where the entire genome is monitored for helix distortions, and transcription-coupled NER, that targets only lesions that are blocking replication. After recognition of the damage, the lesion is removed by dual excision on both sides by structure-specific endonucleases, leaving a ssDNA

gap of 22-30 nucleotides that is then filled and ligated by DNA polymerase and DNA ligase activities (Marteijn et al. 2014).

Base excision repair

DNA bases are susceptible to oxidation mediated by ROS with 8-oxoguanine being the most common product of oxidative damage to DNA. Failure to remove 8-oxoguanine before replication results in G to T mutations, making it a highly mutagenic DNA lesion. This type of damage is repaired by the base excision repair (BER). The ROS-induced lesions are specifically recognized by variety of DNA glycosylase enzymes that catalyze the base removal, after which the undamaged nucleotide is reinstalled to complete the repair (David et al. 2007). Notably, BER is one of the few repair pathways that has been shown to clearly operate in the mitochondria, where the mitochondrial DNA is subjected to high levels of ROS damage.

Mismatch repair

Many cancers exhibit microsatellite instability. Microsatellites are repeated A or CA nucleotide sequence motifs which are sometimes re-annealed incorrectly during DNA synthesis. This results in heteroduplex DNA molecules known as insertion-deletion loops. These are monitored by MMR system along with base-base mismatches that have escaped DNA polymerase proofreading function. A dysfunctional MMR system results in a mutator phenotype, which can contribute to the development of many different cancers. MMR proteins are mutated in HNPCC, a condition that has high risk of colon cancer, as well as other cancer types. Several human MMR proteins have been identified based on their homology to the *Escherichia coli* (*E. coli*) MMR proteins MutS and MutL. These are adenosine triphosphate (ATP)ases that form complexes and travel along DNA, recognizing and binding to mismatches. These complexes interact with proliferating cell nuclear antigen (PCNA) that helps to load exonuclease 1 (EXO1). Along with other nucleases, EXO1 makes nicks in DNA and resects to create a single stranded gap which will be filled by DNA polymerases and then ligated (Jiricny 2006; Bak et al. 2014).

Single strand break repair

Single strand DNA breaks are normal intermediates of BER and arise in case of abortive TOP1 activity or after IR treatment. Unrepaired SSBs can cause replication blockage or replication fork collapse during S phase, possibly leading to DSB formation. PARP1 detects SSBs, rapidly binds them and promotes their repair by remodeling the chromatin surrounding the break and recruiting factors, such as X-ray repair cross complementing protein 1 (XRCC1) that serves as scaffolding protein for other repair factors (Brem & Hall 2005; K W Caldecott 2014). Most SSB ends need to be processed by various XRCC1-interacting proteins to restore the damaged 3'- terminus. This is followed by gap filling by DNA polymerases, which is also stimulated by XRCC1 and PARP1. The final step of SSB repair is DNA ligation (Keith W Caldecott 2014).

Double strand break repair pathways

DSBs form when both DNA duplex strands are broken. They are considered extremely toxic and can cause genome rearrangements that lead to cancer development. Defective DSB repair is also associated with various hereditary disorders characterized by severe pathologies that are described earlier in this chapter. The major exogenous agents that cause DSBs are IR and chemotherapeutic drugs such as topoisomerase inhibitors. In addition, DSBs arise from endogenous sources such as DNA replication and programmed recombination events, such as lymphocyte development (V(D)J recombination and CSR) and meiosis (Stracker & Petrini 2011).

There are two major pathways that repair DSBs: non-homologous end joining (NHEJ) and homology-directed repair (HDR). NHEJ is active throughout the cell cycle and religates the broken DNA ends, sometimes in an error-prone manner. In contrast, HDR, which uses an undamaged homologous sequence, normally from the sister chromatid, as a template, is considered highly accurate (Chapman et al. 2012; Stracker & Petrini 2011). NHEJ can accurately repair "clean" DSB ends, where no nucleotides are damaged or missing. However, it is also capable of joining ends that are processed by enzymes to generate ligateable ends and are therefore missing nucleotides. It can also join ends from

two non-homologous chromosomes, causing chromosomal translocations. DSB pathway choice is therefore critical to maintain genomic stability and is strictly controlled during cell cycle. One major impact of the choice of repair pathways is whether the DSB ends will undergo resection that is 5'-3' nucleolytic degradation to create 3′-ssDNA overhangs. ssDNA is essential for HDR and the presence of this structure has been shown to strongly inhibit NHEJ (Symington & Gautier 2011; Chapman et al. 2012; Daley & Sung 2014). While standard HDR uses ssDNA for strand invasion and template repair, ssDNA is also the basis for alternative DSB repair pathways such as microhomology-mediated end joining (MMEJ) and single-strand annealing (SSA) (McVey & Lee 2008) (Figure 4). MMEJ uses short (1-25 nt) microhomologies to initiate the end joining process. MMEJ always results in deletions and is associated with chromosome translocations that contribute to the development of certain forms of cancer, mainly leukemias and lymphomas (Simsek & Jasin 2010; Wang et al. 2009). SSA, like MMEJ also results in genomic deletions by annealing long (over 30 nt) homologous sequences. Those alternative pathways are therefore highly mutagenic solutions that are likely used when other repair pathways fail (Dueva & Iliakis 2013; McVey & Lee 2008).

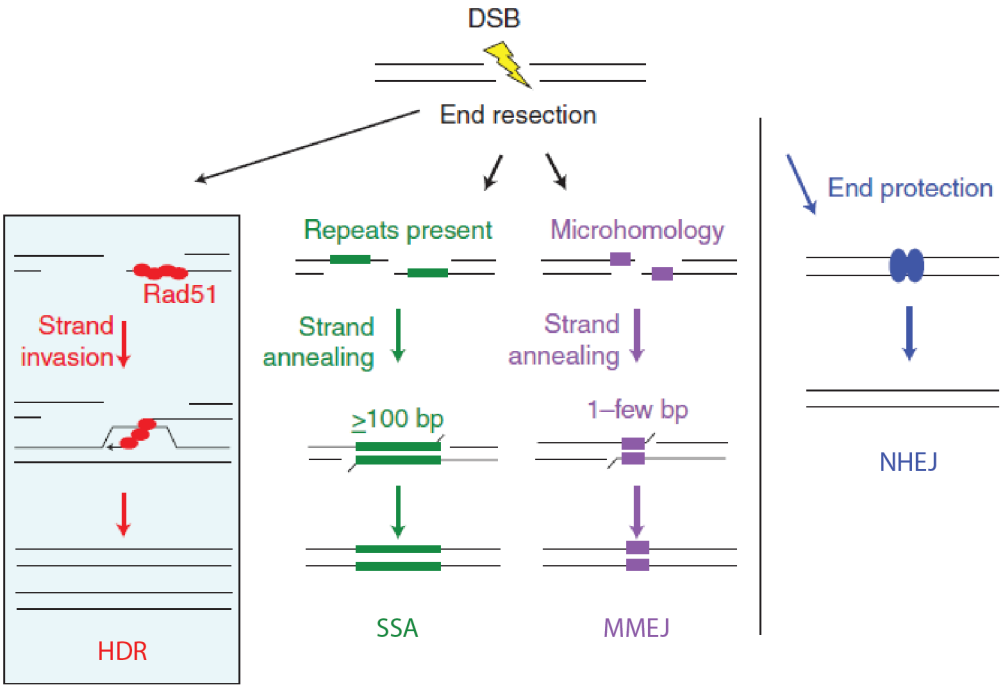

Figure 4. DSB repair pathways. An important determinant of repair pathway choice is DNA end resection, which is essential for HDR but inhibits NHEJ where DNA ends are protected from the resection machinery. A defining step in HDR is the strand invasion by RAD51. DNA end resection also provides an intermediate for alternative, error prone pathways such as SSA and MMEJ, which that generally occur when NHEJ core factors are absent. Adapted from (Jasin & Rothstein 2013).

DNA end resection is normally restricted to S and G2 phases when a sister chromatid is present. Many enzymes that regulate resection are therefore under the control of CDK activity that is normally low in G1 and higher in S and G2 (Chapman et al. 2012). Important regulators of break resection during the cell cycle are 53BP1 and BRCA1. 53BP1 rapidly accumulates on the chromatin near DSB, which is mediated by ATM-dependent phosphorylation of γ-H2AX (Lukas et al. 2011). 53BP1 promotes NHEJ by protecting DSB ends from resection in G1 phase. BRCA1 has been suggested to promote the removal of 53BP1 from DSBs in S-phase, thereby favoring resection. That explains the chromosomal rearrangements in cells lacking BRCA1, where resection in S-phase in impaired, leading to unfavorable NHEJ events (Bunting et al. 2010).

Homology-directed repair

HDR is defined by invasion of ssDNA into homologous duplex, creating a strand invasion intermediate that can be resolved in different ways, ultimately leading to a noncrossover (NCOs) or crossover (COs) products (Jasin & Rothstein 2013). In addition to DSB repair in mitotic cells HDR is essential in meiotic recombination, a developmentally programmed breakage where chromosomes pair with their homologous partners and exchange DNA. Meiotic DSBs are catalyzed by SPO11 enzyme that induces DSBs. HDR machinery is resolving them, providing physical connection between chromosome homologs and promotes their pairing (Kauppi et al. 2013). HDR is initiated by MRE11 complex that recognizes DSBs and promotes the activation of ATM, which governs cell-cycle checkpoint induction and mediates DNA repair. DNA end resection to create ssDNA overhangs is initiated by the MRE11 complex in cooperation with CtIP. Further resection is carried out by the EXO1 5'-3' exonuclease and the DNA2 helicase/nuclease in cooperation with the BLM helicase, creating longer ssDNA tracts (Mimitou & Symington 2008). These are bound by RPA, and this RPA bound ssDNA structure activates ATR via ATRIP, which further promotes CHK1 activation and the checkpoint responses. RPA is replaced by RAD51 recombinase, forming nucleoprotein filaments with DNA and with the help of BRCA2 mediates the invasion of the undamaged template (San Filippo et al. 2008; Moynahan et al. 2001). The formed strand invasion intermediate has many possible fates, resulting in NCO or CO. In meiotic cells, at least one DSB per chromosome pair must be resolved as a CO to ensure proper segregation of homologous chromosomes (Jasin & Rothstein 2013). In mitotic cells, CO can lead to loss of heterozygousity of the segment of chromosome distal to CO, which is a mechanism for initiation of some tumor types (Moynahan & Jasin 2010). Synthesis-dependent strand annealing (Figure 5A) is a primary pathway in mitotic cells that allows the repair without the exchange of adjacent sequences. In this case, the newly synthesized DNA strand dissociates from the template to anneal with its complement on the other side of the double-strand break. A key pathway of mitotic cells involves capture of the other DNA end to form double Holliday junction (dHJ), which are resolved either by combined

activities of MMR components together with EXO1, forming a CO (Figure 5B) or topoisomerase activity of the complex consisting of BLM, topoisomerase 3α (TOP3α) and RecQ mediated genome instability 1 (RMI1) to form a NCO (Figure 5C) (Wu & Hickson 2003; Zakharyevich et al. 2012). Resolution of intermediates that escape the BLM complex result from the action of different resolvases, such as MUS81 endonuclease (Figure 5D) (Ho et al. 2010).

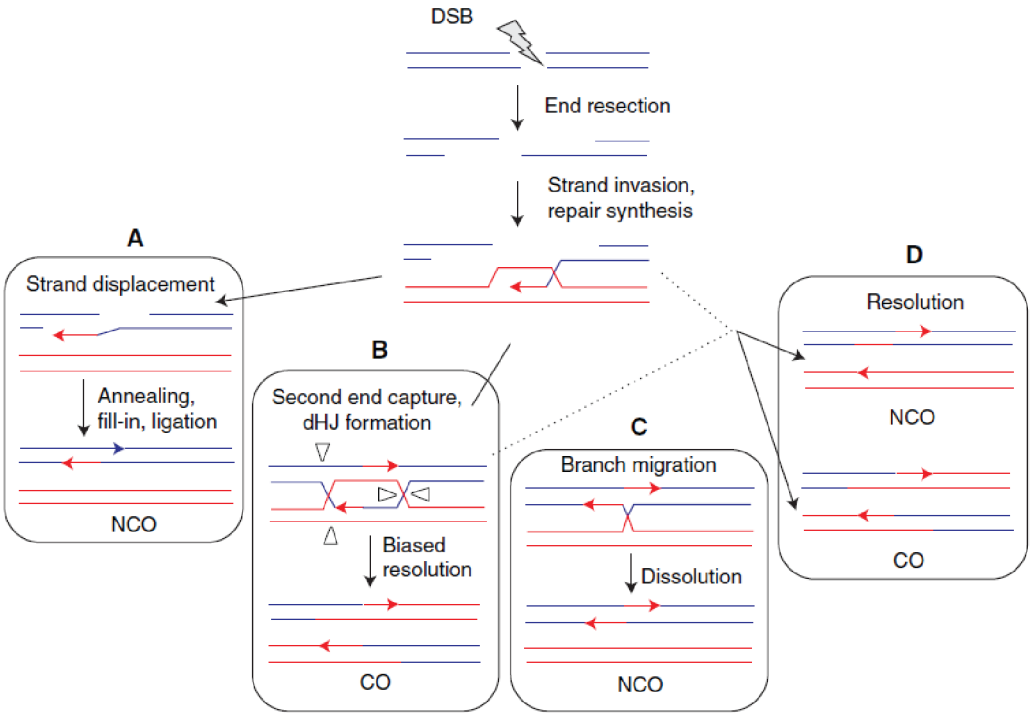

Figure 5. Different resolution pathways of resected DSB by HDR. (A) Synthesis-dependent strand annealing involves displacement of the newly synthesized strand and the complementary ends can anneal. (B) dHJs are formed when the second DNA end is captured. In meiotic cells, dHJ resolution is biased to form COs. (C) dHJs can be also dissolved without crossover by BLM/TOP3a/RMI1 complex. (D) Different resolvases, such as MUS81, can also resolve the dHJs. Figure from (Jasin & Rothstein 2013).

Non-homologous end joining

NHEJ it is essential for DSB repair in G1 and plays a major role in V(D)J recombination and CSR associated chromosome translocations (Chaudhuri et al. 2007). Therefore, the absence of any of the core NHEJ components leads to severe combined immunodeficiency (De Villartay 2009). NHEJ (Figure 6) is started by the binding of ends by the conserved Ku heterodimer, consisting of Ku70 and Ku80. Ku70/80 localizes to DSB ends and loads and activates the

catalytic subunit of DNA-PK (DNA-PKcs). DNA-PKcs has weak kinase activity that is enhanced in the presence of double stranded DNA (dsDNA) ends and Ku. The DNA-PKcs–Ku–DNA complex is referred to as DNA-PK (Gottlieb & Jackson 1993; Mahaney et al. 2009). Autophosphorylation of DNA-PKcs is required for its release from DSBs, which provides access to the end-modifying nuclease ARTEMIS that removes non-ligateable groups and other lesions from DNA ends (Merkle et al. 2002). End processing potentially results in loss of nucleotides, making NHEJ an error-prone process. Depending on the break, different processing enzymes may be required to process the DNA ends. Once the DNA ends have been processed the ligation is carried out by DNA ligase IV, which exists in complex with X-ray repair cross complementing protein 4 (XRCC4), which acts as a scaffolding protein, facilitating the recruitment of other NHEJ proteins to the break (Critchlow et al. 1997; Li et al. 1995).

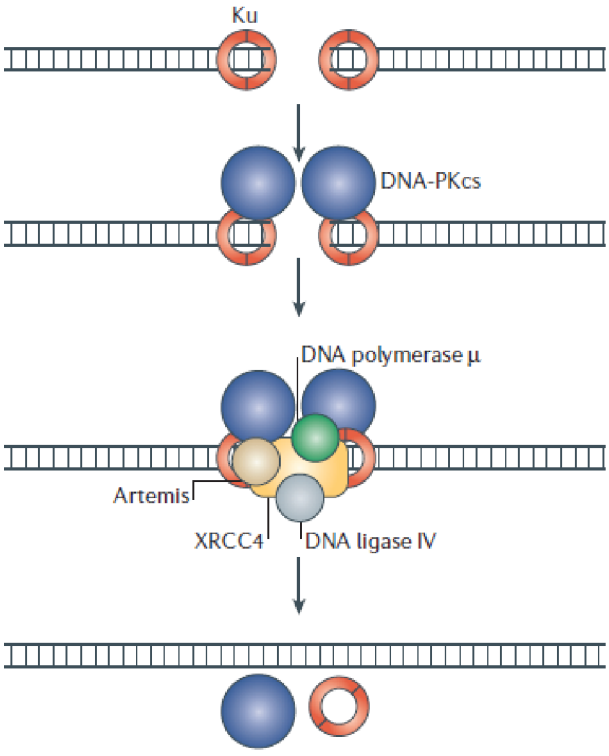

Figure 6. Non-homologous end joining. Ku70 and Ku80 bind DNA double-stranded breaks and recruit DNA-PKcs to the site of DNA damage. The DNA-PK holoenzyme, which comprises the Ku proteins and DNA-PKcs, recruits ARTEMIS, XRCC4, DNA ligase IV and DNA polymerase μ to the site of DNA damage. The endonuclease activities of ARTEMIS are activated by DNA-PKcs-dependent phosphorylation and are required to resolve complex DNA ends. DNA polymerase μ then fills in the gaps, and XRCC4 and DNA ligase IV ligate the processed DNA ends. Figure from (Xu 2006).

DNA damage-induced cell death

Chronic DDR signaling triggers p53-dependent cell death by apoptosis or cellular senescence if the damage cannot be removed, thereby suppressing tumorigenesis. The presence of the chronic DNA damage has been detected in early stage tumors (Halazonetis et al. 2008). Cells are also entering into apoptosis or senescence when chronic DDR is also activated in telomeres that lack terminal telomeric repeats (de Lange 2009), which are recognized as DSBs and can trigger chromosome fusions. Telomere shortening occurs during natural aging and consistent with that, unrepaired DSBs accumulate with age in human and mouse cells (Sedelnikova et al. 2004) and in certain DDR-defective progeroid syndromes, such as Werner's syndrome (Mohaghegh & Hickson 2002). In response to DNA damage, p53 can be activated via parallel pathways, that are controlled mainly by the signaling activities of ATM and MRE11 complex, DNA-PK and CHK2 (Stracker et al. 2007; Stracker & Petrini 2008; Callén et al. 2009).

3. The MRE11 complex

The highly conserved MRE11 complex (or MRN complex) has a key role in different aspects of the DDR. The MRE11 complex is a sensor of DSBs, and its signaling leads to ATM and ATR kinase activation, thereby coordinating diverse cell fate decisions after DSB detection. Various post-translational modifications and MRE11 complex intrinsic enzymatic activities play an important role in DSB repair, which is essential for preventing severe pathologies. Biochemically, MRE11 exhibits endonuclease and 3'-5'exonuclease activity, RAD50 has ATPase activity and bridges sister chromatids during recombination or repair, and NBS1 promotes nuclear localization of the complex and mediates its interactions with other proteins (Stracker & Petrini 2011; Mimitou & Symington 2009).

Structure of the complex

The MRE11 complex consists of a central globular domain, in which MRE11 and NBS1 associate with the Walker A and B domains of RAD50, and the extended coiled-coil domain of RAD50, in which the amino(N)-terminal and carboxy(C)-terminal parts of the coils associate in an antiparallel manner (Figure 7A) (Stracker & Petrini 2011). At the top of the RAD50 coils, the N-terminal and C-terminal stretches fold back to form RAD50 zinc-hook domain. This domain is a highly conserved interface that joins MRE11 complexes, thereby bridging DNA molecules during the DDR (Figure 7B). Studies with RAD50 mouse models show that the hook domain is essential for MRE11 complex functions, including DDR signaling, tumorigenesis and tissue homeostasis (Roset et al. 2014). NBS1 acts as a phosphoprotein sensor and recruitment platform for MRE11 complex. The N-terminal region of NBS1 contains two phosphopeptide-binding modules, the FHA and tandem BRCT domains. NBS1 crystal structures revealed an extended and flexible center, with FHA and BRCT domains linked to C-terminal MRE11 and ATM-binding motifs (Williams et al. 2009).

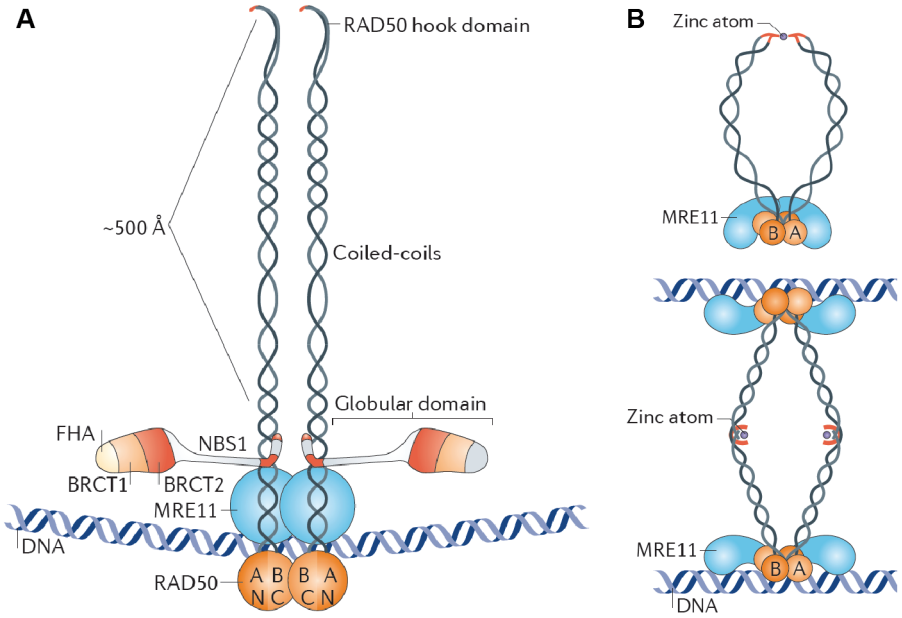

Figure 7. The MRE11 complex structure. (A) MRE11 and NBS1 associate with RAD50 and DNA via a large globular domain and coiled-coil domains of RAD50 associate in an antiparallel manner. (B) MRE11 complex without and with DNA, upon DNA binding, the coiled-coil domains of RAD50 adopt a rigid parallel structure that bridges two DNA strands via the RAD50 zinc-hook domain. Adapted from (Stracker & Petrini 2011).

The ATPase activity of RAD50 is important for many key functions of the complex, including the nuclease activity of MRE11. MRE11 complex exists in 2 different conformations, depending on ATP binding and hydrolysis by RAD50. ATP-bound "closed" MRE11 complex is necessary conformation for the DNA binding and ATM activation. DNA end resection is promoted by the "open" conformation that occurs during ATP hydrolysis (Lee et al. 2013; Deshpande et al. 2014). The dynamic transition between these states is essential to promote end resection, ATM activation and facilitate DNA repair. Observing the DNA duplex opening in real time showed that ATP-dependent MRE11 complex interaction with DNA ends promotes conformational changes in DNA structure, leaving 15-20 DNA base pairs held open by a complex, probably allowing access of the end resection machinery to DNA ends. Consistent with this, RAD50 mutant with impaired duplex opening activity also blocked DNA end resection in vitro (Cannon et al. 2013).

MRE11 is a sensor of DSBs

The molecular mechanism by which MRE11 complex recognizes DSBs and induces ATM activation is not entirely understood. The MRE11 complex is recruited to the breaks within seconds and remains there at later time points, visible in punctate foci (Nelms et al. 1998; Lukas et al. 2003; Lisby et al. 2004; Mirzoeva & Petrini 2001). The initial recruitment is independent of any known post-translational modifications, but the subsequent retention depends largely on FHA and BRCT domains of NBS1 (Lukas et al. 2004).

BRCT domain of NBS1 recognizes PAR, which is polymerized massively by PARPs after the DNA damage (Li et al. 2013). PAR recognition by NBS1 is proposed to mediate the initial recruitment of the MRE11 complex to DNA damage sites, and early ATM activation. Inhibiting PARP by olaparib or mutating the BRCT domain of NBS1 was shown to impair the early localization of MRE11 complex to laser-induced DNA breaks.

MRE11 complex accumulation in chromatin surrounding the DSB involves the interaction of NBS1 via its FHA and BRCT domains with phosphorylated MDC1. MDC1 promotes the accumulation of MRE11 complex at breaks through interactions with its functional partner, γ-H2AX. Therefore, cells deleted for H2AX still recruit MRE11 complex to break sites but are not able to retain it (Lukas et al. 2004; Chapman & Jackson 2008). The alternative clamp loader RAD17 has also been reported to be important for MRE11 complex recruitment to DSB sites through the interaction with the FHA domain of NBS1. This interaction requires prior RAD17 phosphorylation by ATM and leads to increased ATM activation, thus creating a positive feedback loop to promote ATM signaling (Q. Wang et al. 2014).

MRE11 activates ATM

The MRE11 complex plays an important role in ATM activation (Uziel et al. 2003). Following DSB sensing by MRE11 complex, ATM rapidly undergoes autophosphorylation on several residues that promote a conformational change into active monomers where the kinase domain is unmasked (Bakkenist & Kastan 2003; Stracker et al. 2013; Lavin & Kozlov 2007). MRE11 complex also promotes the loading of active ATM at breaks through via the extreme C terminus of NBS1 (You et al. 2005; Lee & Paull 2004). However, ATM can be also activated in MRE11 complex-independent manner, either directly via exposure to ROS (Guo et al. 2010) or through ATM INteracting protein (ATMIN) that is able to activate ATM in response to some types of stress (Kanu & Behrens 2007). ATMIN is proposed to compete with NBS1 for ATM binding as deletion of either protein enhances ATM signaling through the other (Zhang et al. 2012).

Activated ATM can phosphorylate proteins that control DNA damage signal transduction. Over 1000 proteins have been identified as potential substrates for ATM (Matsuoka et al. 2007; Shiloh & Ziv 2012). Many ATM targets play a critical role in the activation of cell cycle checkpoints, such as p53, CHK2, SMC1, MRE11 complex itself and DNA end processing enzymes which activities activate ATR and CHK1 (Ahn et al. 2004; Stracker et al. 2013).

MRE11 enzymatic roles in resection

After localizing to DSBs, the MRE11 complex promotes 5'-3' resection of the DNA to generate ssDNA overhangs that are necessary for the proper break repair via HDR. MRE11 collaborates with 5'-3' exonuclease EXO1 and 5'-3' endo/exonuclease DNA2 that works together with BLM helicase, as demonstrated from yeast studies, where these enzymes show partially redundant activities (Mimitou & Symington 2008). MRE11 itself has 3'-5' exonuclease activity, seemingly incompatible with the required polarity of 5'-3'. Using MRE11 complex mutants in *Saccharomyces cerevisiae* (*S. cerevisiae*) it was shown that Mre11 initiates resection with the Sae2 endonuclease (CtIP in

mammals) by making a nick in the DNA strand and resecting towards the broken DNA end. More extensive resection involves Exo1 or the combined activities of Sgs1 (BLM in mammals) and Dna2 (Garcia et al. 2011; Mimitou & Symington 2008; Zhu et al. 2008). Specific MRE11 inhibitors recently provided evidence that extends this model to the mammalian system. Using the structure of the previously characterized MRE11 exonuclease inhibitor mirin (Dupré et al. 2008), specific endo and exonuclease inhibitors of MRE11 were identified. Specific targeting of endonuclease activity showed that it was essential for initiating resection and committing breaks to HDR. Endonuclease inhibition also promoted NHEJ, which is otherwise inhibited by resected ends or ends that are bound by Ku complex. Further, they showed that the inhibition of MRE11 exonuclease activity combined with the siRNA mediated depletion of EXO1 and BLM restored NHEJ by minimizing resection, even in the presence of the MRE11 endonuclease activity. This data supports the bidirectional resection model (Figure 8) and establishes the roles of MRE11 enzymatic activities as key regulators of DSB pathway choice and DNA repair through HDR (Shibata et al. 2014).

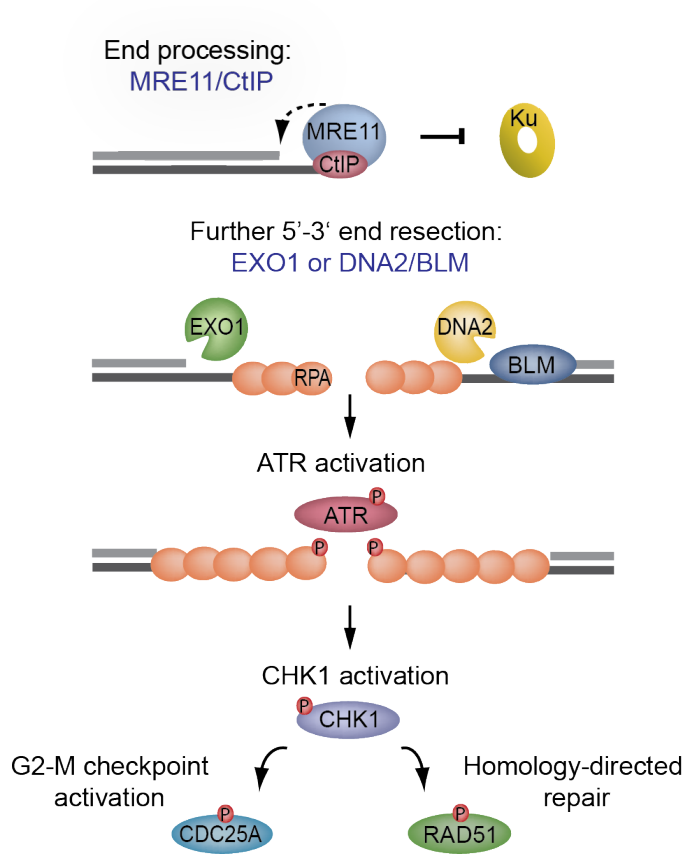

Figure 8. Model for DSB end resection. DSB resection is initiated by MRE11 complex with CtIP, and this creates a substrate that is unfavorable for Ku complex mediated NHEJ. Longer range resection is carried out by EXO1 and/or DNA2 and BLM activities. ssDNA is bound by RPA, which leads to ATR activation. This promotes CHK1 activation, leading to checkpoint arrest and HDR.

Many studies have shown a complex interplay between MRE11 nuclease activity and the Ku heterodimer in determining the DSB repair pathway used. MRE11 mediated resection creates a substrate that is not accessible to the Ku complex, and Ku, on the other hand, blocks access of EXO1 to DSB ends. In strains deficient for Ku, initial resection by the Mre11 complex was not necessary in *S. cerevisiae* cells, as ends could be accessed directly by Exo1 (Mimitou & Symington 2010). Similarly, depleting Ku80 by siRNA in mammalian cells enhanced the recruitment of EXO1 and RPA following IR treatment and the DNA-PKcs was shown to block EXO1 recruitment and resection, thereby promoting NHEJ (Zhou & Paull 2013).

The CtIP protein interacts with the MRE11 complex and plays a key role in determining DSB pathway choice. CtIP is phosphorylated in G2 and S phases of the cell cycle by CDKs which promote CtIP interaction with BRCA1, facilitating the removal of 53BP1 that blocks resection (Polato et al. 2014). CtIP also directly binds the MRE11 complex and its phosphorylation by CDKs promotes an interaction with the NBS1-FHA domain (Wang et al. 2013; Sartori et al. 2007). CtIP itself exhibits 5' flap endonuclease activity, and was found to have a specific role in the removal of DNA adducts or secondary structures from DNA ends. CtIP deficient cells show increased sensitivity to topoisomerase poisons and IR, where adduct removal is necessary, but are not defective in repairing unmodified DNA breaks (Makharashvili et al. 2014; H. Wang et al. 2014).

MRE11 roles in replication fork stability and ATR activation

In mice, deletion of any MRE11 complex members leads to embryonic lethality (Buis et al. 2008; Zhu et al. 2001; Luo et al. 1999). Studies have shown that one of the key functions of the MRE11 complex is facilitating DNA replication and preventing damage during S-phase. Using mouse models with hypomorphic or conditional mutations have shown that MRE11 complex is required in a variety of developing tissues (Stracker & Petrini 2011). The HDR machinery was shown to escort the replication fork, ensuring high fidelity replication by sealing ssDNA gaps behind forks, protecting nascent forks from degradation and helping with fork restart (Carr & Lambert 2013). As the MRE11 complex promotes ATR activation and subsequent phosphorylation of CHK1 that leads to G2-M checkpoint activation, defects in this pathway may explain the essential nature of MRE11 during replication and development (Stracker & Petrini 2011). ATR responds to broader DNA damage than DSBs and is essential for the survival of proliferating cells, even without extrinsic DNA damage (Ruzankina et al. 2007). Moreover, ATM is not essential for development, but inactivation of either ATR or CHK1 leads to embryonic lethality (Brown & Baltimore 2000; Liu et al. 2000; Xu et al. 1996).

To observe fate of cells that have lost functional MRE11 complex, NBS1 was conditionally deleted and cells were monitored using high content microscopy. NBS1 deficient cells accumulated replication intermediates that were converted to DSBs in G2 phase, activating CHK1 and slowing down G2-M progression, which led to chromosomal instability. Interestingly, several cell cycles were needed until this chromosomal instability led to activation of p53, causing further cell-cycle arrest and cell death (Bruhn et al. 2014).

ATR is activated in response to many different kinds of DNA damage, but a single structure – transition from dsDNA to ssDNA, might be responsible for ATR activation. ssDNA is coated with RPA, that is recognized by ATRIP-ATR complex, but that is not yet activating ATR. Another complex – consisting of RAD9, RAD1 and HUS1 (termed 9-1-1 complex) is loaded the DNA adjacent to ssDNA-RPA by RAD17 and this activates TOPBP1, that is essential for ATR activation (Cimprich & Cortez 2008). In *Xenopus* extracts, ATR activating structures, ssDNA or dsDNA-ssDNA junctions, were found to recruit also MRE11 complex. MRE11 recruitment was found to be essential for TOPBP1 recruitment, and thereby ATR and CHK1 activation. In addition, MRE11 was proposed to act redundantly with RAD17, as only co-depletion of both of these components completely blocks CHK1 activation (Duursma et al. 2013; Lee & Dunphy 2013).

After resection, RPA binding to ssDNA is also essential to protect the 3' ssDNA ends from further degradation by nucleases, which can lead to genomic rearrangements. Without RPA ssDNA was also shown to form fold-back structures that are inhibitory to RAD51 binding (H. Chen et al. 2013). Toledo and colleagues showed that following its activation by ATR, CHK1 diffuses through the nucleus and suppresses replication by preventing new origin firing. If ATR signaling fails, dormant origins start firing and the new ssDNA can deplete pools of RPA, which is essential to cover and protect the ssDNA. When ssDNA is unprotected this leads to their conversion to DSBs, thus creating more DNA damage. Therefore ATR protects ongoing replication forks by ensuring

that limiting pools of RPA are not depleted by excess firing of dormant origins (Toledo et al. 2013).

While functional MRE11 complex is essential for replication forks, MRE11 must be precisely regulated, as its uncontrolled activity can lead to degradation of replication forks. When replication fork stalling occurs, BRCA2 is required to stabilize RAD51 filaments and protect ssDNA to prevent MRE11 from degrading nascent DNA behind the fork. MRE11 activity can thereby drive chromosomal instability in BRCA2 or RAD51 deficient cells by first starting the HDR and then further degrading unprotected forks (Schlacher et al. 2011; Ying et al. 2012). Common fragile sites (CFSs) contain sequences that can form secondary structures during DNA replication and are therefore more sensitive to replication stress. MRE11 activity is also harmful for CFSs, which require ATR to protect the replication forks (Koundrioukoff et al. 2013).

DNA2, that works together with MRE11 during resection, is an endonuclease/helicase that processes different structural intermediates that arise during DNA metabolism, such as Okazaki fragments from lagging strand synthesis or G-quadruplexes (Kang et al. 2010; Lin et al. 2013). The ATR pathway has been shown to target the DNA2 nuclease to process stalled forks, preventing fork reversal. Studies in *Schizosaccharomyces pombe* (*S. pombe*) revealed an important role for DNA2 in protecting genome integrity. It was shown that Cdc1 (mammalian CHK2), activated in the intra S-phase checkpoint in response to replication stalling, phosphorylates Dna2, which then cleaves regressed leading or lagging strands. Fork regression occurs when a stalled replication fork actively reverses allowing the nascent strands behind the fork to anneal. The resulting structure resembles Holliday junctions and may trigger unwanted homologous recombination (Hu et al. 2012; Branzei & Foiani 2010).

MRE11 complex mouse models

Complete knockouts of any MRE11 complex members lead to embryonic lethality (Buis et al. 2008; Zhu et al. 2001; Luo et al. 1999). Therefore, to study MRE11 complex functions *in vivo*, different hypomorphic mutants based on alleles identified in human syndromes or conditional alleles have been generated.

MRE11 mouse models

To recapitulate ATLD, mice carrying a truncated allele of MRE11 were created based on one of the more severe mutations identified in patients. *Mre11*$^{ATLD1/ATLD1}$ mice recapitulated checkpoint defects, chromosomal instability and fertility issues. However, despite severe defects in ATM activation, these mice were not prone to cancer. This allele mildly accelerated tumorigenesis in *p53*$^{+/-}$ mice, suggesting that loss of heterozygosity may be accelerated (Theunissen et al. 2003). Notably, like ATM deficient mice, these animals also did not recapitulate the ataxia observed in human ATLD patients.

In mammalian cells, MRE11 nuclease activity has been implicated in ATM activation (Uziel et al. 2003). A nuclease dead allele of *Mre11*, leads to embryonic lethality characterized by rapidly senescing cells carrying chromosomal aberrations by embryonic day E9.5. However, ATM activation in these cells is normal and ATM null mice are viable, indicating that the nuclease function of MRE11 is essential for reasons unrelated to ATM activation and signaling (Buis et al. 2008).

NBS1 mouse models

Conditional null alleles of *Nbs1* lead to checkpoint defects, chromosomal damage, increased sensitivity to DNA damaging agents and cell death. *In vivo*, the null mutation affects fast proliferating tissues, such as bone marrow, thymus, spleen and lymphatic tissue (Demuth et al. 2004).

The majority of human NBS patients carry a five base pair deletion in exon 6 of NBS1, termed Nbs1^{657del5} mutation. This results in the production of two

different fragments of NBS1: an N-terminal 26 kDa product (p26) containing the FHA and BRCT domains and a C-terminal 70 kDa product (p70) containing the MRE11 interaction domain and ATM phosphorylation sites (Maser et al. 2001). To model this in mouse, 3 hypomorphic mutants were created. In *Nbs1*$^{\Delta B/\Delta B}$ mice, exons 4 and 5 were disrupted, resulting in deletion of the BRCT domain and production of a C-terminal fragment of the protein, similar to the human disease p70 fragment (Williams et al. 2002). *Nbs1*$^{m/m}$ mouse carry a disruption of exons 2 and 3, resulting in similar N-terminal truncation (Kang et al. 2002). Both mouse mutants recapitulated NBS cellular phenotypes, displaying defective cell-cycle checkpoints, higher sensitivity to DNA damaging agents and chromosomal instability. Unlike NBS patients, *Nbs1*$^{\Delta B/\Delta B}$ mice do not exhibit immune system defects and they are not prone to cancer but do exhibit subfertility. The similar *Nbs1*$^{m/m}$ mice displayed NBS patient characteristics such as growth retardation, immunodeficiency, infertility and cancer predisposition, although the protein generated was not well characterized. In an attempt to more closely mimic the human allele, a “humanized” transgenic mouse line was created. Human bacterial artificial chromosomes (BACs) containing mutant alleles of human NBS1 were used to complement Nbs1-deficient ES cells. Using this approach, *NBS1*$^{675\Delta 5}$*Nbs1*$^{-/-}$ mice were generated that express the human allele containing a 5-bp deletion (Difilippantonio et al. 2005). Similar to the previous murine models, these mice express only the C-terminal fragment of the NBS1 protein, show checkpoint and fertility defects and are not prone to cancer.

All of the *Nbs1* alleles described above lack the N-terminal FHA and BRCT domains. These N-terminal domains regulate IRIF formation and chromatin association, but are not necessary for the nuclear localization of the MRE11 complex or ATM activation (Zhao et al. 2002; Lee et al. 2003). To understand better the role of the NBS1 FHA domain *in vivo*, the inactivating point mutation H45A was generated in the human allele and introduced in a BAC to create *NBS1*^{H45A}*Nbs1*$^{-/-}$ mice (Difilippantonio et al. 2005). These mice have defects in T-cell and oocyte development similar to *NBS1*$^{675\Delta 5}$*Nbs1*$^{-/-}$ mice, and cells displayed slight checkpoint defects in response to IR, but not the other

phenotypes of NBS. These defects may be due to impaired interaction with CtIP, as the FHA domain is necessary for CtIP recruitment (Williams et al. 2009). Inactivation of CtIP also leads to early embryonic lethality (Chen et al. 2005).

The C-terminus of NBS1 was shown to interact with ATM and was proposed to be required for ATM activation (You et al. 2005; Falck et al. 2005). In contrast to the cellular data, mice that lack the NBS1 C-terminal domain do not show defects in ATM activation, MRE11 complex formation, IRIF formation, checkpoint arrest or nuclear localization (Difilippantonio et al. 2007; Stracker et al. 2007). Thus, the C-terminus of NBS1 is dispensable for ATM activation and checkpoint signaling. Nevertheless, ATM was not fully functional as these cells displayed a defect in IR-induced apoptosis that was largely epistatic to loss of ATM.

ATM phosphorylates NBS1 in response to DNA damage (Zhao et al. 2000) and this phosphorylation was implicated in checkpoint activation and shown to occur at sites of damage (Lukas et al. 2003). However, humanized mouse models lacking ATM phosphorylation sites at Ser278 and Ser343 showed normal checkpoint responses (Difilippantonio et al. 2007). Thus, the role of ATM mediated phosphorylation of NBS1 remains unclear.

A-T, ATLD, NBS and NBSLD are all diseases characterized by neuropathologies. However, they differ in their clinical presentation as A-T and ATLD patients present with neurodegeneration and NBS and NBSLD patients with microcephaly (McKinnon 2004; Taylor et al. 2004; van der Burgt et al. 1996). In order to understand better the reason for these distinct neuropathologies, mouse models of ATLD (*Mre11*$^{ATLD1/ATLD1}$) (Theunissen et al. 2003) and NBS (*Nbs1*$^{\Delta B/\Delta B}$) (Williams et al. 2002) were used to analyze the functional consequence of these mutations in the nervous system. Both of these mutations led to defective ATM phosphorylation in the nervous system following the introduction of DNA breaks, but only the Mre11$^{ATLD1/ATLD1}$ mutation blocked the induction of apoptosis by ATM. This is similar to *Atm*$^{-/-}$ cells, where damaged neural cells accumulate and contribute to the mature nervous system, resulting

in neurodegeneration. On the other hand, in *Nbs1*$^{\Delta B/\Delta B}$ cells, ATM dependent apoptosis functions, resulting in increased apoptosis during brain development and microcephaly (Shull et al. 2009). The deletion of *Nbs1* in the brain using a conditional allele phenocopies patient microcephaly to some extent and can be rescued to a large degree by the elimination of p53, the main effector of apoptosis in response to DNA breaks (Frappart et al. 2005).

RAD50 mouse models

As RAD50 mutations were only recently identified in human NBSLD patients, initial in vivo analysis was based on yeast separation of function mutations termed *Rad50*^{S} (Alani et al. 1990) Based on these studies a *Rad50* hypomorphic mutant carrying a K to M mutation at amino acid residue 22, termed *Rad50*$^{S/S}$, was generated. Mice were viable but exhibited growth defects, severe anemia and cancer predisposition (Bender et al. 2002). The anemia resulted from hematopoietic stem cell attrition and was dependent on ATM and CHK2 mediated apoptosis triggered by the *Rad50*^{S} allele (Morales et al. 2005). Other recently reported mouse models with reduced hook domain function were inviable while carrying homozygous mutations, but cells and tissues heterozygous for mutant hook alleles exhibited increased ATM activation and DDR signaling in the absence of exogenous damage (Roset et al. 2014). In addition, these mice exhibited severe defects in immune system and germline development and were predisposed to liver tumorigenesis. This work highlights the fact that heterozygous mutations in RAD50 may be highly relevant to cancer predisposition in humans.

Mouse models related to the MRE11 complex

ATM knockout mice have been well studied in relation to the human syndrome. *Atm*$^{-/-}$ mice display the same phenotypes as A-T patients, recapitulating many of the clinical features, including neurologic dysfunction, immunologic abnormalities, chromosomal instability, infertility and they are dying of thymic lymphomas at an early age (Barlow et al. 1996). In contrast, ATR knockout is lethal (de Klein et al. 2000), but a hypomorphic allele based on human Seckel syndrome patients, termed *Atr*^{S}, is viable. Similar to human Seckel patients,

these mice have growth defects, microcephaly with brain defects and the protruding nose “bird-head” phenotype. In addition, they displayed a progeroid phenotype, dying in less than half a year with accumulation of replicative stress and chromosomal instability evident in tissues (Murga et al. 2009). Similarly, the conditional knockout of ATR leads to the attrition of stem and progenitor cells resulting in several phenotypes indicative of premature aging (Ruzankina et al. 2007)

The inactivation of CHK1 also results in early embryonic death with increased levels of apoptotic cells evident at the blastocyst stage (Takai et al. 2000), similar to ATR knockout mice (Brown & Baltimore 2000). CHK2 deficient mice, on the other hand, are viable and grow normally with no clear spontaneous phenotypes. However, they are resistant to IR-induced apoptosis mediated by p53, demonstrating that CHK2 regulates p53 functions in response to IR (Takai et al. 2002).

The importance of the MRE11 complex in tumor suppression

Oncogene activation causes stalling or collapse of replication forks that can lead to DSB formation and contribute to genomic instability that is present in many cancers. The DDR functions as a barrier to tumorigenesis by inducing apoptosis or senescence in response to oncogene-induced stress. In addition, DSBs activate p53 that is required for apoptosis or senescence, thus mutations in p53 enable the propagation of damaged cells that can contribute to tumor formation (Halazonetis et al. 2008; Bartek et al. 2007).

The MRE11 complex promotes p53 dependent apoptosis induction through either ATM or CHK2, or both, depending on the cell type and stimulus. Apoptosis in hematopoietic cells of $Rad50^{s/s}$ mice is rescued with alleles that have reduced ATM activity, such as $Atm^{-/-}$, $Mre11^{ATLD1/ATLD1}$, $Nbs1^{\Delta C/\Delta C}$ and $Nbs1^{\Delta B/\Delta B}$, as well as in mice lacking CHK2 or p53 (Morales et al. 2005; Stracker et al. 2007). However, in the immune system, CHK2 dependent apoptosis following IR is unaffected by mutations in MRE11 complex members, delineating parallel signaling pathways (Stracker et al. 2008; Stracker et al.

2007; Stracker & Petrini 2008). This likely reflects a redundant function for DNA-PKcs that can activate CHK2 in this tissue in the absence of ATM or a functional MRE11 complex (Callén et al. 2009).

The role of the MRE11 complex as a barrier to oncogene-induced tumorigenesis was tested in mouse a model of human epidermal growth factor receptor 2 (HER2) driven breast cancer. *Mre11*$^{ATLD1/ATLD1}$ mice exhibited increased hyperplasia, defective G2 checkpoint responses and accelerated tumorigenesis with metastatic tumors being present more often. Interestingly, *Nbs1*$^{\Delta B/\Delta B}$ and *Chk2* null alleles did not enhance HER2 driven tumorigenesis (Gupta et al. 2013) leaving the exact role of MRE11 complex in tumor suppression unclear.

The RAD50 zinc hook is an important domain for MRE11 function as it facilitates proper folding of RAD50 and assembly of the complex (Hopfner et al. 2002). It is also necessary for MRE11 complex recruitment to DSBs and to bridge the DNA molecules during repair. Loss of this domain leads to destabilization of the whole complex, phenocopying complete RAD50 deficiency (Wiltzius et al. 2005). Recently, it was shown that homozygous mice carrying mutations in hook domain were inviable, but heterozygous mutants were phenotypically similar to the *Rad50*$^{S/S}$ allele, exhibiting increased ATM activation, immune system and germline defects. In addition, they were more prone to liver tumors (Roset et al. 2014).

Chk2$^{-/-}$ mice are not tumor prone, despite defects in p53 dependent apoptosis regulation and impaired G1-S checkpoint arrest (Hirao et al. 2002). Defects in apoptosis were restored by complementing cells by wild type CHK2 but not by CHK2 where ATM phosphorylation sites were mutated. Although CHK2 is an ATM target, the only shared phenotype in mutant mice appears to be the defective p53 stabilization and function in response to IR (Hirao et al. 2002). To understand better the relationship between the MRE11 complex and CHK2, double mutant *Mre11*$^{ATLD1/ATLD1}$ *Chk2*$^{-/-}$ and *Nbs1*$^{\Delta B/\Delta B}$ *Chk2*$^{-/-}$ were created. Loss of CHK2 did not change the checkpoint defects or chromosomal instability of MRE11 complex mutant cells, but double mutant mice exhibited increased

apoptotic defects and were prone to a variety of tumors, in contrast to *Atm*$^{-/-}$ mice that develop only thymic lymphomas. This suggests that CHK2 is responsible for tumor suppression in response to replication-associated DNA damage, characteristic of the *Mre11*$^{ATLD1/ATLD1}$ and *Nbs1*$^{\Delta B/\Delta B}$ mutants (Stracker et al. 2008). This is also consistent with the fact that viability of mice that are severely defective for NHEJ due to Ligase IV mutations can be rescued by CHK2 without being predisposed to tumorigenesis (Foster et al. 2012).

4. Exonuclease 1

Exo1 was first described in *S. pombe* as a nuclease that is induced during meiosis (Szankasi & Smith 1992). Subsequently, Exo1 was implicated in mitotic recombination in *S. cerevisiae* (Huang & Symington 1993; Fiorentini et al. 1997). Human EXO1 was described as highly related to yeast Exo1 and the expression was high in testis, consistent with the proposed role of EXO1 in meiosis (Tishkoff et al. 1998).

EXO1 has been shown to have a role in MMR, DSB repair, immune system development, meiosis and telomere maintenance (Vallur & Maizels 2010). EXO1 belongs to xeroderma pigmentosum group G (XPG)/RAD2 family of metallonucleases and biochemically possesses 5'-3' exonuclease and 5' flap-endonuclease activities (Lee & Wilson 1999). EXO1 interacts with several other proteins involved in replication and DNA repair, including PCNA and MMR proteins (Kirkpatrick et al. 2000; Tsubouchi & Ogawa 2000; Lee & Alani 2006; Schmutte et al. 2001; X. Chen et al. 2013).

EXO1 in mismatch repair

By screening proteins that functionally interact and are redundant with Exo1 in *S. cerevisiae*, it was found that Exo1 functionally interacts with the majority of known MMR proteins. It was hypothesized that multiprotein complexes are formed during MMR and that EXO1 plays a structural role in MMR, by stabilizing these complexes (Amin et al. 2001). Biochemical assays with purified human protein show that EXO1 is also required in the excision step of MMR (Genschel et al. 2002). Exo1 mutants show a mutator phenotype in yeast, however, Exo1 mutant strains were shown to be less defective than another MMR protein MutS protein homolog 2 (Msh2) mutants, suggesting alternative activities that can function without Exo1 (Tishkoff et al. 1997).

MMR defects have been described to lead to increased mutation rates and are associated with HNPCC and up to 25% of sporadic colorectal cancers. Since

EXO1 is implicated in MMR, it was suggested that it might be a target for mutation in tumorigenesis. In majority of the cases, the defective genes in HNPCC are MSH2 and MutL homolog 1 (MLH1), smaller proportion of cases are caused by other MMR genes (Peltomäki 2003; Mueller et al. 2009). Although germ line variants of EXO1 were detected in patients with HNPCC, it is not clear whether EXO1 mutations predispose to HNPCC. Germ line mutations of EXO1 display a weak mutator phenotype, and may predispose to late onset of cancer, a phenotype that is not classified as HNPCC, but as sporadic cancer (Liberti & Rasmussen 2004; Alam et al. 2003; Jagmohan-Changur et al. 2003; Tran et al. 2001).

Role of EXO1 in the regulation of resection

Many studies demonstrated the role of EXO1 in long-range DSB resection that generates a structure that is essential for ATR activation and HDR (Mimitou & Symington 2008; Zhu et al. 2008; Nakada et al. 2004; Tomimatsu et al. 2012). Complementary or redundant functions of EXO1 in DSB resection mechanisms have been reported. *S. cerevisiae* genetics experiments showed redundancy between Exo1 and Mre11 nuclease activities in IR sensitivity (Lam et al. 2008). Loss of yeast Sgs1 impairs DSB resection, but only if Exo1 is simultaneously deleted. Similar results in human cells were shown where either EXO1 or BLM downregulation lead to mild impairment of DSB resection and reduction in ATR-mediated signaling, but simultaneous downregulation of both lead to severe defect (Gravel et al. 2008; Zhu et al. 2008). Similar redundancy was reported for EXO1 and DNA2 in human cells (Karanja et al. 2012).

EXO1 has been shown to exhibit limited processivity in DSB end resection *in vitro*, suggesting factors that promote its function *in vivo* (Genschel & Modrich 2003). The MRE11 complex, BLM and RPA were all shown to stimulate EXO1-mediated resection (Cannavo et al. 2013; Nimonkar et al. 2011). EXO1 interacts with the DNA sliding clamp PCNA that promotes processive DNA synthesis by DNA polymerases. PCNA was shown to load recruit EXO1 to DSBs and

promote its function by enhancing its processivity and promoting its retention (Chen et al. 2013).

Competition between the NHEJ machinery and nucleases has been reported. Yeast studies show that in DSB repair, a MRE11 nuclease-deficient HDR mutant is rescued by Exo1 overexpression or by YKu70 (mammalian Ku70) deletion (Muñoz-Galván et al. 2013). The MRE11 complex has also shown to stimulate EXO1 by inhibiting excess binding of the Ku complex (Shim et al. 2010) and the Ku complex was shown to block EXO1-mediated end resection (Sun et al. 2012; Tomimatsu et al. 2012).

Studies with human cells showed that EXO1 is phosphorylated by ATM after IR (Bolderson et al. 2010) and by ATR in stalled replication forks (El-Shemerly et al. 2008). Both of these were found to inhibit EXO1 activity, possibly to prevent excessive resection. Recently, CDKs were reported to phosphorylate EXO1 in S and G2 phases of the cell cycle which was shown to promote resection and HDR (Tomimatsu et al. 2014).

Role of EXO1 in processing stalled replication forks

Since EXO1 is a nuclease that can degrade DNA, its activities must be tightly controlled to avoid DNA resection when it is unfavorable. Several studies showed that in cells with defective S-phase checkpoint responses, various nucleases degrade stalled replication forks (Cotta-Ramusino et al. 2005; Froget et al. 2008; Segurado & Diffley 2008).

Studies with human cells demonstrated that BRCA2 protects replication forks by preventing stalled fork degradation by MRE11. In addition, EXO1 was also proposed to be able to perform excessive degradation in cells with compromised checkpoints (Schlacher et al. 2011). *S. cerevisiae* Exo1 is recruited to stalled replication forks where it resects fork structures in Rad53 (mammalian CHK2) defective cells. This causes the regression of collapsed forks, generating Holliday-like junction. This structure is a target of other nucleases and can potentially generate different recombination substrates

leading to genome instability (Cotta-Ramusino et al. 2005). Moreover, the sensitivity of Rad53 mutants to some DNA-damaging agents was shown to be suppressed by the deletion of Exo1. It was reported that loss of DNA replication fork stability in Rad53 mutants is due to Exo1 activities, and that removal of Exo1 was sufficient to allow proper fork stabilization in the absence of Rad53. This confirms that Rad53 prevents the replication fork degradation from Exo1 activity (Segurado & Diffley 2008). EXO1 was also proposed to promote deletions and contributes to genetic instability at unprotected telomeres. *S. cerevisiae* Exo1 is phosphorylated in response to uncapped telomeres by Rad53, which inhibited Exo1 activity, thereby limiting the accumulation of ssDNA (Morin et al. 2008). Similarly, in *S. pombe*, Exo1 was identified as a target of the ATR pathway at collapsed forks, where Rad3 (mammalian ATR) was shown to prevent Exo1 from inappropriately processing the collapsed fork, leading to genome instability. The 9-1-1 complex, on the other hand, promoted Exo1 activity at the collapsed fork, leading to the proposal that ATR controls resection by targeting EXO1 when sufficient resection has taken place (Tsang et al. 2014). Using purified recombinant proteins in *S. cerevisiae*, RPA was also shown to inhibit the nonspecific binding of Exo1 to ssDNA and prevent excessive DNA degradation (Cannavo et al. 2013).

EXO1 mutant mice

The first *Exo1* mutant mouse had a deletion of exon 6, resulting in a loss-of-function *Exo1* (*Exo1*^{dex6}) allele. These mice showed MMR defects along with microsatellite instability, and a mutator phenotype, albeit lower than of *Msh2*$^{-/-}$ cells. *Exo1*^{dex6} mice had also decreased CSR and changes in the characteristics of SHM, similar to the defects observed in *Msh2* mutant mice. In addition, *Exo1*^{dex6} mice were infertile and displayed decreased survival and predisposition to tumors, especially lymphomas. However, all these phenotypes were fairly mild, as at the age of 17 months there was still 50% survival, compared to 6 months in *Msh2*$^{-/-}$ mice (Wei et al. 2003; Bardwell et al. 2004).

In *Exo1*^{dex6} mutants, EXO1 was both structurally and nucleolytically impaired. To understand better which phenotypes resulted from its nuclease activity, *Exo1* mutant mice carrying either a mutation of the nuclease domain E109K (*Exo1*^{EK}) or a complete knockout (*Exo1*^{null}) were created. *Exo1*^{EK} mice showed normal MMR in contrast with *Exo1*^{null} mice that showed defective MMR, indicating that only a structural function of EXO1 is necessary for MMR. This structural activity of EXO1 was also shown to be necessary for meiosis, as *Exo1*^{EK} mice were infertile. However, EXO1 nuclease activity was found to be necessary for SHM and DSB resection. Both mutants showed reduced survival and they were prone to tumors. Interestingly, *Exo1*^{null} mice developed lymphomas while *Exo1*^{EK} mice developed tumors with a different spectrum, mostly sarcomas and adenomas. Crossing them with p53 resulted in decreased survival in *Exo1*^{null} mice but has not effect on *Exo1*^{EK} mice (Schaetzlein et al. 2013).

However, many studies show that EXO1 is controlled by its interaction with MMR protein complexes and that for fully functional MMR, both nuclease and structural roles of EXO1 are important (Dherin et al. 2009; Genschel & Modrich 2003). Two independent studies showed that the mutation of E109K, which was used to create nuclease deficient *Exo1*^{EK} mouse, was actually nuclease-proficient. E109K was demonstrated to be located far from the hydrolytic center and the phenotypes that were seen earlier in *Exo1*^{EK} mice were attributed either to the presence of an N-terminal His tag in the Exo1 mutant construct, or due to the potential structural consequences of the E109K mutation. The EXO1 E109K protein was expressed in *E. coli* and reported to resemble the wild-type enzyme. Also, biochemical assays using the E109K mutant showed similar exonucleolytic activity than wild-type. Instead, another EXO1 mutant, D173A, was shown to be hydrolytically defective and MMR defective (Shao et al. 2014; Bregenhorn & Jiricny 2014).

5. Targeting the DNA damage response in cancer treatment

Many cancer treatments, including radiotherapy and some classes of chemotherapeutic agents, function by inducing DNA damage. These therapies, aimed at killing rapidly dividing cells, often result in toxicities in normal dividing tissues, particularly the gastrointestinal tract and immune system (Jackson & Bartek 2009). However, as cancer cells are heterogeneous and they adapt genetically for growth and survival advantages, they also become resistant to drugs, which is a primary cause of cancer treatment failure. Drug resistance can arise in various ways, for example by reducing drug uptake, mutating or regulating the expression of the specific drug target, modulation of the expression or the activity of drug-metabolizing enzymes, or bypassing the DNA damage caused by drug. To overcome resistance, current drug discovery and development is focused on the identification of novel compounds that act through different and/or complementary mechanisms, which can be combined with existing agents (Cheung-Ong et al. 2013). As cancer cells often have known specific abnormalities in the DDR, for example BRCA1 mutations, therapeutic strategies aimed at exploiting these known weaknesses have been developed (Hosoya & Miyagawa 2014).

DNA damaging drugs in cancer treatment

The first chemotherapy drugs, based on nitrogen mustard, were discovered in the 1940s after soldiers exposed to it were found to have depleted bone marrow and reduced lymph nodes (Cheung-Ong et al. 2013). Nitrogen mustards are alkylating agents, which attach an alkyl group to DNA, inducing a bulky lesion that normally cells repair by NER pathway. Platinum-based agents, such as cisplatin and carboplatin, also induce bulky DNA damage, and when two platinum adducts form close by on the same DNA strand, they form intrastrand crosslinks (Siddik 2003). Platinum compounds have been extremely effective in the treatment of solid tumors (Kelland 2007). A large class of agents that target

DNA metabolism have been identified, including DNA intercalating agents, topoisomerase poisons and antimetabolites. Treatment with these results in DNA adducts, strand breaks or collapsed DNA replication forks, as well as the generation of ROS that further damages DNA (Woods & Turchi 2013). Topoisomerase inhibitors, such as irinotecan and camptothecin (TOP1 inhibitor) and etoposide (TOP2 inhibitor), could be regarded as the first generation of "targeted" DDR inhibitors (Lord & Ashworth 2012).

Inhibitors of ATM, ATR and the MRE11 complex

As ATM, ATR and the MRE11 complex are the central players in the response to DNA damage, they are very attractive targets for the development of novel anticancer agents. Some older inhibitors of ATM, such as caffeine and the fungal steroid metabolite Wortmannin, lack specificity, also inhibiting other PIKK family kinases (Furgason & Bahassi 2013). The small molecule inhibitor KU55933 is the first specific inhibitor of ATM activity. Treatment with KU55933 sensitizes cancer cells to radiation and topoisomerase inhibitors (Hickson et al. 2004) and KU60019, the improved analog of KU55933 being developed by AstraZeneca, effectively radiosensitizes human glioma cells (Golding et al. 2012). CP466722, another specific ATM inhibitor, was shown to be sufficient to sensitize cells to IR in clonogenic survival assays, and suggests that therapeutic sensitization may only require ATM inhibition for short periods of time (Rainey et al. 2008).

Schisandrin B, isolated from the fruit of *Scisandra chinesis*, which is commonly used in traditional Chinese medicine, was identified as a moderately selective ATR inhibitor. In addition to decreasing ATR kinase activity *in vitro*, schisandrin B also inhibited ATM kinase activity, although only at much higher concentrations (Nishida et al. 2009). Two additional ATR inhibitors, NU6027, in breast and ovarian cancer cell lines, and VE821, in pancreatic cancer cell lines, were also shown to sensitize cells to a variety of DNA-damaging agents (Peasland et al. 2011; Prevo et al. 2012). In addition, ATR inhibition is proposed to be useful in malignancies carrying oncogenic mutations, since reduction of

ATR expression levels in oncogenic environments (such as p53 deficiency or Myc overexpression) results in increased cell toxicity, whereas the same reduction is tolerated in normal tissues (Schoppy et al. 2012).

In addition to ATM and ATR, the MRE11 complex has also been investigated as a therapeutic target. Mirin is an inhibitor of the MRE11 complex, which prevents activation of ATM without affecting ATM protein kinase activity and inhibits MRE11-associated exonuclease activity, thereby eliminating HDR pathway in cells (Dupré et al. 2008). Based on the structures of Mirin, new MRE11 inhibitors that specifically target exo- or endonuclease activities are even more promising to specifically target the DSB repair pathway (Shibata et al. 2014).

Inhibitors of CHK1 and CHK2

Activating cell cycle checkpoints is crucial in the DDR, thus checkpoints have also been widely investigated as a potential target for cancer therapy. Human cancers frequently have functional defects in the p53 tumor suppressor, which causes the loss of G1-S checkpoint control, making these cells rely more on the S and G2-M checkpoints. Thus, inhibiting CHK1 or CHK2 can selectively sensitize p53 deficient cancer cells to DNA damaging agents (Furgason & Bahassi 2013). The first CHK1/CHK2 inhibitor to enter clinical trials was UCN01 but it was not continued due to toxicities, likely due to off target effects (Syljuåsen et al. 2005). Some other inhibitors with improved specificities, such as AZD7762, also failed to show good response in clinical trials (Ma et al. 2011). The promising CHK1 inhibitor LY2603618, developed by Eli Lilly, is currently being tested in preclinical studies and is the first CHK1 inhibitor to be tested in patients (King et al. 2014).

Inhibition of DNA repair

While DDR signaling is clearly a viable target, other strategies have aimed at directly inhibiting repair. It has been shown that DNA-PK protein expression correlates with resistance to etoposide in human chronic lymphocytic leukemia samples (Furgason & Bahassi 2013), making it an attractive target to modulate

the resistance to cancer therapeutics. Specific inhibitors of DNA-PK, including NU7026 and NU7441, were found to induce extreme sensitivity to IR as well as variety of chemotherapeutic agents in preclinical studies. However, their clinical application is restricted because of their toxicity to normal cells (Davidson et al. 2013). Another DNA-PK inhibitor, KU0060648, has been reported to enhance sensitivity to TOP2 poisons such as etoposide and doxorubicin (Munck et al. 2012). In addition to DNA-PK, Ligase IV inhibitor, SCR7, has been developed. SCR7 was shown to interfere with DNA binding of Ligase IV, thereby inhibiting NHEJ and activating apoptosis. Moreover, it was preventing tumor progression in mouse models that were treated with DSB-inducing drugs (Srivastava et al. 2012).

PARP inhibitors and synthetic lethality

Germline mutations of BRCA1 and BRCA2 predispose to breast and ovarian cancers, and somatic loss-of-function mutations of these genes have been found in other cancer types. This knowledge has been used to treat BRCA1 and BRCA2 deficient tumors with PARP inhibitors, inducing selective tumor cytotoxicity. PARP inhibition generates unrepaired SSBs that are likely converted to DNA DSBs and collapsed replication forks, which are normally repaired by HDR. As this requires functional BRCA1 and BRCA2, they are not repaired in the BRCA1 and BRCA2 deficient tumor cells, selectively killing them while limiting toxicity in normal tissues (Lord & Ashworth 2008). This concept is termed synthetic lethality, meaning that the mutation of either gene alone is compatible with viability, but simultaneous mutation of both genes leads to increased toxicity (Figure 9) (Kaelin 2005). Clinical trials of the PARP inhibitor olaparib, acquired by AstraZeneca, has produced very impressive results in patients with BRCA1/2 mutated cancers with high response rates and mild side effects (Fong et al. 2009; Balmaña et al. 2011). Now there are several new series of PARP inhibitors being tested in clinical trials in BRCA mutation carriers, alone or in combination with other chemotherapeutic drugs. In addition, several new genetic modulators of PARP-inhibitor responses have been identified, such as ATM, ATR, MRE11 or NBS1 translocations. Moreover,

elevated PARP1 expression has been proposed to be predictive biomarker of PARP inhibitor response in lung cancer (Lord & Ashworth 2013).

Resistance to PARP inhibitors

Although PARP inhibition is a promising tool for cancer treatment, most tumors eventually escape from PARP inhibition. Studies with BRCA2 defective cells have shown an interesting and surprising mechanism for resistance through secondary mutation of BRCA2. Cells from BRCA2 mutation carriers resistant to cisplatin and PARP inhibitors either restore the wild type BRCA2 allele, or acquire a new, functional, non-wild type isoform (Figure 9). This corrects the defect in homologous recombination, leading to a loss of PARP inhibitor sensitivity (Edwards et al. 2008). Mechanism for BRCA1 resistance involves downregulating 53BP1, which is a target of the ATM kinase and an important factor for DSB repair pathway choice. Whereas 53BP1 inhibits resection at G1, BRCA1 was shown to promote the removal of 53BP1 is S-phase to allow resection (Bunting et al. 2010). The loss of 53BP1 in BRCA1 mutant cells restores resection and HDR repair (Bunting et al. 2012). Moreover, the analysis of tumors from *Brca1* deficient mice that were resistant to PARP inhibition revealed partial loss of 53BP1 expression (Jaspers et al. 2013). Alternating PARP protein expression is another mechanism for resistance, a hypothesis that has not yet been validated clinically (Lord & Ashworth 2013). Therefore, studying the detailed mechanisms for resistance is essential to design effective therapies.

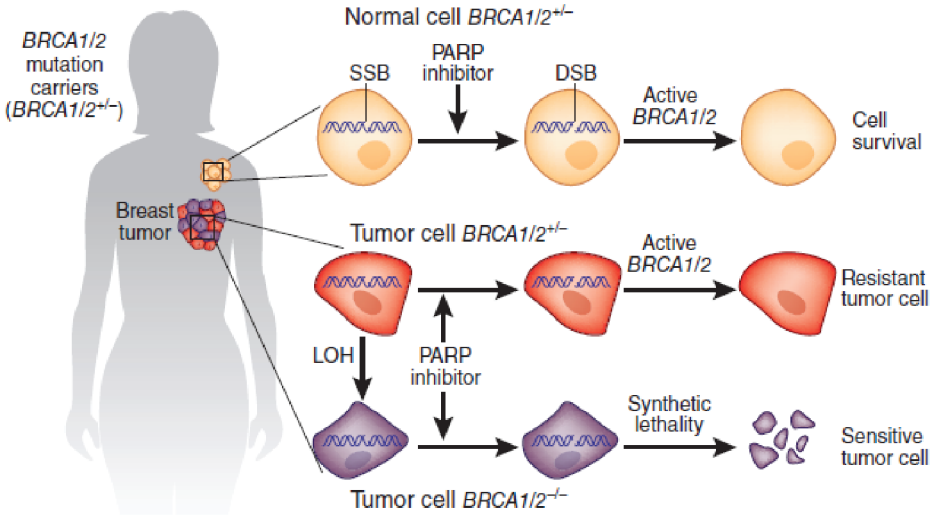

Figure 9. Synthetic lethality in BRCA1 and BRCA2 mutation carriers. PARP inhibitors block the repair of SSB, which will be converted to a DSB. DSB repair by HDR needs at least one copy of functional BRCA1/2. Tumor cells that have lost the functional copy of BRCA1/2 by loss of heterozygosity (LOH) cannot correctly repair the DSBs, leading to tumor cell death. Resistance can arise in tumor cells that have restored the wild-type copy of BRCA1/2 or acquired other compensatory mutations such as deletion of 53BP1. Figure from (Polyak & Garber 2011)

Hypothesis

We hypothesize that EXO1 activity can compensate the defective MRE11 complex in mammalian development, cellular responses to DNA damage and replication fork progression.

Objectives

1. Examine the genetic interaction between hypomorphic *Nbs1* and *Exo1* null allele in mice.
2. Characterize the relative influence of NBS1 and EXO1 on cell growth, chromosomal stability and DNA replication fork progression.
3. Determine whether EXO1 can modify the checkpoint signaling defects of NBS1 hypomorphic cells.
4. Assess the influence of EXO1 deletion in NBS1 hypomorphic cells on DNA damage sensitivity.
5. Examine the role of EXO1 in MRE11 complex mutants in alternative model systems.

MATERIALS AND METHODS

Mouse genotyping

The generation of *Nbs1*$^{\Delta B}$ and *Exo1*$^{-}$ mice was previously described (Wei et al. 2003; Schaetzlein et al. 2013; Williams et al. 2002). Genomic DNA was isolated from the mouse tails using proteinase K in lysis buffer (0.1M Tris-HCl, 200mM NaCl, 0.2% SDS and 5mM EDTA). For genotyping, PCR primers designed for wild-type or gene-trap alleles were used. Forward primer sequences are provided in Table 1 and PCR reaction conditions in Table 2.

Allele	**Primer name**	**DNA sequence (5'-3')**	**PCR product and program**
Nbs1$^{\Delta B}$	mp95.a7	TCCAGTTGTTTGCGGTAAGTCCTC	s3-a7 WT (440 bp) s3-N mut (310 bp) PCR program 1
Nbs1$^{\Delta B}$	mp95.s3	GATAGAGTTACCTTTGGGGTGTTT	
Nbs1$^{\Delta B}$	p95.N	TTTGCCAAGTTCTAATTCCATCAG	
Exo1^{-}	Exo1.A	CTCTTGTCTGGGCTGATATGC	A-B WT (262 bp) B-C mut (300 bp) PCR program 2
Exo1^{-}	Exo1.B	ATGGCGTGCGTGATGTTGATA	
Exo1^{-}	Exo1.C	AGGAGTAGAAGTGGCGCGAAGG	

Table 1. Primer sequences used for mouse genotyping.

Program 1			**Program 2**		
Cycles	Temperature	Time	Cycles	Temperature	Time
1	95^{o}C	3 min	1	95^{o}C	3 min
35	95^{o}C	1 min	35	95^{o}C	1 min
	60^{o}C	1 min		58^{o}C	1 min
	72^{o}C	1 min		72^{o}C	1 min 45 sec
1	72^{o}C	7 min	1	72^{o}C	7 min
1	14^{o}C	hold	1	14^{o}C	hold

Table 2. PCR reaction conditions used for mouse genotyping.

Mouse embryonic fibroblast preparation

Mouse embryonic fibroblasts (*MEFs*) *were isolated* from E14 embryos. The embryos were separated from the uterine wall and amniotic sac and placed in Petri dishes containing PBS. The head and soft tissues were removed from the embryos and the embryonic tissue was placed for overnight in 5ml 0.25% trypsin/EDTA at 4^{o}C. Upon plating, the tissue was further digested in trypsin at 37^{o}C for 20 minutes, minced, and seeded on 3 x 10cm plates. Primary MEFs were transformed by the transfection (MEF2 reagent Amaxa Nucleofector; Lonza) of a linearized, origin-less plasmid containing the simian virus 40 genome.

Cell cultures

All transformed cells were cultured in Dulbecco's modified Eagle medium (DMEM, *Gibco*) supplemented with 10% fetal bovine serum (FBS, Sigma-Aldrich) and 100u/ml penicillin-streptomycin (*Gibco*). Primary cell medium was supplemented with 15% FBS (HyClone), 2mM Glutamax (*Gibco)* and 100u/ml penicillin/streptomycin.

3T3 proliferation assay

Primary MEFs were seeded in every three days at the density of 3 x 10^5 cells per 6-cm plate. Total number of cells was counted at each passage and cumulative cell numbers were plotted.

Senescence-associated (SA) B-galactosidase staining

Primary MEFs were seeded at the density of 70,000 cells per 3.5-cm plate. Senescent cells were stained using the Senescence β-Galactosidase Staining Kit (Cell Signalling). Five representative images were taken from diverse areas of the plate, using Nikon *TE200* inverted microscope with *phase contrast* illumination. Images were analyzed using Fiji software to quantify the number of β-Galactosidase positive cells.

Cell cycle analysis

Transformed MEFs were seeded at the density 2.5 x 10^5 cells per 6-cm plate. Cells were mock treated or damaged with CPT, following trypsinization and overnight fixation in 70% ethanol. Cells were resuspended in 300µl PBS containing 25µg/ml propidium iodide (PI) and 0.1mg/ml RNaseA. The cell cycle based on PI content was determined by flow cytometry and analyzed with FlowJo software.

Cell death analysis

Transformed MEFs were seeded at the density 2.5 x 10^5 cells per 6-cm plate. Cells were mock treated or damaged with CPT. Cells were trypsinized resuspended in 300µl PBS containing 25µg/ml propidium iodide (PI) and 0.1mg/ml RNaseA. The dead cells based on PI incorporation was determined by flow cytometry and analyzed with FlowJo software.

BrdU labeling for G1/S checkpoint assay

Primary or transformed MEFs were seeded at the density 10^6 cells per 10-cm plate. S-phase cells were stained using the BD Pharmingen FITC BrdU Flow Kit (BD Biosciences). The percentage of BrdU positive cells were determined by flow cytometry and analyzed with FlowJo software.

G2-M checkpoint assay

Primary or transformed MEFs were seeded at the density 2.5 x 10^5 cells per 6-cm plate. Cells were mock treated or damaged with IR. Cells were trypsinized and fixed overnight in 70% ethanol 1h after the IR treatment. Cells were washed with dilution buffer (PBS, 1% FBS, 0.1% Triton X-100) and incubated 1h at room temperature in anti-Histone H3 Phospho (Ser10) antibody (1:200 in blocking solution, Merck Millipore). Cells were washed and incubated with FITC-conjugated goat anti-rabbit IgG (1:200 in blocking solution, Jackson ImmunoResearch). Cells were resuspended in 300µl PBS containing 25µg/ml propidium iodide (PI) and 0.1mg/ml RNaseA. The percentage of FITC positive cells were determined by flow cytometry and

analyzed with FlowJo software. A mitotic ratio (% mitotic cells mock or IR treatment) is presented.

γ-H2AX staining

The assay was performed using the same protocol as for G2/M assay. Cells were mock treated or damaged with CPT. The used antibody was γ-H2AX (1:200, Millipore 05-636) following by FITC conjugated goat anti-mouse IgG (1:200, Life Technologies). The γ-H2AX intensity was determined by flow cytometry and the mean intensity change of γ-H2AX staining compared to untreated cells was analyzed with FlowJo software.

Metaphase spreads

Cells were seeded at the density of 10^6 cells per 10-cm plate. For arresting the mitotic cells, colcemid was added to a final concentration of 0.1μg/ml for 30 min (transformed MEFs) or 2 hours (primary MEFs). To harvest cells, media was removed and cells were washed with PBS, treated with trypsin and then pelleted. Cells were hypotonically swollen in 75mM KCl at 37^{o}C for 20 minutes, following the fixation in ice-cold acetic acid:methanol (1:3) overnight at 4^{o}C. For obtaining the metaphase spreads, cells were resuspended in 50-300μl of fixative, 50μl was spread on glass slide steam treated using an 80°C water bath for 3-5 seconds and heat dried. Slides were stained with 5% Giemsa (Sigma-Aldrich) and mounted with DPX mounting medium (Panreac). Metaphases were examined and images were taken using Leica DM6000 microscope with *transmitted light* illumination. Images were analyzed using Fiji software to quantify the number of metaphases.

DNA fibre assay

Transformed MEFs were seeded at the density of 2 x 10^5 cells per 6-cm plate. Cells were pulse-labeled with 25μM 5-Chloro-2′-deoxyuridine (CldU, Sigma-Aldrich) followed by 250μM 5-Iodo-2′-deoxyuridine (IdU, Sigma-Aldrich). For replication restart, cells were treated with 1mM hydroxyurea (HU, Sigma-Aldrich) for 15min after CldU labeling, followed by 40min IdU labeling. Labeled cells were harvested by trypsinization and resuspended in ice-cold PBS at 10^6

cells/ml. For spreading, 2µl of cell suspension was dropped on the top of the microscope slide (Superfrost, Fisher Scientific), dried for 6min, 7µl of spreading buffer (200mM Tris-HCl pH 7.4, 50mM EDTA, 0.5% SDS) was added to each drop, mixed by stirring with the pipette tip, followed by 2min of incubation. Chromatin was spread by tilting the slides (20-30^{o}) and they were air-dried and fixed in acetic acid:methanol (1:3) for 10min. For DNA denaturation, slides were washed 2 times with H_2O for 5min, once with 2.5M HCl, denatured with 2.5M HCl for 1h, and rinsed 2 times with PBS. For immunodetection, slides were blocked for 1h in blocking solution (PBS, 1% BSA, 0.1% Tween20) and incubated over-night at 4^{o}C with a mix of rat anti-BrdU monoclonal antibody (1:500 in blocking solution, AbD Serotec) that recognizes CldU, and mouse anti-BrdU monoclonal antibody (1:500 in blocking solution, Becton Dickinson) that recognizes IdU. Slides were washed 3 times with PBS and fixed with 4% formaldehyde for 10 minutes, following by 3 times washing with PBS and 3 times with blocking solution. The slides were then incubated at 37^{o}C for 2h with a mix of an AlexaFluor 555-conjugated goat anti-rat IgG (1:500 in blocking solution, Life Techologies) and an AlexaFluor 488-conjugated goat anti-mouse IgG (1:500 in blocking solution, Life Techologies). Slides were washed 5 times with PBS, dried, and mounted with Vectashield mounting medium (Vector Laboratories). Fibers were examined with Leica TCS SPE confocal microscope using 63x objective. The lengths of CldU-labeled (red) and IdU-labeled (green) patches were measured using the Fiji software, and micrometer values were converted into kilobytes using the conversion factor 1mm = 2.59kb (Jackson & Pombo 1998).

Clonogenic survival assay

Cells were seeded on 6-cm plates in duplicates either after the treatment (IR) or before the treatment (UVC, CPT, MMC, Cisplatin). The number of the seeded cells were adjusted according to the plating efficiency of the cell line and the cytotoxicity of the treatment. The cells were incubated at 5% CO_2 at 37^{o}C for 12 days, the colonies were stained with crystal violet (Sigma-Aldrich) and counted manually. Results were normalized for plating efficiencies.

DNA damaging agents and drug treatments

IR exposure was performed using the YXLON Smart 200 irradiator with 200kV X-rays at 4.5mA with the dose rate of 0.025Gy/s. UVC irradiation with the dose of 15-25 J/m^2 was performed using UVC crosslinking oven (Stratalinker, Stratagene). CPT (Sigma-Aldrich) was used at final concentration of 5-10μM for 1h or 40-120nM for 24h. MMC (Sigma-Aldrich) was used at 1-2μg/ml for 2h. Cisplatin (Ferrer Farma) was used at 5-15μM for 2h.

Analysis of single strand annealing

The hprtSA-GFP (Bennardo et al. 2009) reporter plasmid was linearized by Sac1/Kpn1, and 10 μg was electroporated into 1-2.5x10^6 MEFs (0.8ml total volume, 780V, 10μF) per electroporation. Following selection in puromycin (1.5 μg/ml), the puro-resistant clones were pooled and expanded. For the reporter assay, 0.4x10^5 cells were seeded onto 24 well dishes one day prior to transfection with 0.4 μg of the I-SceI expression vector (pCBASce) or the GFP expression vector (pCAGGS-GFP), along with 0.2 μg of empty vector (pCAGGS-BSKX) or Nbs1 expression vector (pCAGGS-Nbs1). All plasmids were previously described (Bennardo et al. 2009). Transfections were performed with 1.8 μl Lipofectamine 2000 transfection %GFP+ cells were examined using a CyAN ADP flow cytometer (Dako). Repair frequencies were normalized to transfection by dividing the GFP frequencies from the I-SceI transfections by those of a parallel GFP transfection. Repair frequencies reflect the mean of at least 6 independent transfections, and the error bars are the SD. To examine Nbs1 expression, cells were extracted 2 days after transfection using NETN (20 mM Tris, pH 8, 100 mM NaCl, 1 mM EDTA, 0.5% IGEPAL, 1.25 mM DTT, and Roche Protease Inhibitor Mixture) using several freeze/thaw cycles. Blots of these extracts were probed with antibodies against buffer and several freeze thaw cycles, and were probed with Nbs1 (Bethyl A301-284A) and Actin (Sigma A2066) antibodies.

RNA isolation and real-time PCR

Total RNA was isolated using Trizol (Life Technologies) reagent followed by chloroform extraction. RNA was precipitated with isopropanol, washed with 70% ethanol and dissolved in DEPC-treated water. RNA was quantified using Nanodrop. cDNA was prepared using High Capacity cDNA Reverse Transcription Kit (Applied Biosystems), using 2µg of RNA. mRNA levels were detected by quantitative real-time PCR with TaqMan Gene Expression Assay (Applied Biosystems). GAPDH was used as an endogenous control. The following TaqMan probes were used: *Exo1* Mm00516302_m1; *Gapdh* Mm99999915_g1; *EXO1* Hs00243513_m1; *GAPDH* Hs02758991_g1**.** MUS81 and FBH1 amplification was performed using SYBR Green Expression Assay using GAPDH as an endogenous control. Primer sequences are provided in Table 3.

Gene	**DNA sequence (5'-3')**
GAPDH	Sense: GCACAGTCAAGGCCGAGAAT Antisense: GCCTTCTCCATGGTGGTGAA
MUS81	Sense: TCCCTTCTTTCCAGATGGTG Antisense: ACTCCAGCACTTCGGAGACA
FBH1	Sense: GCTGAGTCACAGCCAAATGA Antisense: GGAAAGGCTGAATGTCCG

Table 3. Primer sequences used for MUS81 and FBH1 amplification.

Total protein isolation and Western Blotting

Cells were lysed with TNG-150 lysis buffer containing 50mM Tris-HCl, 150mM NaCl, 1% Tween 20, 0.5% NP-40, 1x Phosphatase Inhibitor Cocktail 2 (Sigma-Aldrich) and 1x Protease Inhibitor Cocktail (Roche). Protein concentration was quantified with DC Protein Assay Kit (Bio-Rad). 30-80µg of total protein was separated by SDS-PAGE (8-12% gels) or *NuPAGE* Novex *Tris-Acetate* SDS (3-8% gels, Life Technologies) followed by transfer to Immobilon-P PVDF membrane (Merck-Millipore). For blocking solution, 5%

milk in PBST was used, membranes were incubated in primary antibody at 4^{o}C overnight and in secondary antibody for 1h at room temperature. ECL reagent (Amersham) with X-ray film (Fujifilm) were used to detect the signal. The used antibodies are provided in Table 4.

Primary antibody	**Source**	**Dilution**
ATM	Sigma-Aldrich A1106	1:3000
P-ATM (Ser1981)	Cell Signalling 4526	1:3000
CHK1	Santa Cruz sc7898	1:500
P-CHK1 (Ser345)	Cell Signalling 2341	1:1000
CHK2	Merck-Millipore 05-649	1:500
RPA	Merck-Millipore NA19L	1:1000
P-RPA (S4/S8)	Bethyl A300-245A	1:2000
CtIP	Santa Cruz sc271339	1:500
NBS1	Novus NB100-143	1:1000
EXO1 (human)	Thermo Scientific MS1534-P1	1:1000
EXO1 (mouse)	Bethyl A302-640A	1:5000
α-Tubulin	Sigma-Aldrich T5168	1:8000
Secondary antibody	**Source**	**Dilution**
Goat anti-Mouse IgG HRP	Thermo Scientific Pierce	1:30000
Goat anti-Rabbit IgG HRP	Thermo Scientific Pierce	1:30000

Table 4. Antibodies used for Western Blotting.

Immunofluorescence

Cells were seeded on 8-well dish with the density of 15,000 cells/well. Cells with fixed in 4% formaldehyde for 10 min in room temperature, followed by permeabilization with PBS + 0.2% Triton X-100 for 10 minutes at room temperature. Cells were blocked for 20 min in PBS + 2% FBS. Cells were

incubated with primary antibodies in PBS + 2% FBS + 0.25% Tween-20 for 1h. Cells were incubated with secondary antibodies and DAPI for 1h, mounted in Vectashield mounting media and analyzed with Leica DM6000 microscope. The used antibodies are provided in Table 5.

Primary antibody	**Source**	**Dilution**
γ-H2AX	Millipore 05-636	1:500
53BP1	Novus 100-304	1:500
ER	Santa Cruz sc543	1:100
Secondary antibody	**Source**	**Dilution**
Alexa Fluor 488 Goat anti-*Mouse* IgG	Life Technologies	1:500
Alexa Fluor 594 Goat anti-*Mouse* IgG	Life Technologies	1:500
Alexa Fluor 488 Goat anti-*Rabbit* IgG	Life Technologies	1:500
Alexa Fluor 594 Goat anti-*Rabbit* IgG	Life Technologies	1:500

Table 5. Antibodies used for immunofluorescence.

Generation of lenti- or retroviral-construct expressing cell lines

For production of lenti- or retrovirus, HEK293T cells were transfected with the vector of interest and with lentiviral packaging vectors (REV, RRE and VSV-G) or with retroviral packaging vectors (VSV-G and Gag-Pol) using PEI (1mg/ml) and NaCl (150mM). Viral supernatants were harvested 48 and 72 hours post transfection, filtered (0.45um) and placed directly on transformed MEFs. Cells containing the constructs were selected with 5 μg/ml of puromycin (Calbiochem) or 400 μg/ml of hygromycin (Invitrogen) for 1 week.

siRNA-mediated knockdown of proteins

Small interfering (si)RNAs were designed using siRNA Selection Program (Whitehead Institute for Biomedical Research) and manufactured by Invitrogen. Transformed MEFs were transfected using Lipofectamine

RNAiMAX (Invitrogen) for 2 times within a 24-hour interval. All experiments were done 48h after the first transfection. Mock transfections targeting GFP were used as a control. The sequences of the forward siRNAs are provided in Table 6.

Gene	RNA sequence (5'-3')
Exo1	CCGAUAUCGUGAAGGUUAU [dT][dT]
GFP	GGCUACGUCCAGGAGCGCCGCACC [dT][dT]
Fbh1	GGGAUGGCGUUACUAAGAA [dT][dT]
Mus81	GUGAAGCGAACCAUGGAUA [dT][dT]

Table 6. Sequences of siRNAs for EXO1, FBH1 and MUS81.

shRNA-mediated knockdown of proteins

Short hairpin (sh)RNAs were used form Sigma MISSION lentiviral library: EXO1 (NM_130398) and sh nontargeter (shNT, SHC016) and lentiviral-expressing stable cell lines were generated.

Plasmids used in the study

Human cDNA of EXO1 was amplified with PCR using primers with appropriate restriction sites and cloned into pENTR/D-TOPO vector (Life Technologies). EXO1 was then subcloned using the LR clonase reaction (Life Technologies) into the pDEST53 vector (Life Technologies), into retroviral pLPC backbone containing a C-terminal fusion of the Strep-tag II and the FLAG-tag (Gloeckner et al. 2009) or lentiviral pTRIPz backbone for doxycycline-inducible expression (Campbell et al. 2011). For EXO1-pTRIPz expression, doxycycline (Sigma) was used at the concentration of 1 µg/ml.

In order to obtain EXO1-pBabe constructs, vectors and DNA inserts were digested with appropriate restriction enzymes (Biolabs) and separated by electrophoresis. DNA bands were excised from the gel and purified with PureLink Quick Gel Extraction Kit (Life Technologies). Fragments were

quantified using NanoDrop, and ligated using 1U of T4 DNA Ligase (Biolabs) at 16°C 24 hours. Ligated product was transformed into competent DH5α cells. Severel transformed clones were selected for plasmid purification in order to verify the presence DNA insert using appropriate restriction enzymes (Biolabs) and separated by electrophoresis. Positive clones were sequenced to verify the correct nucleotide sequence.

TopBP1-pMX-PIE retroviral inducible construct (Toledo et al. 2008) expression was induced by 4-OHT (Sigma) at the at the concentration of 1 μM.

CPT sensitivity with *S. cerevisiae*

The *S. cerevisiae* strains used in this assay were present in the laboratory collection of Dr. Lorraine Symington. For dilution spot assays, yeast cells grown in synthetic complete (SC) medium to logarithmic phase were initially diluted to 1×10^7 cells/ml. Subsequent tenfold dilutions were made and 5 μl were spotted onto medium containing different concentrations of CPT and incubated at 30°C for 3 days.

RESULTS

1. Deletion of EXO1 leads to embryonic lethality in mice expressing a hypomorphic allele of Nbs1

Previously characterized *Nbs1*$^{\Delta B/\Delta B}$ mice are viable, show normal longevity and are not predisposed to cancer (Williams et al. 2002). The *Nbs1*$^{\Delta B}$ mutation results in the production of a truncated NBS1 protein that is unstable and lacks the FHA and first BRCT domain in the N-terminus, but maintains interactions with the MRE11 and RAD50 proteins. At the cellular level, *Nbs1*$^{\Delta B/\Delta B}$ cells exhibit a mild defect in ATM signaling and the G2-M checkpoint, elevated chromosomal instability and sensitivity to DSB inducing agents, such as IR and CPT (Williams et al. 2002; Stracker et al. 2009). *Atm*$^{-/-}$ cells display similar defects, albeit all of them more severe than in *Nbs1*$^{\Delta B/\Delta B}$ cells (Barlow et al. 1996). As ATM is the central transducing kinase following DSB detection (Stracker & Petrini 2011) and *Nbs1*$^{\Delta B/\Delta B}$ cellular defects are intermediate to those observed in *Atm*$^{-/-}$ cells, we reasoned that some ATM dependent activities must exist in *Nbs1*$^{\Delta B/\Delta B}$ cells that could provide some compensatory functions when MRE11 complex functions are compromised. The main candidate for this activity was EXO1, as the current model of DSB resection proposes that EXO1 acts in tandem with MRE11 complex during the resection of DSBs (Garcia et al. 2011; Mimitou & Symington 2008; Zhu et al. 2008) and ATM has been shown to directly phosphorylate EXO1 (Bolderson et al. 2010). Moreover, deficiency of MRE11 complex members in yeast together with loss of EXO1 leads to severe synthetic phenotypes (Mimitou & Symington 2010; Nicolette et al. 2010; Nakai et al. 2011).

To determine if EXO1 modifies the cellular defects observed in *Nbs1*$^{\Delta B/\Delta B}$ cells, we established crosses between *Nbs1*$^{+/\Delta B}$ (Williams et al. 2002) and *Exo1*$^{+/-}$ (Wei et al. 2003; Schaetzlein et al. 2013) double heterozygous mice to generate *Nbs1*$^{\Delta B/\Delta B}$*Exo1*$^{-/-}$ double mutant mice. We observed that the single mutant mice were born at expected Mendelian ratios, but no viable double mutant mice were born, suggesting embryonic lethality (Figure 10A). Therefore, we examined the double mutant embryos at embryonic day 14.5 (E14.5). Expected Mendelian

ratios were observed at E14.5 (Figure 10B), but the double mutant embryos were runted and displayed developmental defects, such as malformation of the cranium and neural tube closure defects (Figure 10C). These results indicate that EXO1 is essential for mammalian development when MRE11 complex functions are compromised.

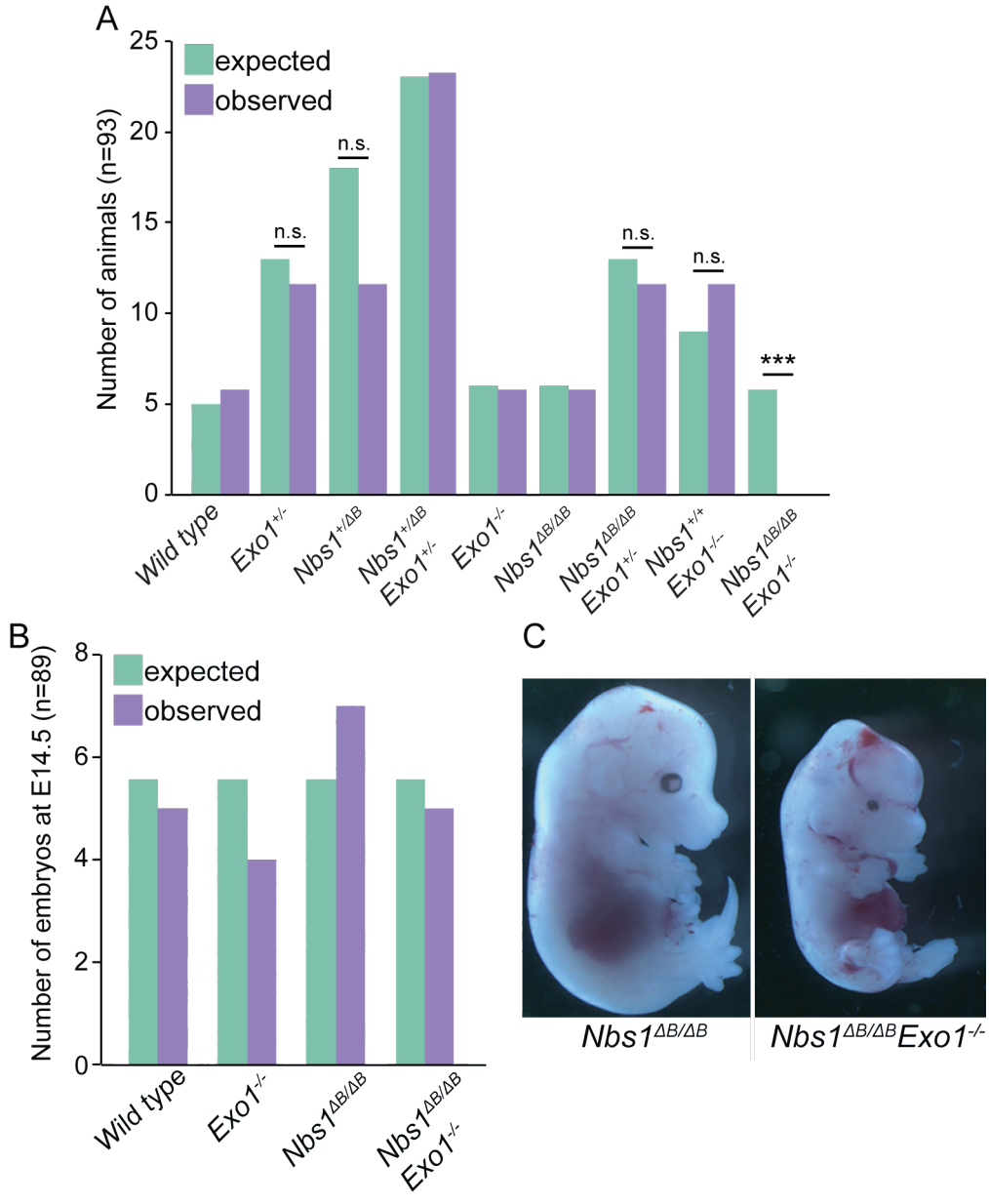

Figure 10. Embryonic defects resulting from NBS1 and EXO1 mutations. (A) Expected (based on normal Mendelian ratios) and observed genotypes from of a total 93 live born pups from *Nbs1*$^{+/\Delta B}$ and *Exo1*$^{+/-}$ crosses. Synthetic lethality was observed in *Nbs1*$^{\Delta B/\Delta B}$*Exo1*$^{-/-}$ mice. Statistical analysis was performed using an unpaired T-test. *** = p<0.0001, ns = nonsignificant. (B) Expected and observed genotypes from a total of 89 analyzed embryos from *Nbs1*$^{+/\Delta B}$ and *Exo1*$^{+/-}$ crosses. (C) Representative images of E14.5 embryos of the indicated phenotype.

2. EXO1 suppresses the chromosomal instability and promotes the replication fork progression in *Nbs1* mutants

We derived primary mouse embryonic fibroblasts (MEFs) from E14.5 embryos in order to understand better the mechanism by which EXO1 suppressed the defects of NBS1 mutants. Expected NBS1 and EXO1 protein expression was verified in single and double mutant MEF cell lines (Figure 11A). We next examined cell proliferation by following a modified 3T3 protocol that involves counting and plating the same number of MEFs every three days. Double mutant MEFs exhibited a strong growth defect (Figure 11B) compared to single mutant or wild type cells. We observed that many of the double mutant cells detached from the culture plate, indicating increased cell death.

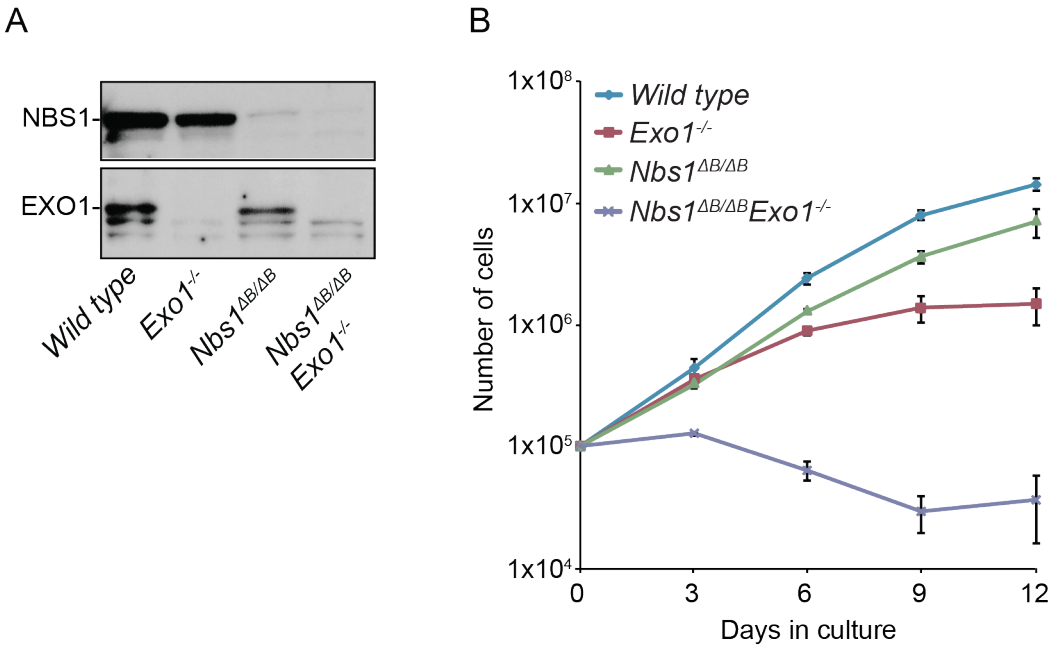

Figure 11. Cell growth defects in double mutant MEFs. (A) Western blotting of NBS1 and EXO1 levels in MEFs of the indicated phenotypes (B) 3T3 growth curve for primary MEFs of the indicated phenotypes. Number of cells represents the average of three plates counted at each time point. Error bars indicate standard deviation. Consistent data was obtained from three independent experiments.

In addition to increased cell death of the double mutant, we noticed the appearance large, flat cells, a morphology characteristic of senescence. Senescence-associated β galactosidase (SA-βgal) staining (Figure 12A) revealed that nearly 70% of the double mutant cells became senescent by passage 6, compared to very low percentage in single mutant cells (Figure 12B).

As the cells grew poorly, we also examined DNA synthesis by 5-bromo-2-deoxyuridine (BrdU) uptake. Cells were incubated with BrdU for 30 minutes and BrdU positive cells were detected with a FITC-conjugated anti-BrdU antibody and co-stained with propidium iodide (PI) to measure DNA content by flow cytometry (Figure 12C). Consistent with the growth defect, we observed a notable reduction in DNA synthesis in double mutant cells (Figure 12D). Taken together, these results indicate that EXO1 is crucial for the cell growth when MRE11 complex functions are impaired.

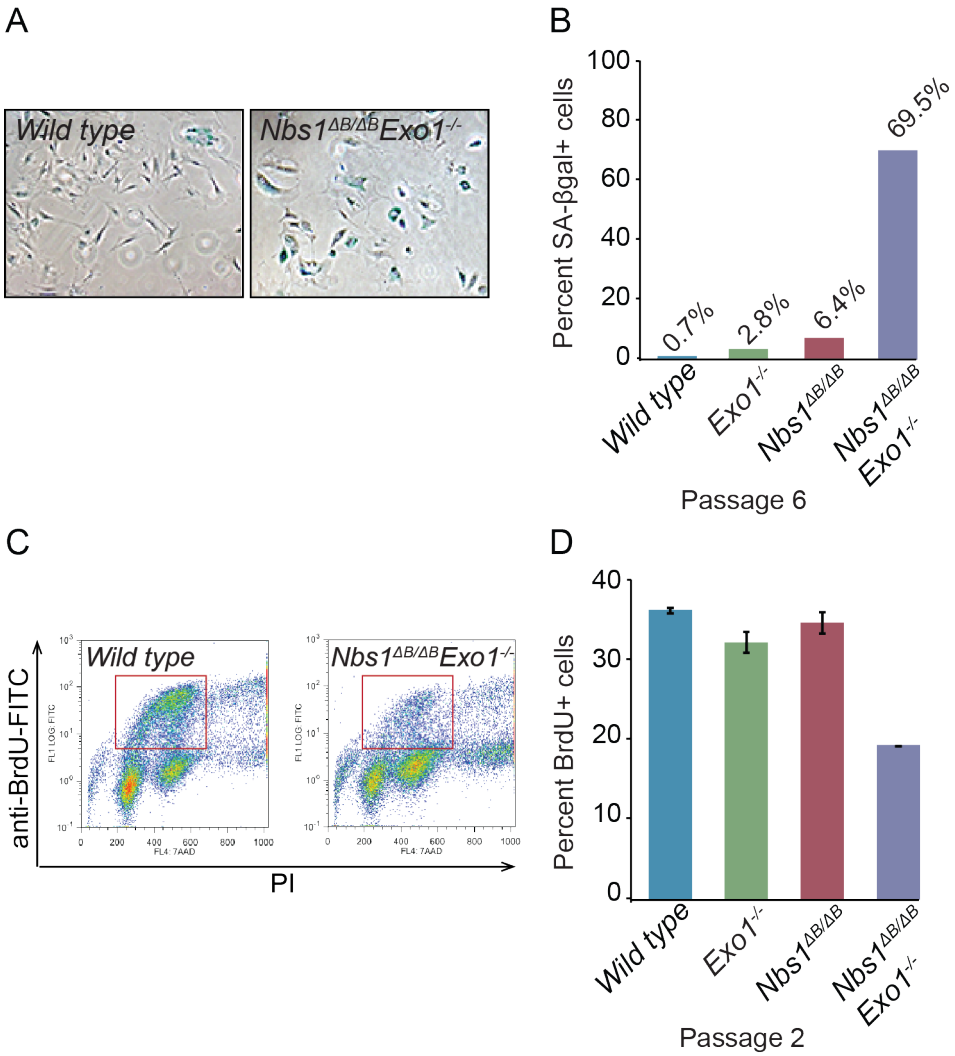

Figure 12. Increased cellular senescence and decreased DNA synthesis in double mutant cells. (A) Representative images of senescent cells determined by increased SA-βgal activity (blue) of wild type and double mutant cells. (B) Cellular senescence in MEFs at passage 6. Percentage of SA-βgal positive cells are indicated on top of the column of each phenotype. At least 200 cells were counted to determine the percentage of senescent cells. (C) Representative flow cytometry profiles of BrdU staining of wild type and double mutant cells. S-phase cells, determined by BrdU uptake are marked with the red square. (D) DNA synthesis in MEFs at passage 2 of the indicated phenotypes. Results from two independent experiments performed in duplicate are shown. Error bars indicate standard deviation.

In order to determine whether the cell growth defects and premature senescence were a result of increased chromosomal instability, we examined chromosomal aberrations in metaphase spreads. We scored four different types of aberrations that are visible by light microscopy: chromatid breaks, chromosome breaks, fusions and fragments (Figure 13A). The chromosomal

aberrations were highly elevated in double mutant cells (Figure 13B) with a high incidence of chromatid breaks (Figure 13C), suggesting that they arouse during S-phase.

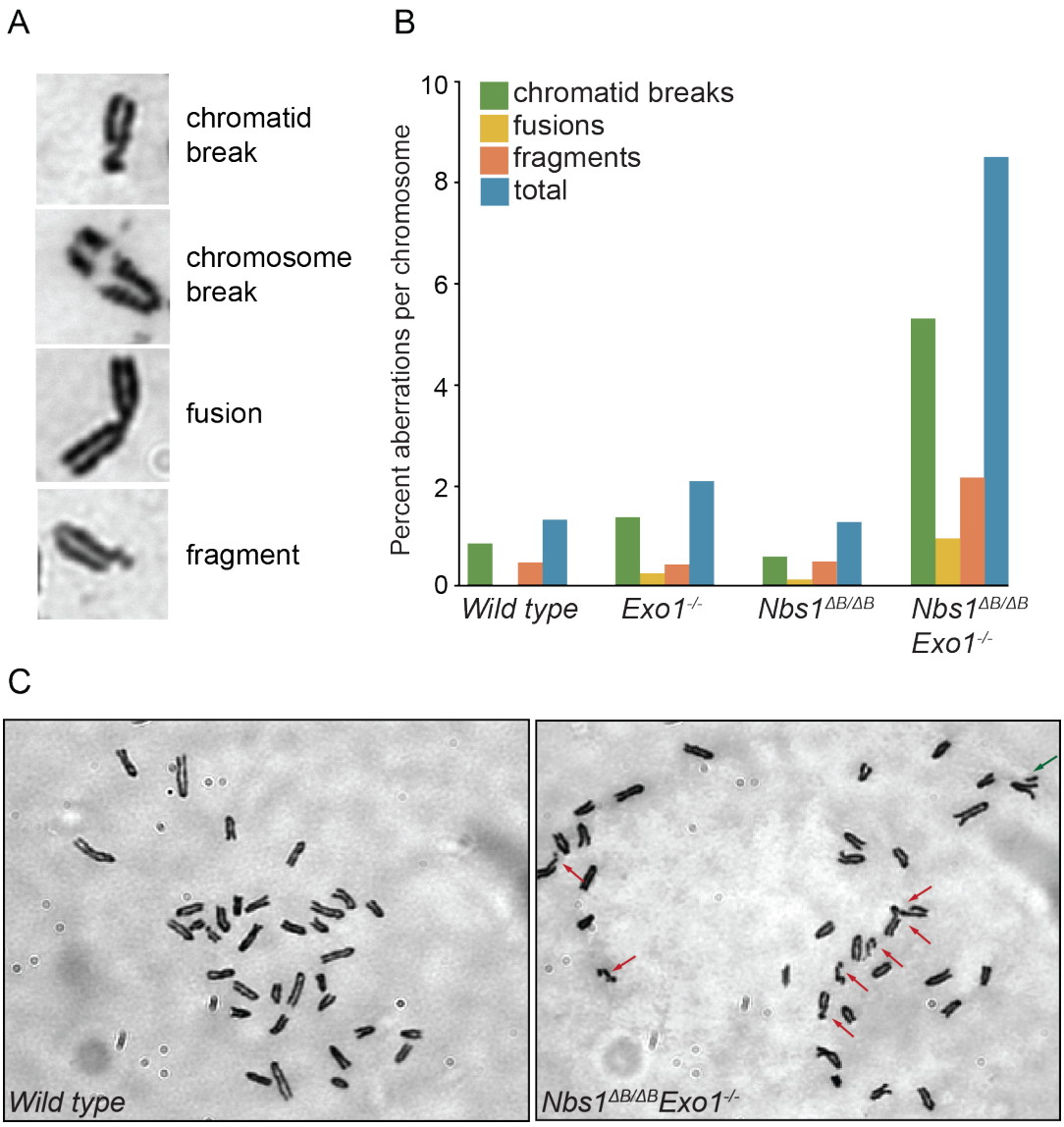

Figure 13. Chromosomal instability in primary MEFs. (A) Examples of the scored metaphase aberrations. (B) Metaphase aberrations in early passage primary MEFs of the indicated genotype were scored. (C) Representative images of chromosomes comparing wild type and double mutant cells. Chromatid breaks are indicated with red arrows and a fragment by green arrow.

Cells that have not accurately completed S-phase can enter mitosis, leading to abnormal sister chromatid segregation. The appearance of anaphase bridges, micronuclei and 53BP1 foci have all been linked to under-replicated DNA

entering mitosis (Mankouri et al. 2013). We analyzed these structures in passage 3 primary MEFs together with the appearance of foci positive for both γ-H2AX and 53BP1, which indicates the presence of DSBs. We observed a pronounced increase of anaphase bridges (Figure 14A) and micronuclei (Figure 14B) using 4',6-diamidino-2-phenylindole (DAPI) staining, together with an increase in colocalized 53BP1 and γ-H2AX (Figure 14C) in double mutant cells (Figure 14D). This indicates that the *Nbs1*$^{\Delta B/\Delta B}$*Exo1*$^{-/-}$ MEFs are progressing through S-phase with defects and enter mitosis with damaged DNA, suggesting defective cell-cycle checkpoints and replication stress.

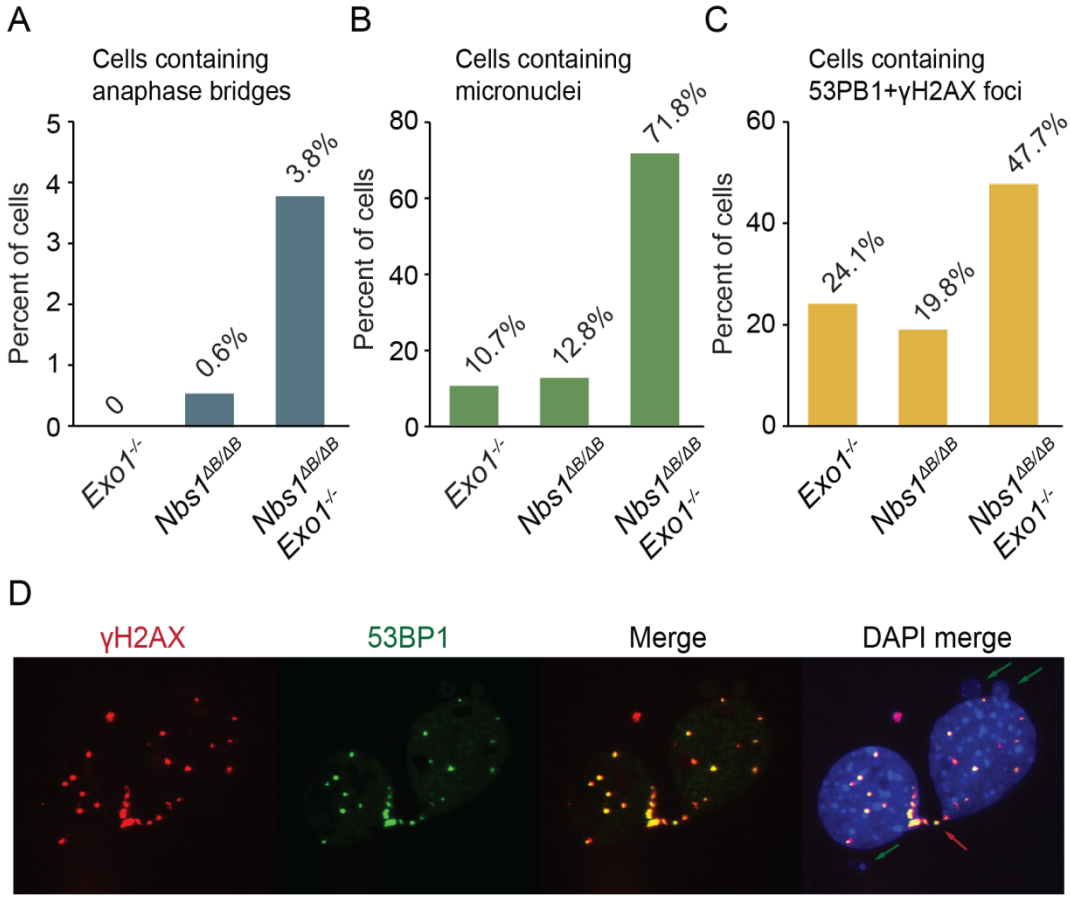

Figure 14. Unresolved mitotic DNA structures and accumulation of DSBs in primary MEFs. (A) Percentage of cells containing anaphase bridges. (B) Percentage of cells containing micronuclei. (C) Quantification of DSBs by 53BP1 and γ-H2AX foci colocalization. Results were plotted from passage 3 MEFs; at least 150 cells were scored. (D) Representative images of the double mutant cells. Merged photo is indicating 53BP1 and γ-H2AX foci colocalization, anaphase bridge (red arrow) and micronuclei (green arrows) are visible from DAPI merged photo.

As the strong growth defect of double mutant cells made their expansion and further experiments difficult, we immortalized single and double mutant cells by electroporation of a plasmid containing the simian virus 40 (SV40) genome without the origin of replication. SV40 achieves immortalization by associating with and inactivating the tumor suppressor genes *Tp53* and *Rb*, that would normally induce a state of replicative senescence in cells (Zhu et al. 1991). We monitored the growth of transformed MEFs and analyzed metaphase spreads to determine if the defects observed in primary cells persist when p53 is inactivated. We observed a similar phenotype as the transformed double mutant MEFs continued to display growth defects (Figure 15A) and increased chromosomal aberrations (Figure 15B).

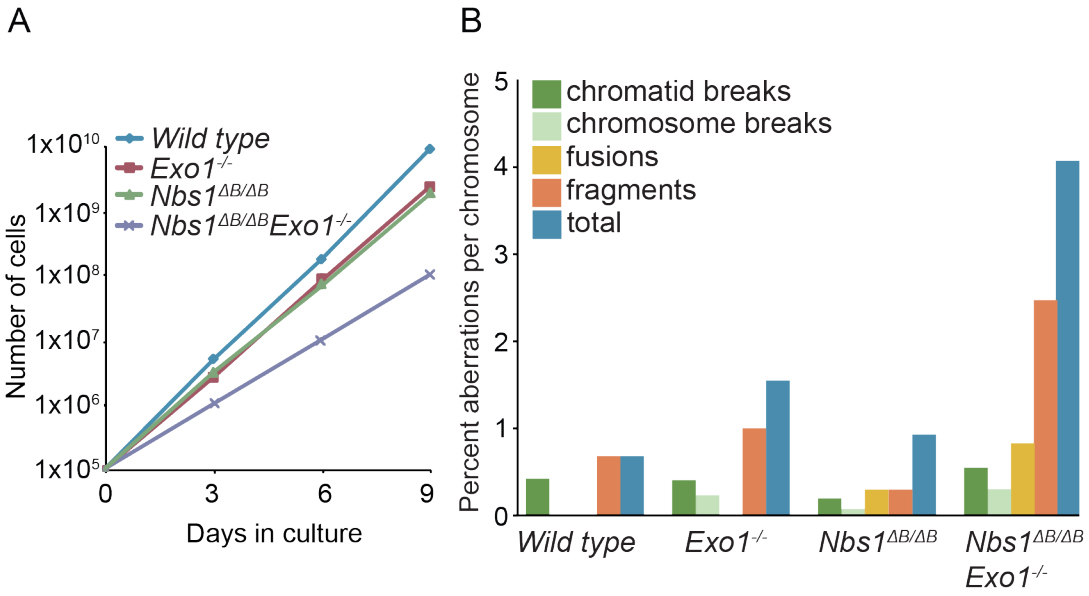

Figure 15. Cell growth and chromosomal instability in transformed MEFs. (A) 3T3 growth curve for transformed MEFs of the indicated phenotypes. The cell number represents the average of three plates counted at each time point. (B) Metaphase spread analysis of transformed MEFs of the indicated genotype.

The defects in cell growth and DNA synthesis suggested that replication fork progression is slower in the double mutant cells. To analyze replication fork progression, we performed DNA fibre analysis by incubating transformed MEFs with BrdU analogues 5-chloro-2′-deoxyuridine (CldU) and 5-iodo-2'-deoxyuridine (IdU). DNA was spread onto slides and visualized using antibodies

that specifically recognize CldU and IdU (Figure 16A). Replication tract lengths were measured and converted into kilo bases (kb) using the conversion factor 1 μm = 2.59 kb (Henry-Mowatt et al. 2003). We consistently observed shorter DNA fibres in double mutant cells (Figure 16A), indicating slower replication fork progression. Analysis of fibre lengths of all the genotypes revealed that the replication speed was similar in wild type and single mutant cells, but notably reduced in double mutant cells (Figure 16B). This data confirms that EXO1 promotes replication fork progression in the absence of fully functional MRE11 complex.

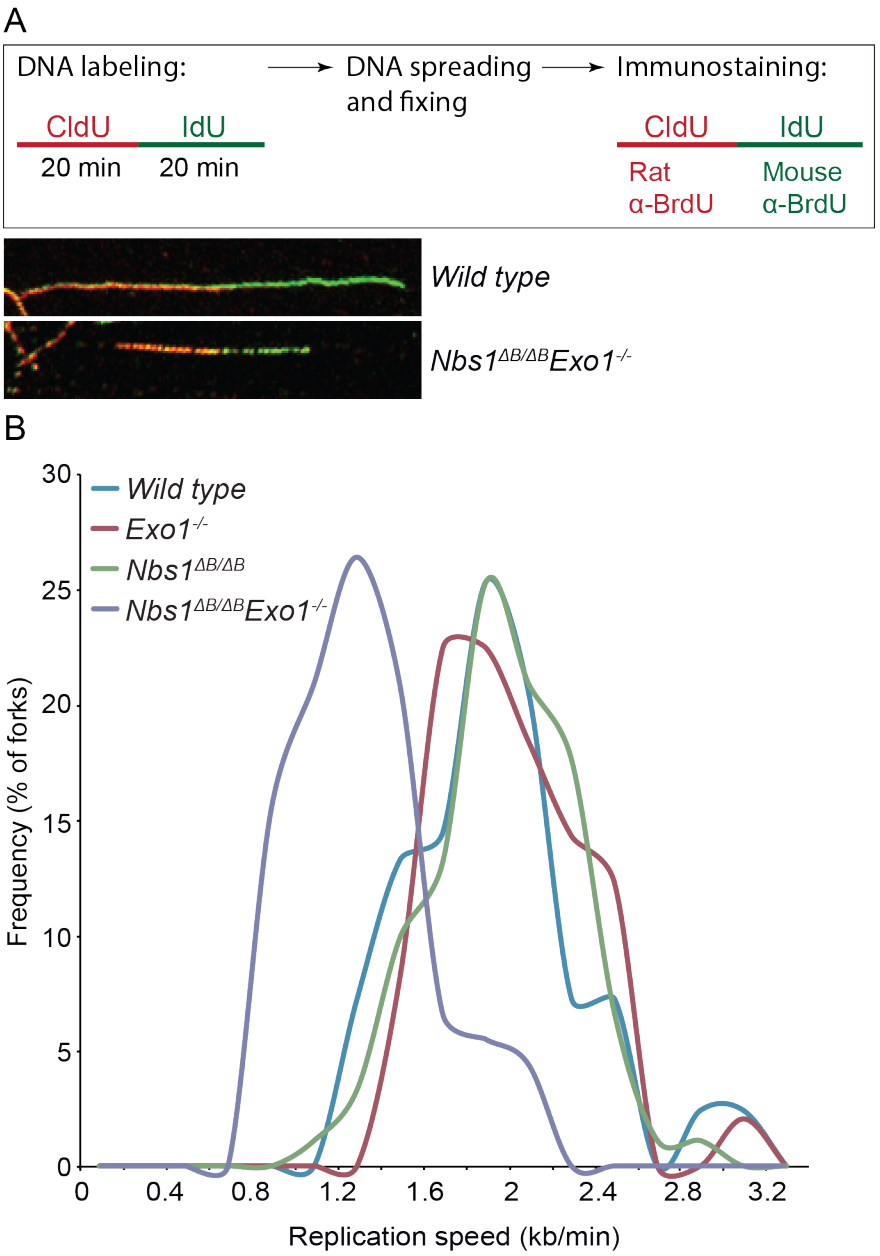

Figure 16. DNA fibre analysis of replication fork speed. (A) Schematic illustration of the fibre assay with representative images of the DNA fibres of the indicated phenotype. (B) Replication fork speed of the indicated genotypes. DNA fibres were distributed according to the frequency of the replication speed. At least 100 fibres were measured from each genotype.

3. EXO1 is required for ATM and ATR dependent checkpoint signaling and DNA repair in NBS1 mutant cells

The activation of the ATM kinase by the MRE11 complex is essential for G2-M checkpoint arrest (Stracker & Petrini 2011). In addition, the MRE11 complex promotes the resection of DNA ends that leads to ATR activation, which is also required for G2-M checkpoint arrest (Cimprich & Cortez 2008). Therefore, we asked whether the loss of EXO1 influenced the mild checkpoint defect that *Nbs1*$^{\Delta B/\Delta B}$ cells exhibit following IR treatment (Stracker et al. 2009; Williams et al. 2002). For the G2-M checkpoint assay we irradiated the cells and stained them with the phospho-specific histone 3 serine 10 (H3S10) antibody that is a well-established marker of mitotic cells. The population of mitotic cells was defined as cells positive for H3S10 that had 4N DNA content (G2 and mitotic cells), determined by PI staining using flow cytometry (Figure 17A). We observed the previously reported, mild checkpoint defect in *Nbs1*$^{\Delta B/\Delta B}$ cells and found that the loss of EXO1 alone did not influence the G2-M checkpoint (Figure 17B). Double mutant cells, however, displayed a strong checkpoint defect (Figure 17B) that was worse than that of *Nbs1*$^{\Delta B/\Delta B}$ and comparable to the checkpoint defect of ATM deficient cells.

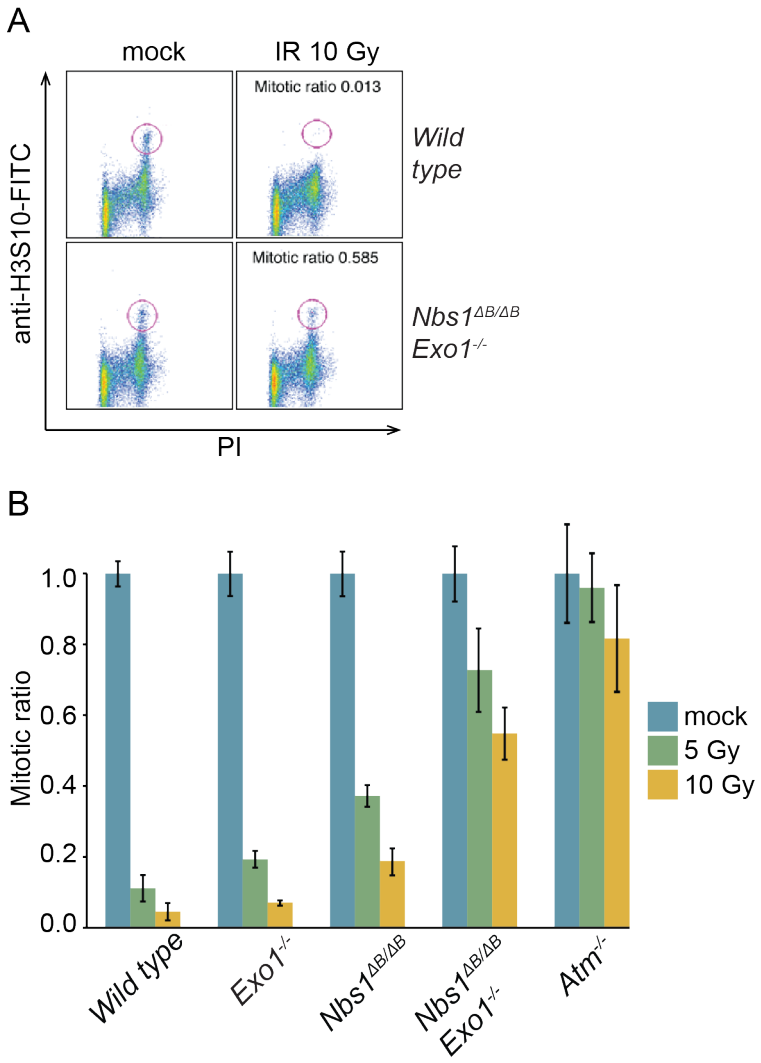

Figure 17. G2-M checkpoint in primary MEFs. (A) Example of the flow cytometry profile of wild type and double mutant cells before (mock) and after IR (10Gy). The gated mitotic cell population (4N DNA content and H3S10+) is marked with a circle. (B) The mitotic ratios of primary MEFs at 1h post-treatment. The mitotic ratio of irradiated cells is normalized to mock-treated cells. Results from 3 representative experiments performed in duplicate are shown. Error bars indicate standard deviation.

We confirmed the G2-M checkpoint results in transformed MEFs (Figure 18A) and in transformed double mutant cell lines derived from 3 different embryos (Figure 18B). Taken together, this data indicates that EXO1 activities are essential for G2-M checkpoint activation when MRE11 complex functions are compromised.

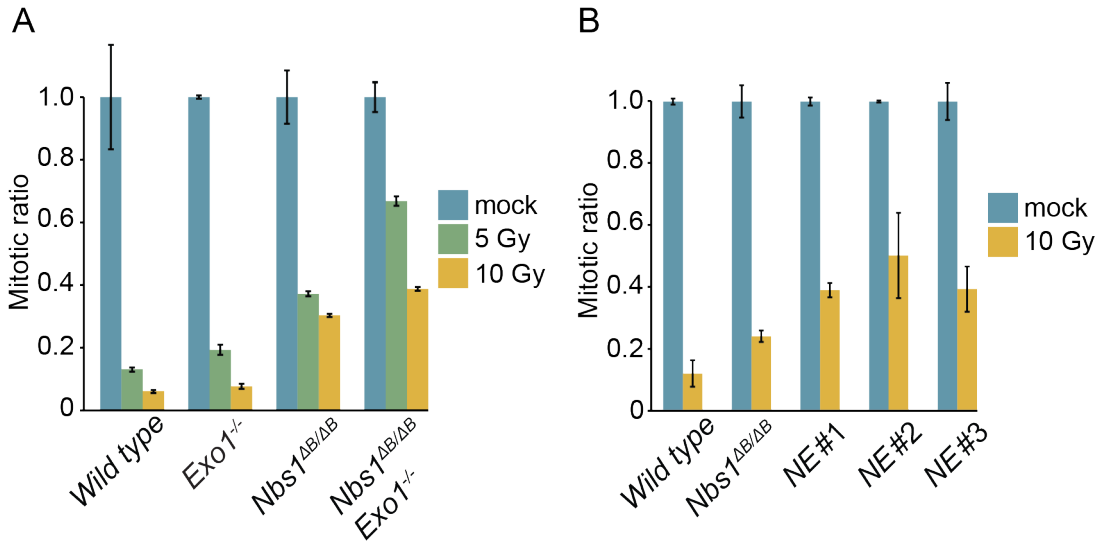

Figure 18. G2-M checkpoint in transformed MEFs. (A) The mitotic ratios of transformed MEFs at 1h post-treatment. (B) G2-M checkpoint comparing different *Nbs1*$^{\Delta B/\Delta B}$*Exo1*$^{-/-}$ *(NE)* cell lines. The mitotic ratio of irradiated cells is normalized to mock-treated cells. Error bars indicate standard deviation.

The defective G2-M checkpoint observed in double mutant cells suggests impaired resection, which is essential for both checkpoint activities and repair pathways that require the generation of ssDNA. To study whether the resection was affected by the loss of EXO1, we examined resection dependent DNA repair using an integrated reporter for SSA, a sub-pathway of homologous recombination that requires extensive resection. For this, we used a green fluorescent protein (GFP) reporter that contains two homologous fragments of the GFP expression cassette separated by a puromycin marker gene with a recognition site for I-SceI endonuclease in the 3' fragment. A DSB is induced with I-SceI, and SSA repair uses homologous sequence in the GFP fragments to restore GFP expression which causes a 2.7 kb deletion between the repeats (Bennardo et al. 2009). Therefore, cells positive for GFP require at least 2.7 kb of end resection to reveal the homologous sequence needed for SSA mediated repair (Figure 19A). The GFP reporter was integrated in transformed MEFs, I-SceI was expressed and the GFP positive cells were identified by flow cytometry, normalizing to parallel transfections with GFP expression vector. *Exo1*$^{-/-}$ cells did not show any reduction in SSA, whereas *Nbs1*$^{\Delta B/\Delta B}$ and *Nbs1*$^{\Delta B/\Delta B}$*Exo1*$^{-/-}$ cells showed a significant reduction compared with wild type

(2.3 fold and 5.6 fold, respectively) (Figure 19B). Cells lacking functional NBS1 (*Nbs1*$^{\Delta B/\Delta B}$ and *Nbs1*$^{\Delta B/\Delta B}$*Exo1*$^{-/-}$) were also complemented with wild-type NBS1 (Figure 19C). *NBS1* expression resulted in a similar increase in SSA in both *Nbs1*$^{\Delta B/\Delta B}$ and *Nbs1*$^{\Delta B/\Delta B}$*Exo1*$^{-/-}$ cells (2.2 fold) (Figure 19B). These results indicate that the loss of EXO1 alone does not cause a reduction in SSA, whereas the loss of functional NBS1 reduces the SSA capacity of the cell. This defect is further diminished by the loss of EXO1, as double mutants show an even stronger reduction in SSA. As SSA mediated repair requires 2.7 kb of resection, this result is consistent with a requirement for EXO1 in resection when MRE11 complex functions are impaired and may explain the observation that double mutant cells exhibit an increased G2-M checkpoint defect.

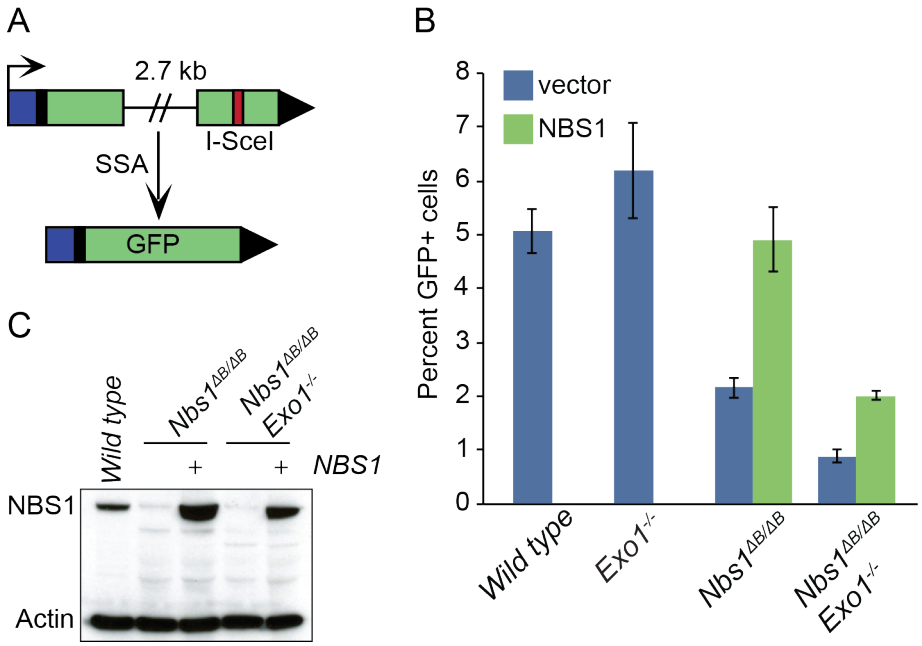

Figure 19. Single strand annealing assay in transformed MEFs. (A) Schematic illustration of the SSA assay. (B) SSA measured by the percentage of GFP positive cells, which is normalized to GFP transfection in parallel. Error bars indicate standard deviation. (C) Western blot of NBS1 from cells of the indicated phenotypes, "+" indicates samples complemented with NBS1.

To understand more clearly how EXO1 loss influenced the checkpoint and impaired resection in *Nbs1*$^{\Delta B/\Delta B}$, we examined key ATM and ATR dependent signaling events by Western blotting following IR and CPT treatment. While IR treatment generates SSBs and DSBs in all stages of the cell cycle, CPT inhibits

TOP1, thereby damaging the cells primarily in S-phase. Cells were either irradiated (10 Gy) or treated with CPT (1 μM) for 1 hour and the whole cell lysates were collected at 1 hour post-treatment.

We first examined the activation of ATM using a phospho-specific antibody against ATM S1987, one of the ATM autophosphorylation residues that promote ATM kinase activity (Lavin & Kozlov 2007; Bakkenist & Kastan 2003). We found that following both IR (Figure 20A) and CPT (Figure 20B) treatments, neither the *Nbs1*$^{\Delta B}$ mutation alone, as previously reported (Stracker et al. 2008), nor the loss of EXO1 affected ATM activation, as the levels of ATM S1987 phosphorylation were similar to that of wild type. However, in *Nbs1*$^{\Delta B/\Delta B}$*Exo1*$^{-/-}$ cultures, ATM activation was markedly reduced (Figure 20A and B).

Both CtIP and CHK2 participate in DNA end resection and checkpoint activation in S and G2 phases and have been reported to be hyperphosphorylated in an ATM dependent manner following DNA damage and depend on NBS1 as a mediator for phosphorylation (Wang et al. 2013; Matsuoka et al. 1998; Buscemi et al. 2001). The hyperphosphorylation of CtIP, which initiates resection, together with the MRE11 complex, was not affected in any of the cell lines, including *Nbs1*$^{\Delta B/\Delta B}$ and double mutant cells following IR (Figure 20A) and CPT (Figure 20B). These results are in contrast to the data reporting that the NBS1 FHA domain is essential for CtIP phosphorylation by ATM (Wang et al. 2013), as the NBS1$^{\Delta B}$ protein lacks the FHA domain. This suggests that CtIP phosphorylation could occur in the absence of the NBS1 FHA and BRCT domains and full activation of ATM, which is consistent with a role for CDKs for CTIP hyperphosphorylation (Wang et al. 2013). In agreement with the previous reports that CHK2 hyperphosphorylation is deficient in *Nbs1*$^{\Delta B/\Delta B}$ thymocytes after IR treatment (Stracker et al. 2008), we observed defective CHK2 phosphorylation after IR treatment in *Nbs1*$^{\Delta B/\Delta B}$ fibroblasts (Figure 20A), which was not further affected by EXO1 deletion. Together these results suggest that the loss of EXO1 in *Nbs1*$^{\Delta B/\Delta B}$ cells leads to reduced ATM activation but does not grossly alter the phosphorylation status of key targets CHK2 and CTIP.

We next examined signaling following CPT treatment that leads to more extensive resection and is a more potent activator of ATR. As we do not have antibodies to directly assess ATR activity, we examined the phosphorylation of CHK1 on S345 that is ATR dependent. Following CPT treatment, we noted a marked reduction in CHK1 phosphorylation only in double mutant cells indicating reduced ATR signaling (Figure 20B) in agreement with the results showing that resection is further impaired in double mutant cells (Figure 19). However, the phosphorylation of RPA on S4 and S8, which is considered a surrogate of DNA resection, was reduced in *Nbs1*$^{\Delta B/\Delta B}$ and in double mutant cells (Figure 20C) after CPT treatment to equivalent levels. Taken together, these data indicate that DNA resection is defective in NBS1 hypomorphic cells and reduced further by EXO1 depletion. This likely underlies the reduced ATM and ATR activation in double mutant cells following IR or CPT treatment.

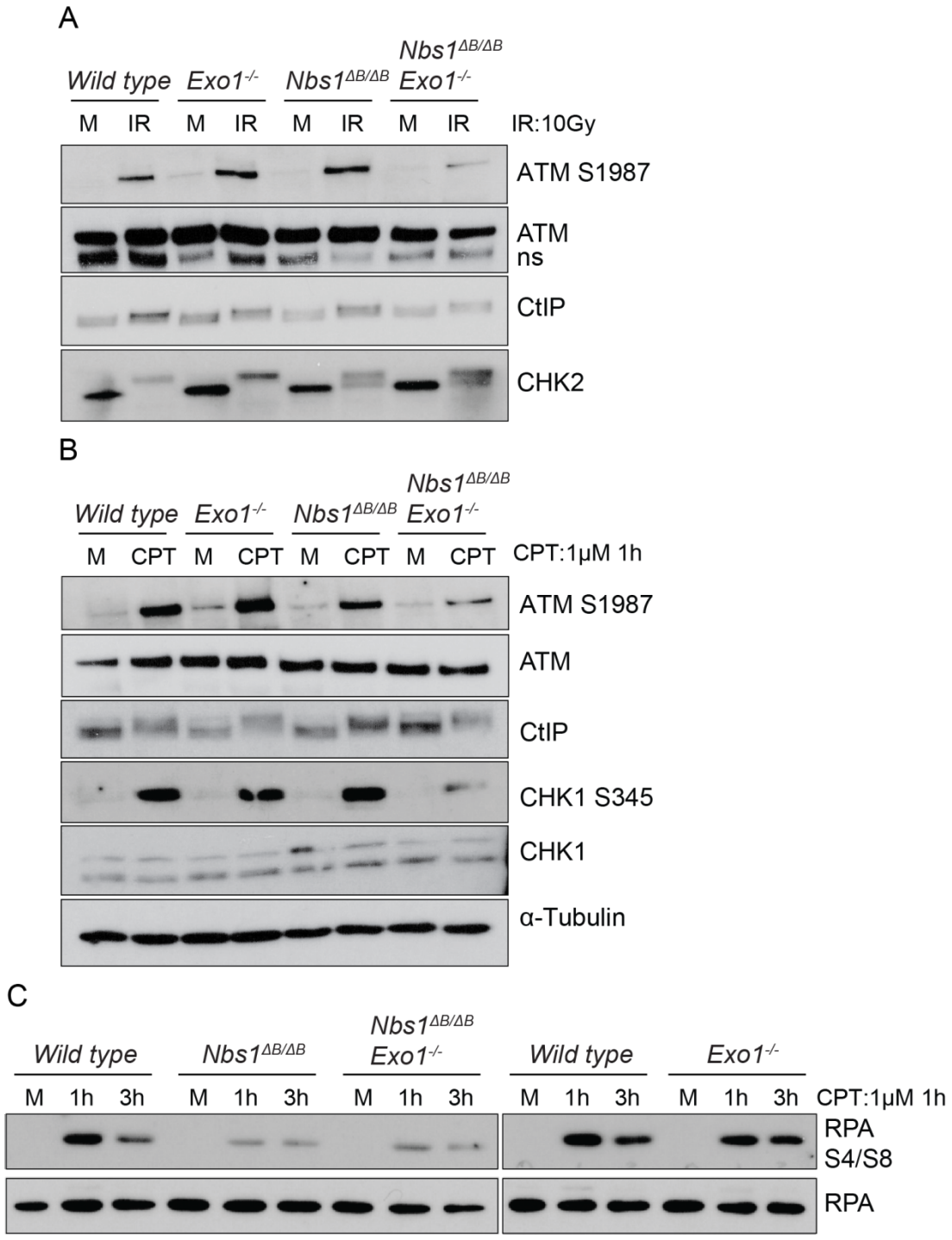

Figure 20. Western blot analysis of the signaling events following IR and CPT treatment. (A) Signaling events after 1h following IR treatment. M indicates mock treated cells, IR indicated cells treated with 10Gy of IR. Membranes were probed with indicated antibodies, and ns indicates nonspecific band. (B) Signaling events following 1h of CPT treatment. M indicates mock treated cells; CPT indicates 1μM CPT treated cells for 1h. α-Tubulin was included as loading control. (C) RPA phosphorylation after 1h and 3h following CPT treatment for 1h. Total RPA was included as loading control.

4. EXO1 loss differentially influences the sensitivity of NBS1 mutant cells to IR, crosslinking agents and CPT

As checkpoint signaling and repair were more severely compromised in double mutant cell cultures, we next examined the impact of this on the sensitivity to DNA damaging agents. The clonogenic survival assay was employed to measure the sensitivity of cell cultures of different genotypes to a spectrum of DNA damaging agents. For this assay, cells are sparsely plated before the treatment and left to form colonies during 12 days after the treatment. Colonies are stained with crystal violet and visible colonies (>50 cells) are counted and normalized for plating efficiency. The number of colonies reveals the ability of the cells to survive and proliferate after the treatment with a certain damaging agent.

The clonogenic survival assay confirmed that *Nbs1* hypomorphic cells are hypersensitive to IR (Figure 21A), MMC (Figure 21C), cisplatin (Figure 21D) and CPT (Figure 21E and F) but not to UV (Figure 21B). EXO1 deficient cells are mildly sensitive to UV (Figure 21B), and this was not further affected by *Nbs1* mutation in the double mutants. However, EXO1 loss in *Nbs1* hypomorphic cells increased their sensitivity to IR (Figure 21A) and strongly increased the sensitivity to crosslinking agents MMC (Figure 21C) and cisplatin (Figure 21D). UV lesions are mainly repaired by the NER pathway, and EXO1 has been implicated in the processing of NER intermediates (Giannattasio et al. 2010). Conflicting data regarding the role of the MRE11 complex in UV sensitivity has been reported (Yanagihara et al. 2011; Brugmans et al. 2009) but these results are consistent with previous studies in our lab that indicate that the MRE11 complex is dispensable. Lesions created by crosslinking agents, on the other hand, can be converted to DSBs during their processing, that sometimes involves end resection (Kottemann & Smogorzewska 2013), and this requires both the MRE11 complex and EXO1, although their relative roles

remain unclear. These results suggest that EXO1 is crucial for preventing crosslinker toxicity when MRE11 complex function is impaired.

Mutations in the MRE11 complex confer a high sensitivity to CPT treatment that results in covalently attached proteins, replication fork stalling and DSBs. Unexpectedly, we observed that loss of EXO1 rescued the sensitivity of *Nbs1*$^{\Delta B/\Delta B}$ mutants to CPT treatment (Figure 21E and F). *Exo1* deficiency also reduced the CPT sensitivity of wild type cells, suggesting that EXO1 promotes CPT induced cell death. In both cases, the cellular sensitivities and the rescue were notably more pronounced with low dose of CPT treatment during 24 hours than high dose treatment during 1 hour (Figure 21E and F). It has been shown that the low dose CPT (25-100 nM) treatment leads to replication fork reversal without DSBs even after prolonged CPT treatment (24 hours), whereas higher CPT treatment (≥1 μM) leads to blocked replication forks and DSBs (Ray Chaudhuri et al. 2012). Therefore, considering that we observe more pronounced rescue of CPT sensitivity with low dose treatment, our results indicate that EXO1 could promote cell death in response to aberrant replication fork structures in response to CPT.

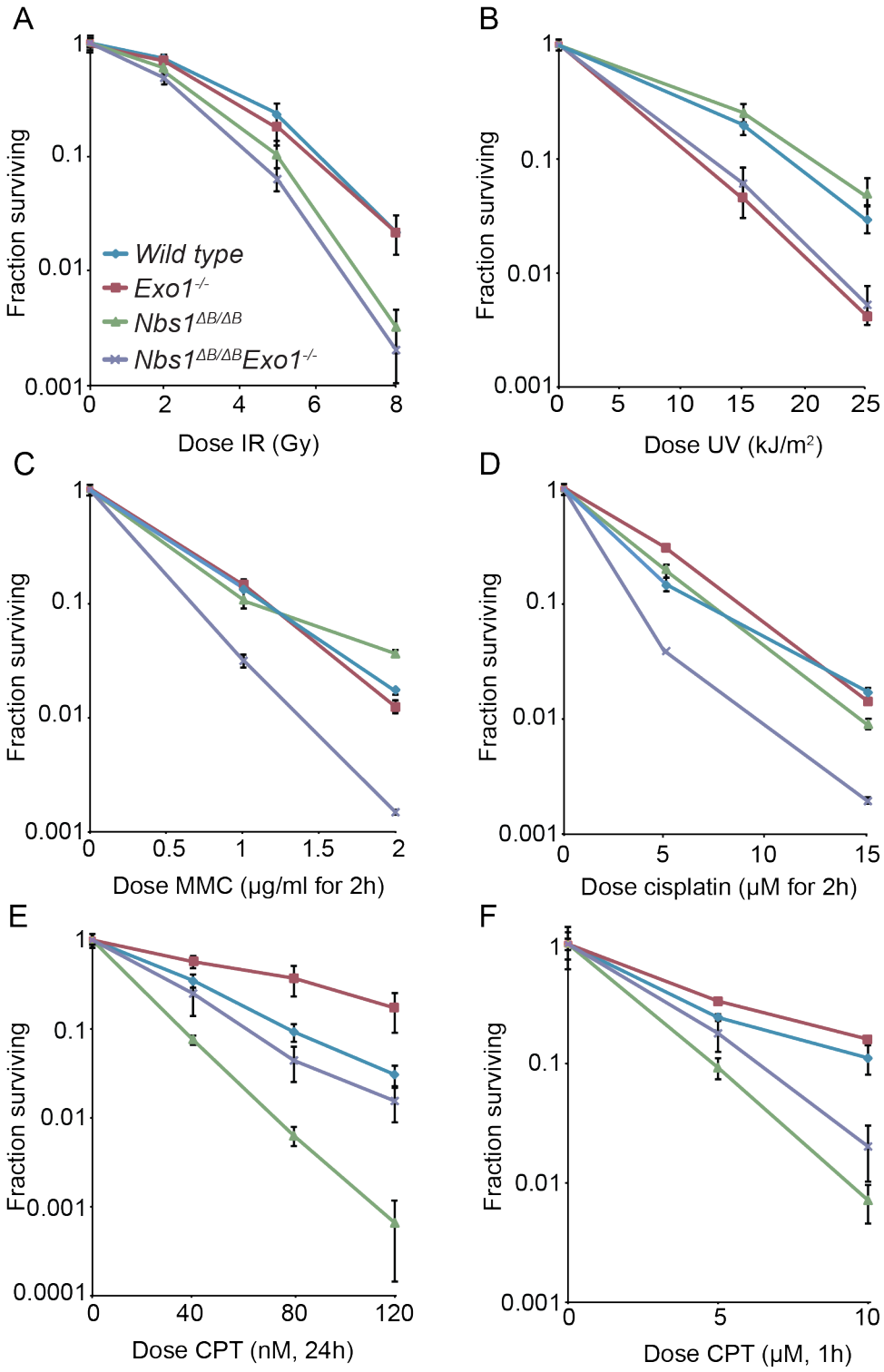

Figure 21. Cellular sensitivities to DNA damaging agents determined by the clonogenic survival assay. (A) IR sensitivity. (B) UVC sensitivity. (C) MMC sensitivity. (D) Cisplatin sensitivity. (E) CPT sensitivity with low dose CPT treatment. (F) CPT sensitivity with high dose CPT treatment. The surviving fractions (normalized to mock-treated cultures) are plotted in a dose-dependent manner. All the data is a result of at least 3 independent experiments performed in duplicate. Error bars indicate standard deviation.

5. EXO1 promotes cell death in response to CPT

To understand the basis of why EXO1 deficiency results in rescue of CPT sensitivity, we first wanted to rule out the possible off-target effects that could result from SV40 transformation or the *Exo1* targeting construct. *Exo1*$^{-/-}$ mice were generated using a construct with a hygromycin cassette in the targeting vector (Wei et al. 2003; Schaetzlein et al. 2013). As *Nbs1*$^{\Delta B/\Delta B}$ cells do not carry hygromycin resistance, we wondered whether this selectable marker could change the cellular sensitivity to CPT. We infected wild type and *Nbs1*$^{\Delta B/\Delta B}$ cells with an empty pBabe vector carrying a hygromycin cassette (pBabe-hygro), verified that the newly created cell lines were resistant to hygromycin and performed the CPT sensitivity assay. We observed that hygromycin resistance does not influence CPT sensitivity (Figure 22A) and that the sensitivity of both wild type and *Nbs1* mutated cells was similar to the cell lines without the pBabe-hygro vector (Figure 22B).

Next, we asked whether the transformation process itself could result in mutations in the *Top1* gene, which is the target of CPT, as this is a common occurrence in acquired resistance to CPT (Rasheed & Rubin 2003). Therefore, we amplified the *Top1* gene from wild type, single mutant and double mutant cell lines and sequenced it. No mutations were found, indicating that transformation did not result in mutation of the *Top1* gene and the CPT resistance that we observe in cells lacking EXO1 is not due to mutated TOP1.

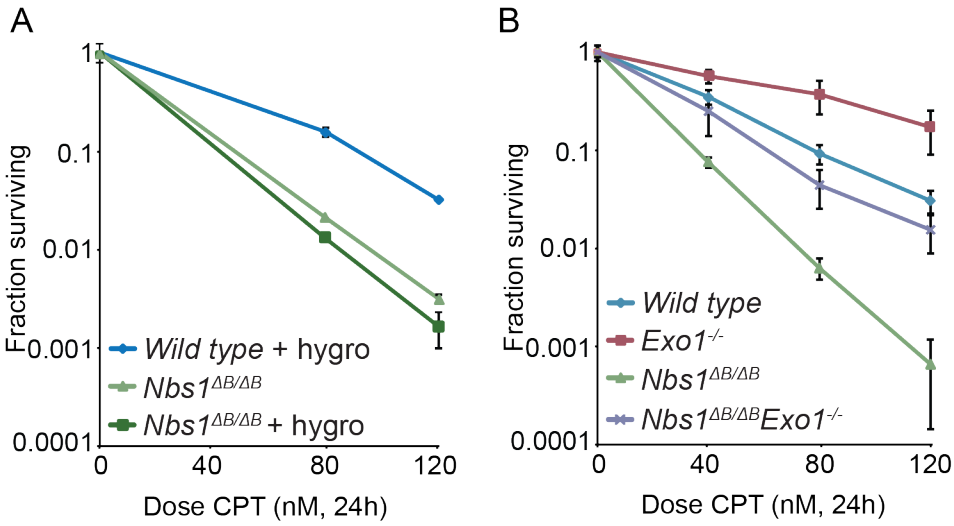

Figure 22. Hygromycin resistant transformed MEF sensitivities to CPT. (A) CPT sensitivity with low dose CPT treatment using hygromycin resistant cell lines. Experiment performed in duplicate, error bars indicate standard deviation. (B) Previous CPT sensitivity results for comparison.

To better understand how EXO1 influenced sensitivity to CPT, we analyzed cell cycle progression after CPT treatment. We incubated the cells with a low dose of CPT (80 nM) for 24 hours and then assessed the cell cycle profile by flow cytometry using PI staining at different time-points after removal of the CPT from the cells (Figure 23). The analysis revealed that after 24 hours of CPT treatment, wild type cells had accumulated in the G2-M phase of the cell cycle, which became more evident 3 hours after drug removal. 24 hours after drug removal, the cell cycle profile looked normal, with a small increase in the sub-G1 population, indicating dead cells. *Nbs1*$^{\Delta B/\Delta B}$ cells showed a much more dramatic accumulation in the G2-M phase immediately after drug removal and this became even more pronounced 8 hours after the removal of CPT. However, 24 hours after drug removal, *Nbs1*$^{\Delta B/\Delta B}$ cells had a very large sub-G1 population and many more cells with greater than 4N DNA content, indicating both increased cell death and polyploidy, likely due to failed mitotic divisions. *Exo1*$^{-/-}$ cells, on the contrary, accumulated in G2-M phase 3 hours after drug removal, but after 8 hours, the cell cycle profile looked normal, with very little increase in the G2-M phase and these cultures exhibited few dead cells 24 hours after drug removal. The cell cycle profile of the double mutant cells

following CPT treatment was very similar to wild type cells with a pronounced G2 arrest at 3 and 8 hours following drug removal and a return to a near normal cell cycle profile with little cell death by 24 hours after CPT removal. These results indicate that the toxicity of low dose CPT in *Nbs1*$^{\Delta B/\Delta B}$ cells becomes apparent 24 hours after CPT removal and is dependent on EXO1.

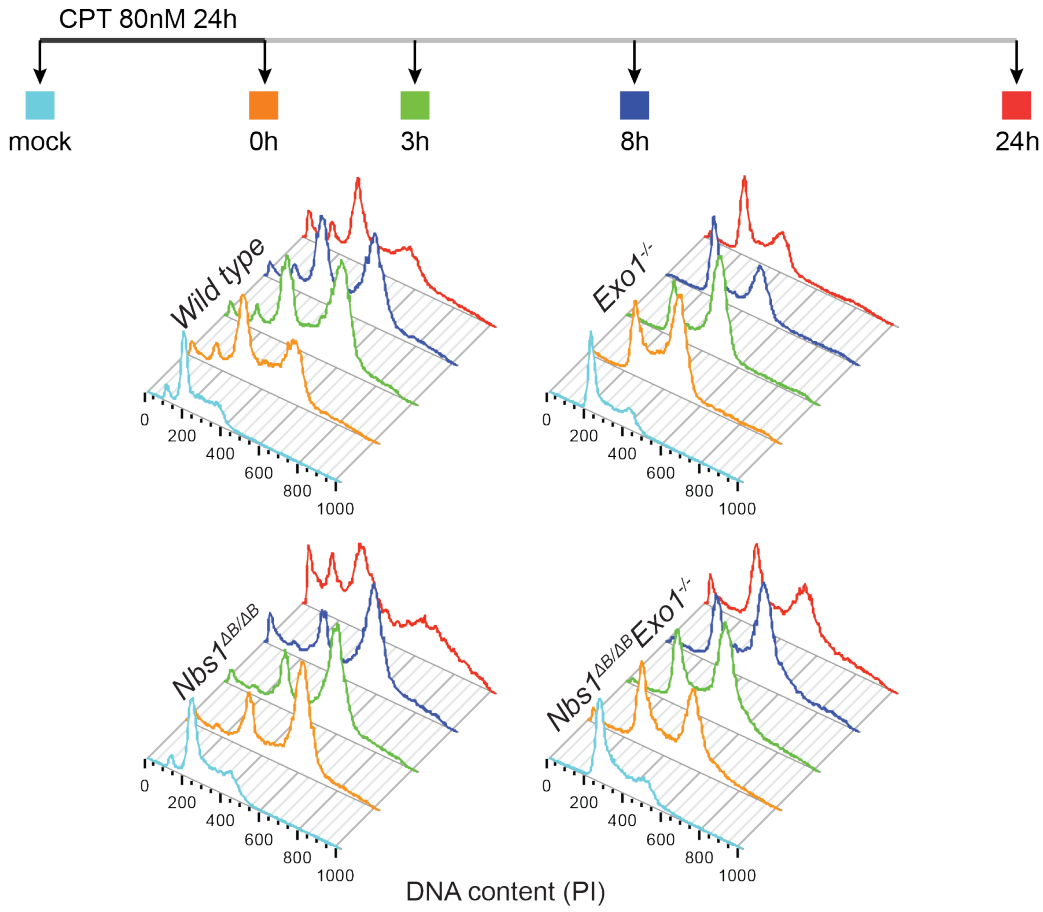

Figure 23. Cell cycle profile after low dose CPT treatment. Cells were treated with 80nM of CPT for 24h and collected for cell cycle analysis at the indicated time points.

Since the cell cycle profiles revealed a high amount of dead cells (sub G1 population) in *Nbs1*$^{\Delta B/\Delta B}$ cultures, we further examined cell death in response to CPT. After incubating the cells with low dose CPT (80 nM) for 24 hours, we measured PI incorporation in non-fixed cells by flow cytometry to identify dead cells with exposed DNA (Figure 24A). The outcome largely correlated with the cellular sensitivity results from the clonogenic assays, as we observed that the cell death is highest in *Nbs1* mutants after CPT treatment (Figure 24B).

However, in double mutant cells, cell death was also high (Figure 24B). This could be the result of the low plating efficiency of the double mutant cells, as even in untreated conditions we observe many dead cells and for clonogenic survival assays the number of plated double mutant cells needs to be higher compared to single mutants or wild type cells. The other possibility is that the cell death continues to increase even more at the later time-points in *Nbs1* mutants after CPT treatment. The latest time-point we observed was 2 days (48 hours) after removal of the drug, and by that time almost 75% of the *Nbs1*$^{\Delta B/\Delta B}$ cells were dead, compared to only 23% in *Exo1*$^{-/-}$ cells (Figure 24B). Taken together, the data confirms that in accordance with the clonogenic survival assay results, EXO1 promotes cell death in response to CPT treatment.

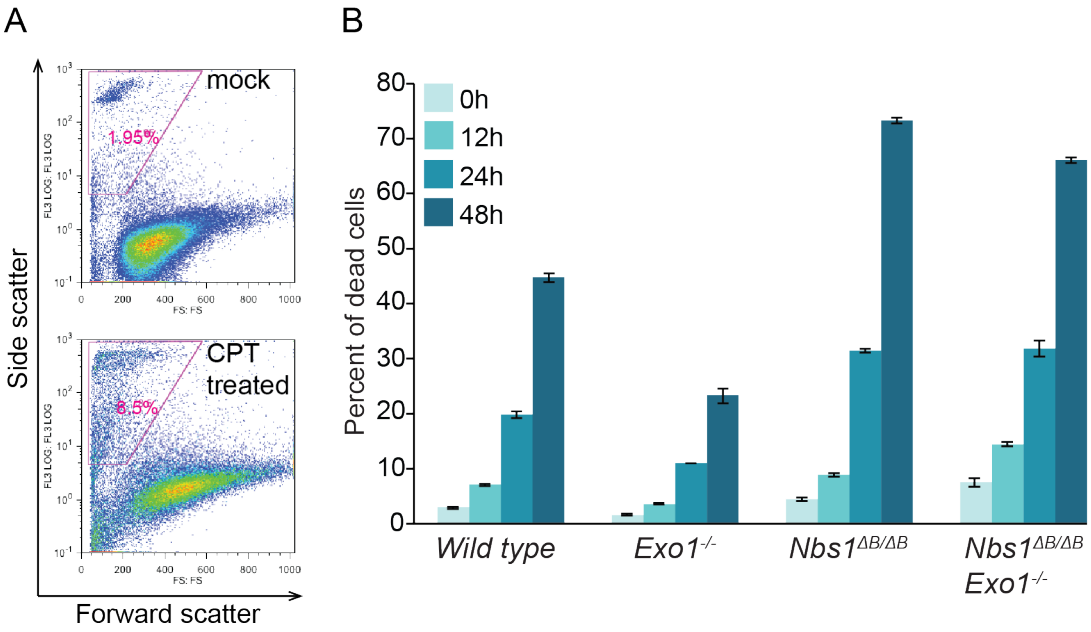

Figure 24. Cell death after low dose of CPT treatment. (A) Representative flow cytometry images of mock-treated and CPT treated cells after PI incorporation. Pink squares indicate dead cells. (B) Cell death of the indicated phenotypes in different time-points after 24h 80nM CPT treatment. Error bars indicate standard deviation.

6. EXO1 reduces the restart of stalled replication forks and promotes sensitivity to low dose CPT

To better understand the fate of cells during low dose of CPT treatment, we evaluated DNA synthesis in the presence of CPT by BrdU uptake. We incubated the cells with low dose of CPT (80 nM) and assessed DNA synthesis 5 hours and 24 hours after CPT addition. We observed that DNA synthesis still continues at a similar extent as in untreated cells in the presence of low dose CPT after 5 hours, and decreased only after 24 hours by around 40% in all the genotypes (Figure 25A) except in *Nbs1*$^{\Delta B/\Delta B}$ cells, where it decreased by 80% (Figure 25A and B). This data suggests that cells continue DNA synthesis in the presence of low dose CPT for several cell cycles until cell cycle arrest occurs. This is most dramatic in the sensitive NBS1 hypomorphic cells that experience the most problems in continuing DNA synthesis following CPT treatment. This is possibly due to a direct effect on replication forks, such as impaired restart of stalled forks, or could reflect the more dramatic arrest of these cultures in G2/M, thus reducing the number of cells entering the next S-phase. The latter effect could be a result of mitotic entry with CPT induced structures that impair cell division, consistent with the increased levels of polyploidy we observed.

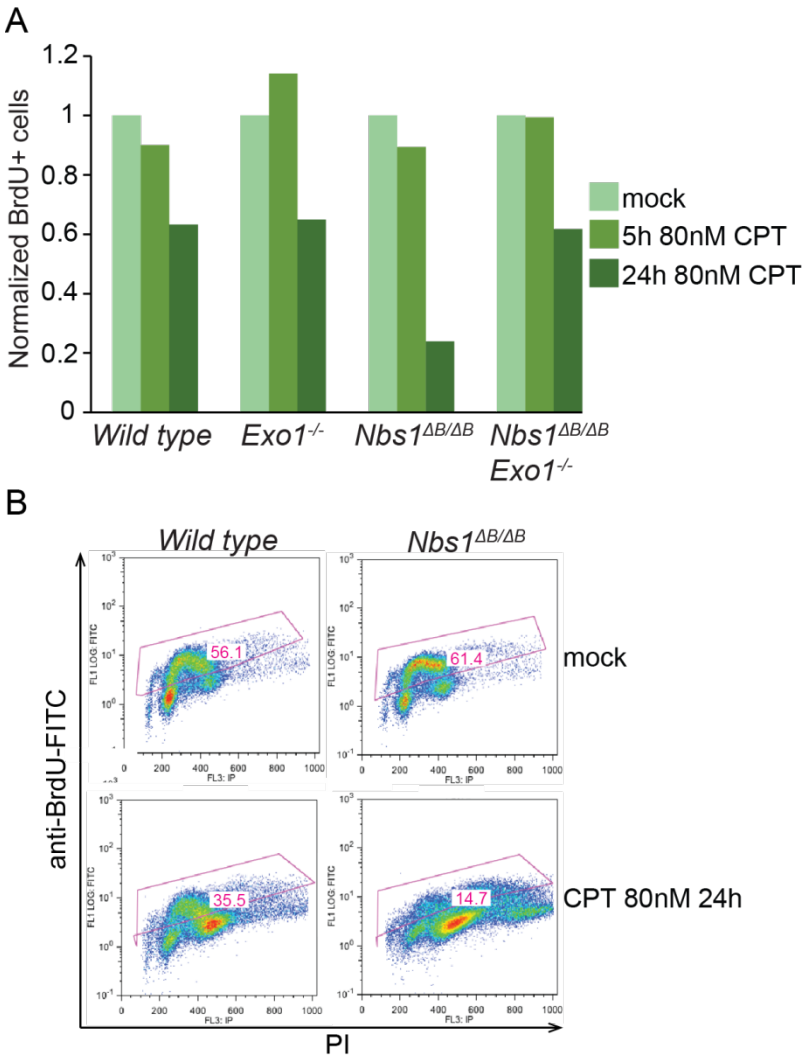

Figure 25. DNA synthesis during the treatment of CPT. (A) DNA synthesis measured by BrdU uptake at the indicated time-points after adding CPT to cells. (B) Representative flow cytometry profiles of wild type and *Nbs1* mutant cells shown before (mock) and after treating them with 80nM CPT for 24h. S-phase cells are marked by the red square; the percentage of S-phase cells is indicated.

To directly address replication fork progression in the presence of CPT, we employed the DNA fibre assay. We incubated the cells with CldU for 20 minutes and added 80 nM CPT to the second analogue, IdU, and incubated the cells for further 20 minutes (Figure 26A). Visually, we did not observe replication fork slowing in the presence of CPT (Figure 26A). We measured the lengths of replication tracts generated in the presence of both analogues and divided the length of the second analogue by the first one. In unperturbed conditions, this should be 1, and if tracks shorten due to CPT addition, less than 1. We

observed that the replication forks do not slow down immediately after CPT addition, as in all the genotypes the ratio between IdU and CldU did not change after CPT was added to the IdU at doses that cause high sensitivity in the NBS1 mutant cells (Figure 26B). Since the BrdU analysis in the presence of CPT indicated the DNA synthesis slows down many hours after CPT addition to the cells (Figure 25A), we incubated the cells with 80 nM of CPT for 2 hours and before the addition of CldU and IdU (Figure 26C). We observed that the fibres appeared aggregated (Figure 26C), which made the measurement of fibre lengths difficult. The observed structures are potentially a result of covalent attachments or torsional issues that CPT treatment can cause.

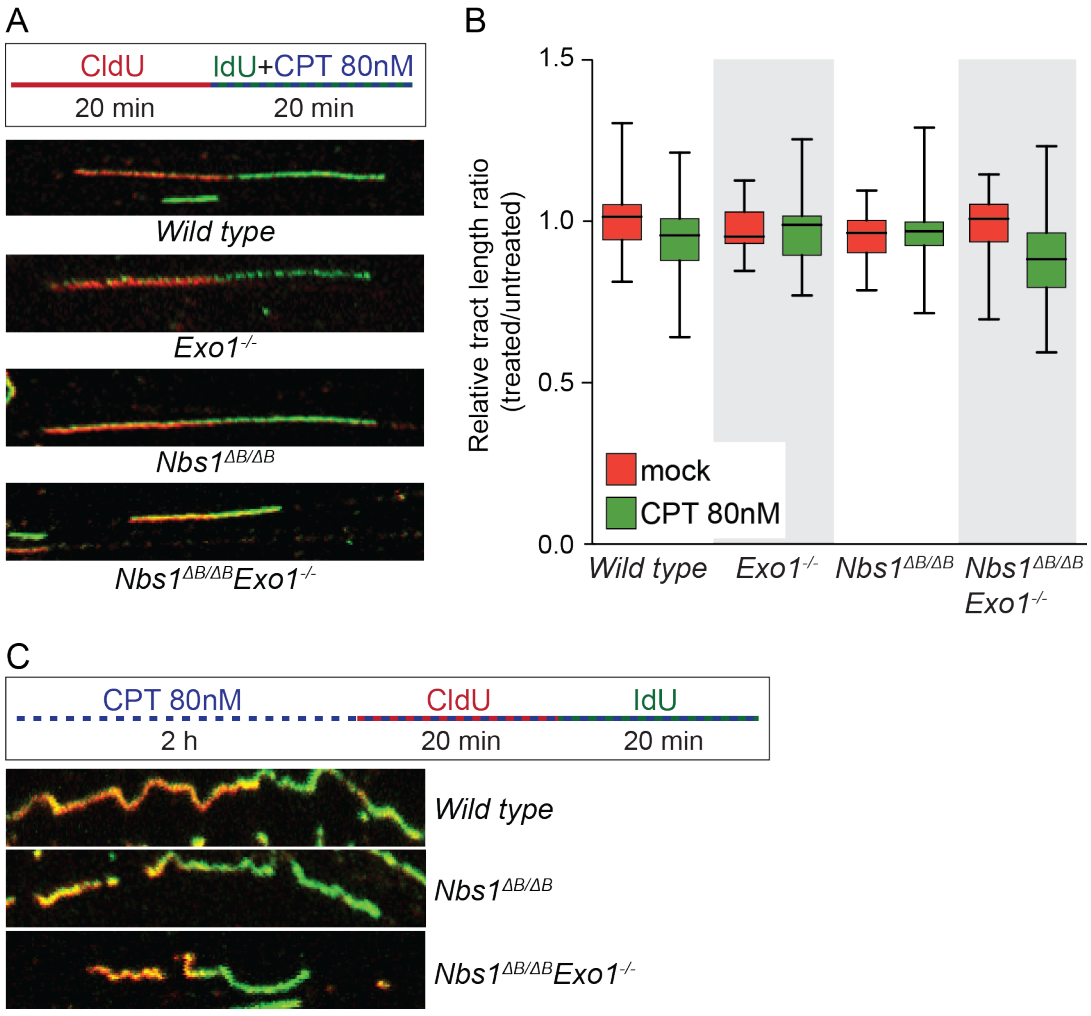

Figure 26. Replication fork progression in the presence of CPT. (A) Schematic illustration of the assay in which CPT is added to IdU with representative images of the DNA fibres of the indicated genotypes. (B) DNA fibres of the indicated genotypes distributed according to the relative IdU/CldU track length ratio. Mock indicates replication fork progression without CPT, CPT 80nM indicates replication fork progression with CPT addition during IdU

incorporation. Error bars indicate standard deviation. At least 50 fibres were measured from each genotype. (C) Schematic illustration of the assay in which CPT is added to the cells 2 hours before CldU and IdU incorporation with representative images of the DNA fibres of the indicated genotypes.

To determine if the influence of EXO1 on sensitivity was reflected in the number or types of chromosomal aberrations generated, we examined metaphase spreads after treating the cells with a low dose of CPT for 2 hours (Figure 27A). We observed that the CPT treated cells had considerably higher level of chromosomal aberrations in double mutant cells (Figure 27B). Based on our clonogenic survival assay results (Figure 21E), this high incidence of chromosomal aberrations does not correlate with cellular survival, indicating that in response to CPT treatment, the double mutant cells are able to continue cell division even in the presence of highly elevated damage. It may also be that we do not see increased damage in the NBS1 single mutants due to the increased arrest prior to mitosis, thus obscuring metaphase analysis, and increased cell death.

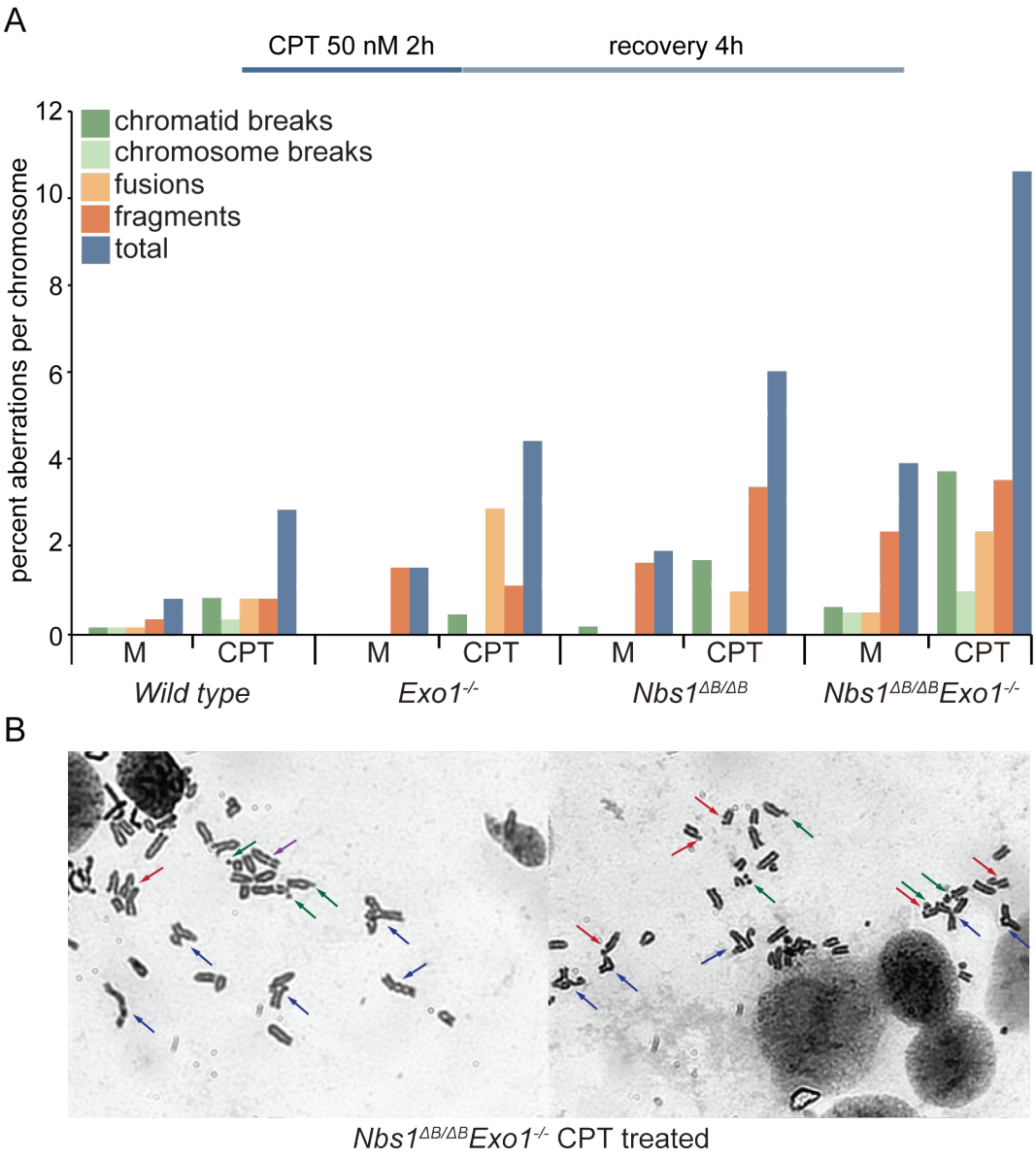

Figure 27. Chromosomal instability in CPT treated TMEFs. (A) Metaphase aberrations in transformed MEFs of the indicated genotype after treating the cells with CPT. M indicates mock treated cells, CPT indicates cells treated with 50 nM CPT for 2h following by 4h recovery. (B) Representative images of chromosomes of CPT-treated double mutants, chromatid breaks are indicated with red arrows, chromosome break by purple arrow, fusions by blue arrows and fragments by green arrows.

Next, we assessed metaphase aberrations after the treatment of the cells with another agent that interferes with replication forks, wondering if the chromosomal aberration pattern was similar to that of CPT treatment in the different genotypes. We treated cells with aphidicolin, a selective inhibitor of DNA polymerase alpha, that at low doses causes dissociation of leading and

lagging strands, resulting in replication fork stalling. Following a low dose (300 nM) treatment with aphidicolin for 24 hours, we examined chromosomal aberrations in each of the genotypes. We observed the most aberrations in *Nbs1* mutant cells, and this was not further increased by the loss of EXO1 (Figure 28). Aphidicolin is known to induce breaks at CFS, structures particularly sensitive to replication stress. This indicates that NBS1 might play a role at CFS during DNA replication, but that CPT affects the replication fork through a different mechanism that is more influenced by EXO1.

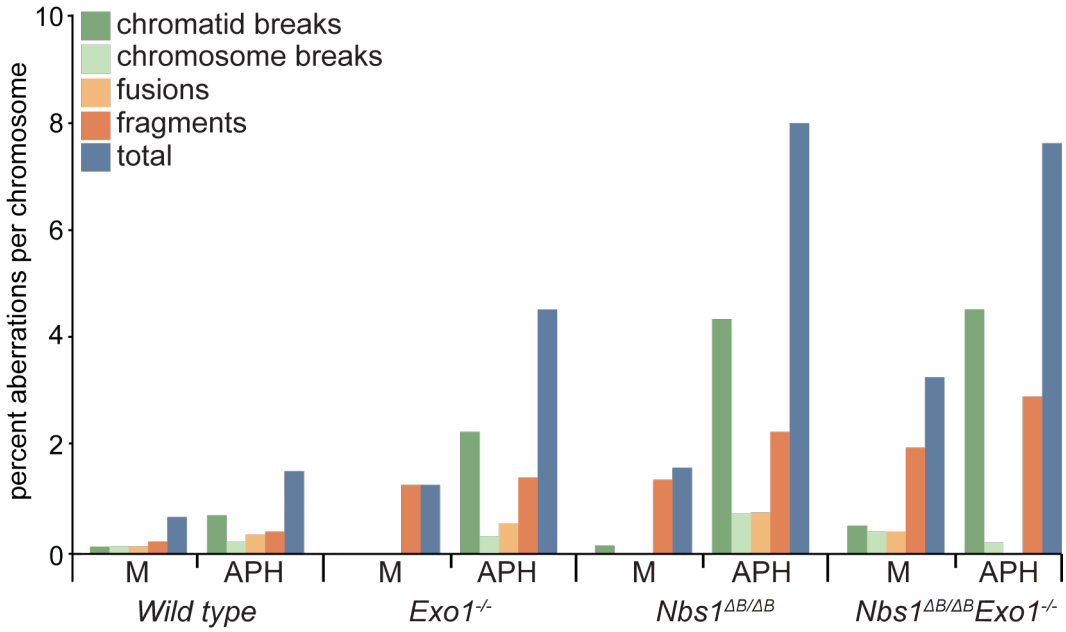

Figure 28. Chromosomal instability in aphidicolin-treated transformed MEFs. Metaphase aberrations in transformed MEFs of the indicated genotype after treating the cells with aphidicolin. M indicates mock treated cells, APH indicates cells treated with 300 nM aphidicolin for 24h.

In order to gain additional insight regarding the type of DNA damage that CPT induces, we monitored the phosphorylation of γ-H2AX, which is activated in response to DSBs and replication stress (Ward & Chen 2001). In odder to assess that, we treated the cells with a low dose of CPT for 24 hours, stained them for γ-H2AX, and evaluated the mean intensity change of γ-H2AX staining compared to untreated cells by flow cytometry (Figure 29A). We did not detect substantial differences between different genotypes in γ-H2AX phosphorylation (Figure 29B) indicating that equal damage was generated in the different

genotypes after 24 hours of low dose CPT treatment, either through breaks or replication stress.

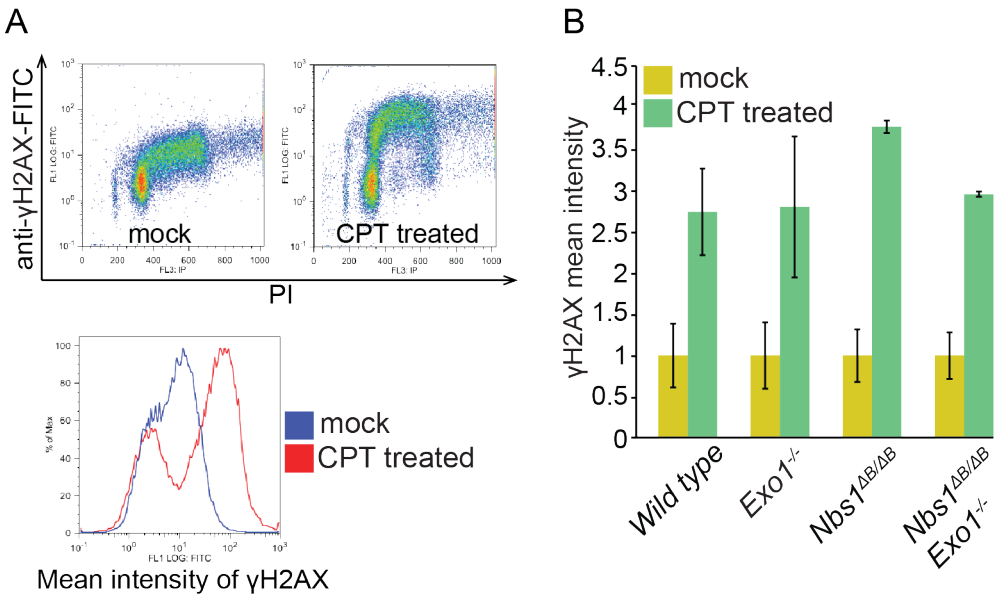

Figure 29. γ-H2AX phosphorylation in CPT treated transformed MEFs. (A) Representative flow cytometry profiles of the indicated phenotypes before and after CPT treatment (up). Results are represented as the mean intensity increase in γ-H2AX phosphorylation (down). (B) γ-H2AX mean intensity increase compared to untreated cells of the indicated phenotypes after 24h 80nM CPT treatment. Error bars indicate standard deviation.

Previous work has shown that the nuclease activity of MRE11 can attack unprotected DNA at stalled forks and prevent restart (Schlacher et al. 2011; Ying et al. 2012; Hashimoto et al. 2010). Additionally, EXO1 has been implicated in stalled fork degradation in yeast (Cotta-Ramusino et al. 2005). To determine if replication fork restart was affected by the mutations in *Nbs1* or EXO1 loss, we again employed the DNA fibre assay. Cells were treated with hydroxyurea (HU) to stall forks after incorporation of CldU, and then IdU was added to measure the length of restarted replication fork tracts (Figure 30A). We observed longer IdU tracks in the cells lacking EXO1 (*Exo1*$^{-/-}$ and double mutant) compared to the IdU track lengths in wild type and *Nbs1*$^{\Delta B/\Delta B}$ cells (Figure 30A), indicating that the cells without EXO1 can restart the replication faster. We measured the lengths of replication tracts of both analogues and divided the length of the second analogue by the first one, which should be 2 if

the replication started immediately after HU removal (as we incubated the cells with IdU twice as long as with CldU) and less than 2 if the IdU tracks shorten because of a delay in replication restart. We observed that the cells lacking EXO1 were able to restart the stalled replication forks faster regardless of NBS1 status (Figure 30B and C). These results suggest that EXO1 opposes replication fork restart.

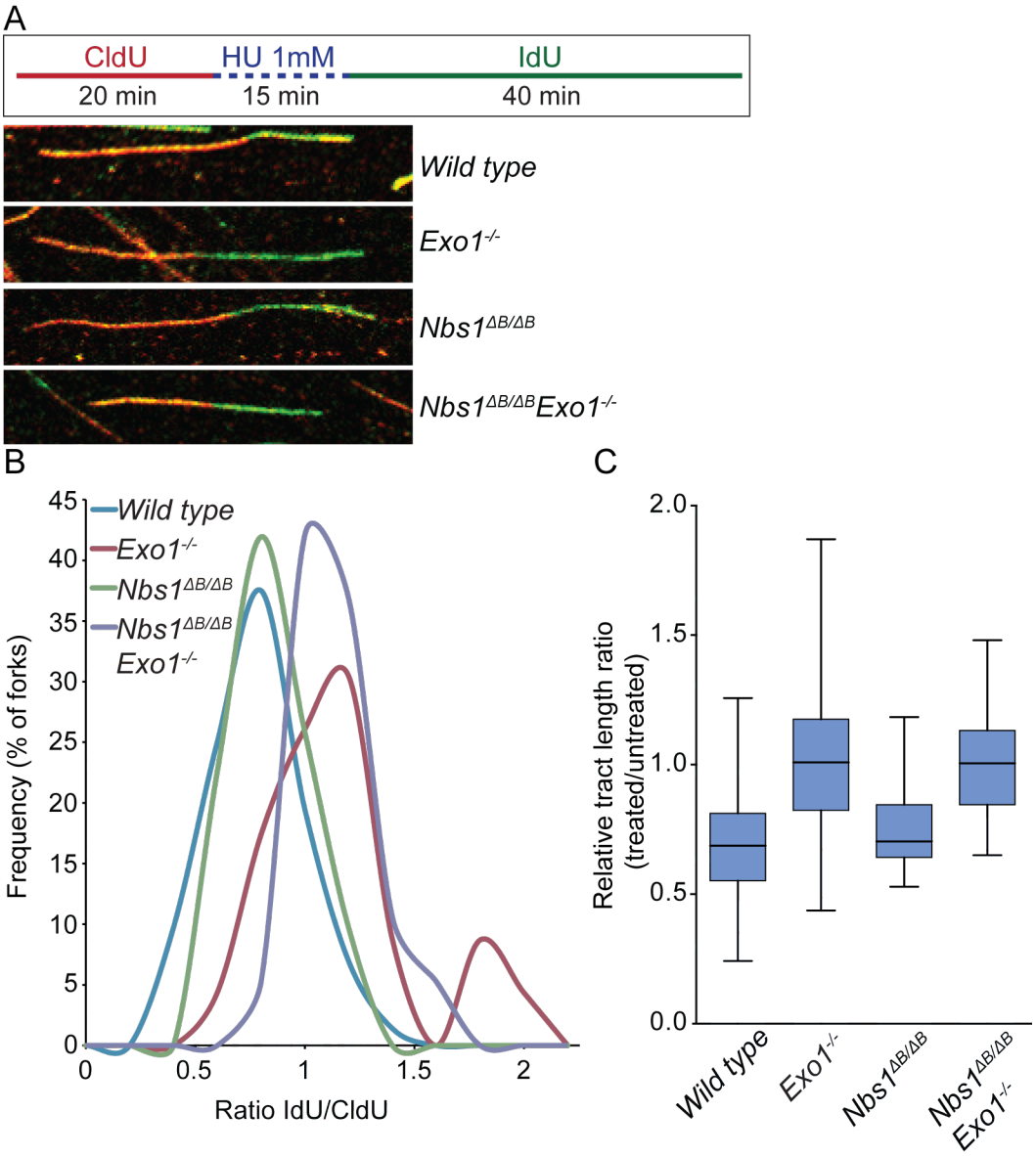

Figure 30. Replication fork restart of transformed MEFs after HU treatment. (A) Schematic illustration of the assay with representative images of the DNA fibres of the indicated genotypes. (B) DNA fibres distributed according to the frequency of IdU/CIdU ratio. Larger ratio indicate faster replication restart. At least 50 fibres were measured from each genotype. (C) Boxplot representation of the results from the same assay. Error bars indicate standard deviation.

Stalled replication forks have been shown activate ATR, and since our results indicate that ATR activation might be impaired in *Nbs1*$^{\Delta B/\Delta B}$ and in double mutant cells (Figure 20), we wondered whether increased activation of ATR might rescue the CPT sensitivity we observe in *Nbs1* mutant cells. We used a retroviral system in which the intracellular domain of ATR-activating fragment of TopBP1 is controlled by 4-hydroxytamoxifen (4-OHT), an estrogen receptor (ER) modulator (Toledo et al. 2008) (Figure 31A). We produced retrovirus in 293T cells and infected transformed MEFs with the virus-containing supernatant, followed by the selection of the cells with puromycin. We visualized the chimeric protein (termed TopBP1^{ER}) with an anti-ER antibody and observed that it was cytoplasmic until the addition of 4-OHT that caused its nuclear translocation (Figure 31B). In order to verify whether TopBP1^{ER} nuclear translocation was sufficient to promote ATR activation, we analyzed phosphorylation of γ-H2AX, which is an ATR target (Ward & Chen 2001). Indeed, whereas small amounts of γ-H2AX can be detected before 4-OHT treatment, we observed higher levels of γ-H2AX phosphorylation after the treatment (Figure 31B). We then assessed whether CPT sensitivity can be rescued by TopBP1^{ER}-mediated ATR activation by employing the clonogenic survival assay. While we saw a rescue in CPT sensitivity in the cells treated with 4-OHT (Figure 31C), we also observed that treating the cells not carrying TopBP1^{ER} with 4-OHT also resulted in a slight rescue of CPT sensitivity (Figure 31C). This suggested that the estrogen pathway altered sensitivity to CPT and made it difficult to discern the specific effects of increased ATR activation.

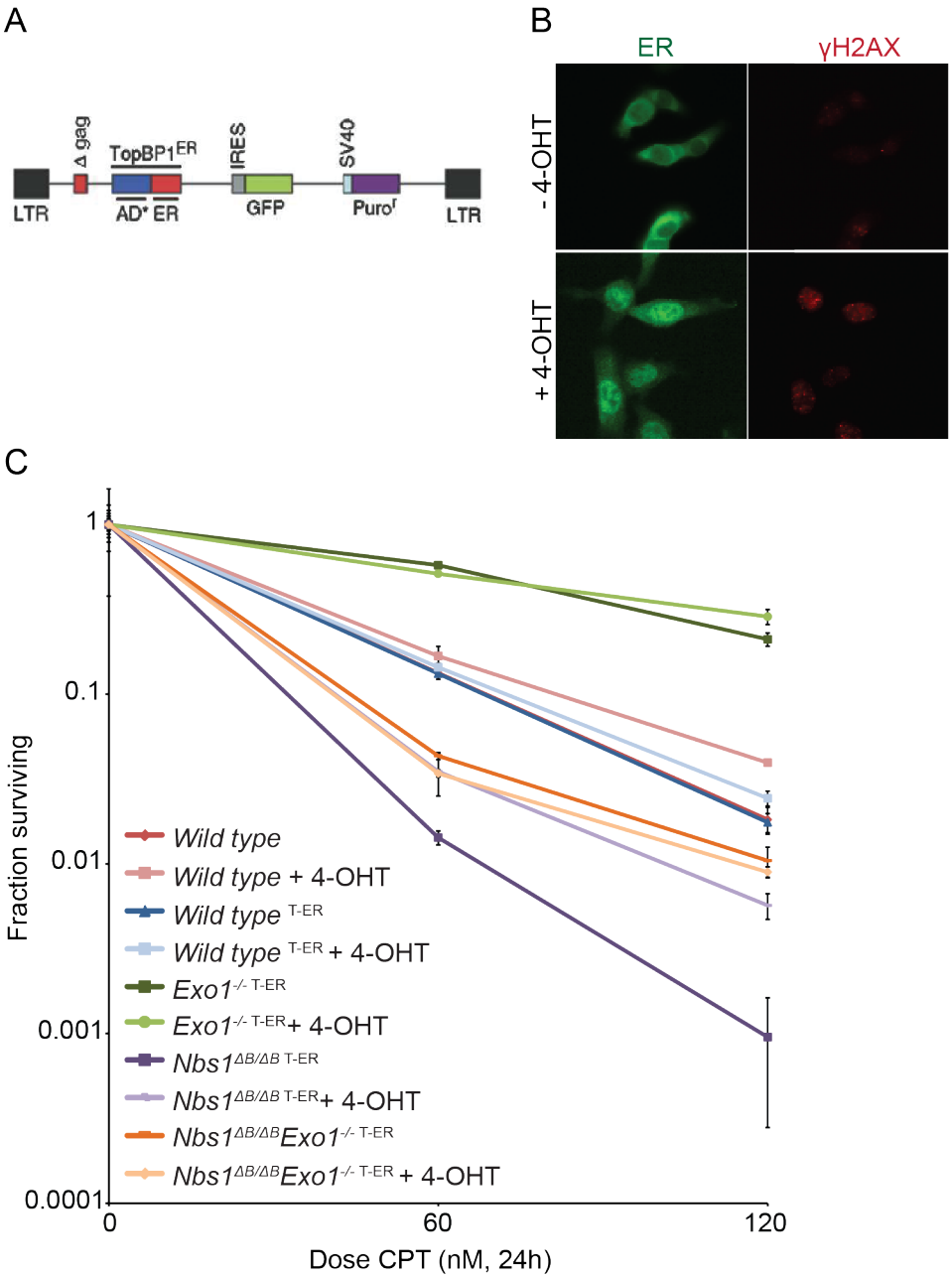

Figure 31. Cellular sensitivity to CPT in ATR activated transformed MEFs. (A) Schematic illustration of the inducible retroviral construct. Adopted from (Toledo et al. 2008). (B) Representative images of TopBP1^{ER} construct translocation to the nucleus in response to 4-OHT treatment. TopBP1^{ER} is visualized with ER-recognizing antibody (green) and γ-H2AX phosphorylation can be seen upon ATR activation (red). (C) Cellular sensitivity assessed by clonogenic survival assay to low dose CPT of the indicated phenotypes upon 4-OHT treatment. TopBP1^{ER} carrying cells are marked as $^{T\text{-}ER}$. Error bars indicate standard deviation.

Analysis of the DNA structures associated with TOP1 inhibition in human cells by electron microscopy has shown that CPT treatment at low doses causes widespread replication fork reversal (Ray Chaudhuri et al. 2012). When a stalled replication fork reverses, this allows the nascent strands to anneal and generates a “chicken foot” structure that is similar to Holliday junction. These structures must be properly resolved, otherwise they can potentially generate different recombination substrates and lead to further genome instability and cell death (Cotta-Ramusino et al. 2005). We reasoned that EXO1 might contribute to the generation of reversed replication fork structures that are necessary for repair and replication restart and that the nucleolytic degradation of these structures could promote sensitivity to CPT. The endonuclease MUS81 and DNA helicase FBH1 have both been implicated in processing abnormal replication structures, eliminating cells with excessive replication stress via apoptosis and preventing mitotic aberrations (Fugger et al. 2013; Mankouri et al. 2013; Jeong et al. 2013). MUS81 is a structure specific endonuclease that acts as a Holliday junction resolvase (Ho et al. 2010) and has been implicated in generating DSBs and causing replication fork collapse in CHK1 deficient cells (Forment et al. 2011). The role of FBH1 is less clear but it is thought to act upstream of MUS81 and has been implicated in replication fork processing (Fugger et al. 2013). In order to test whether cells lacking EXO1 may have reduced numbers of reversed forks, we examined the influence of MUS81 and FBH1 on the sensitivity to low dose CPT in each genotype. We transfected small interfering RNA (siRNA) to downregulate *Fbh1* (Figure 32A) or *Mus81* (Figure 32B) in our transformed MEFs and then performed clonogenic survival assays to determine if downregulating these proteins affected sensitivity to CPT treatment. Indeed, we observed that downregulation of either MUS81 or FBH1 improved cellular survival in all genotypes after low dose CPT treatment. However, this effect was more pronounced in cells with EXO1 as wild type cells showed a 4 fold increase in survival after depletion of either FBH1 or MUS81 and *Nbs1* mutant cells a roughly 3 fold and 7.5 fold increase in survival respectively. The sensitivity of *Exo1* deficient cells was minimally affected as they showed only a 1 fold increase in survival (Figure 32C, D and E). This

suggests that EXO1 promotes fork reversal or the generation of other structures that could be rendered toxic to cells by the activities of FBH1 and MUS81. This is particularly true in *Nbs1*$^{\Delta B/\Delta B}$ cells when MUS81 is downregulated as we observe a close to 8 fold increase in survival (Figure 32C).

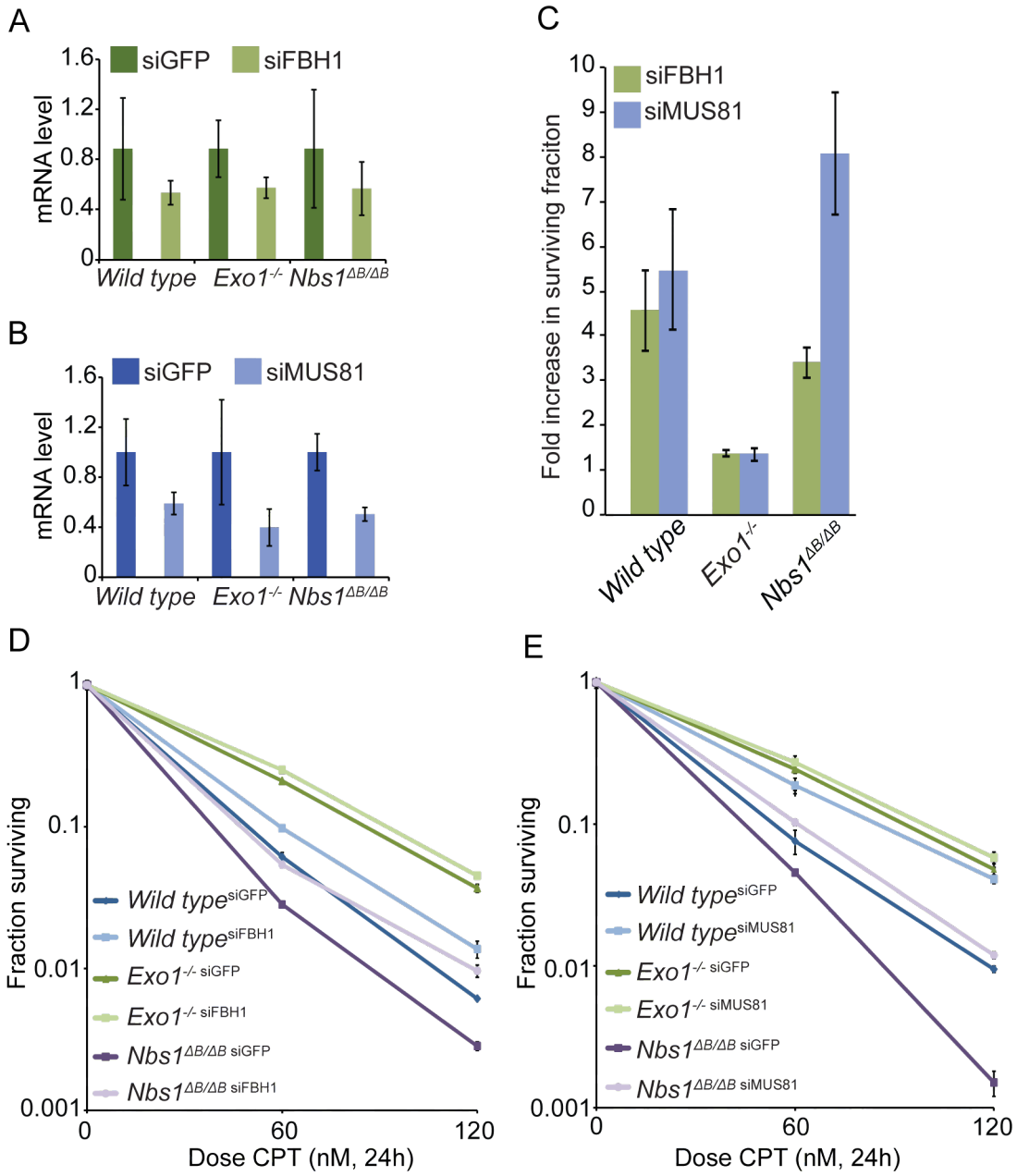

Figure 32. Cellular sensitivity to CPT in FBH1 and MUS81 downregulated cells. (A) Real time PCR showing relative mRNA levels of FBH1 normalized to siRNA GFP transfected cells. (B) Real time PCR showing relative mRNA levels of MUS81 normalized to siRNA GFP transfected cells. (C) Fold increase in survival of the indicated phenotypes of FBH1 or MUS81 downregulation, calculated from the results of clonogenic survival assay presented in D and E. Error bars represent standard deviation. (D) Cellular sensitivity to CPT in FBH1 downregulated cells. (E) Cellular sensitivity to CPT in MUS81 downregulated cells. Error bars indicate standard deviation.

7. EXO1 complementation

As the influence of EXO1 on the DSB response only becomes apparent in the *Nbs1*$^{\Delta B/\Delta B}$ mutant background, little analysis has been performed addressing its regulation by post-translational modifications. In order to better understand the regulation of EXO1, we attempted to overexpress EXO1 using various expression systems in order to eventually perform complementation analysis with mutants.

As a first attempt, we cloned the human cDNA of EXO1 into a mammalian GFP fusion expression vector, pDEST53 (termed EXO1-pDEST53) that is compatible with the Gateway cloning system. We verified the expression of GFP-EXO1 from the pDEST53 vector by transiently transfecting human 293T cells (Figure 33A). Using an antibody against human EXO1, we were not able to detect endogenous EXO1 expression but could detect high levels of the GFP-EXO1 fusion protein (Figure 33A, 293T cells). Next, we cloned the cDNA of EXO1 into the retroviral pLPC expression vector with a cassette for C-terminal fusion of the Strep-tag II and the FLAG-tag (termed EXO1-pLPC-CTAP). We again verified the expression of EXO1 in human 293T cells following transfection of the plasmid (Figure 33A). Next, using EXO1-pLPC-CTAP, we produced retrovirus in 293T cells and subsequently infected transformed MEFs with the virus-containing supernatant and puromycin-selected for stable expression. The cells survived the selection with puromycin, indicating insertion of the retrovirus, but we were not able to detect EXO1 overexpression by Western blotting (Figure 33B), suggesting that stable expression of EXO1 was unfavorable for mouse fibroblasts. Subsequently, we transfected MEFs with EXO1-pDEST53 to determine if we could overexpress EXO1 with direct transfection of the EXO1-pDEST53 construct. While the control transfection with GFP construct worked, after transfecting the cells with EXO1-pDEST53 we could not detect visible GFP, nor EXO1 overexpression by Western blot (Figure 33C). As EXO1 overexpression could be toxic in mouse fibroblasts, we next tried a doxycycline-inducible inducible lentiviral vector, pTRIPz, for EXO1 expression. We cloned

the human *EXO1* cDNA into pTRIPz, produced lentivirus in 293T cells, infected both 293T cells and transformed MEFs with the virus-containing supernatant and selected the cells with puromycin. We were able to easily create an EXO1-pTRIPz 293T cell line, and we confirmed the inducible expression of EXO1 by adding doxycycline to cells (Figure 33D). Unfortunately, we were not able to create stable cell lines with transformed MEFs, which died during the selection. This could reflect leaky expression that was not tolerated by the MEFs or problems with the infection of this cell type.

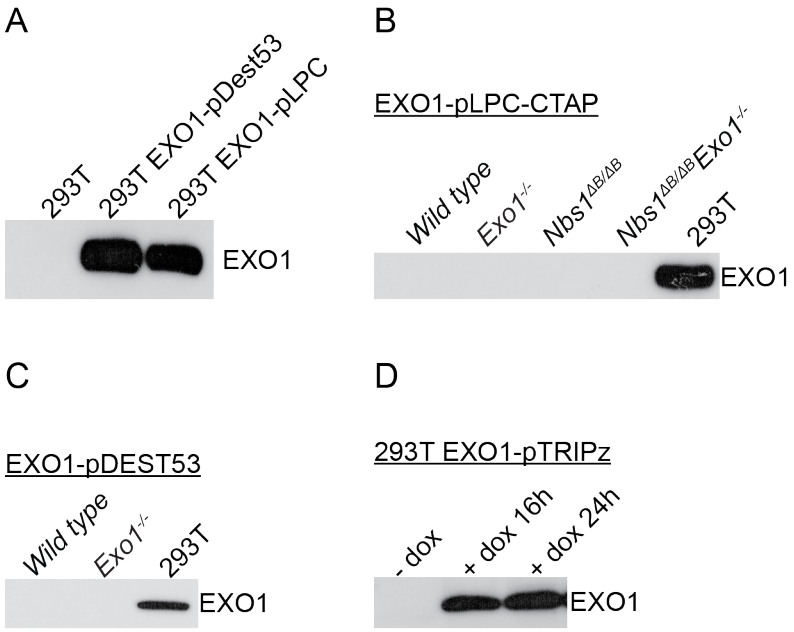

Figure 33. EXO1 expression by Western blot. (A) Different constructs transfected to 293T cells overexpressing EXO1 compared to untransfected cells. (B) Stable transformed MEF cells lines carrying EXO1 construct. 293T cells expressing the same construct are shown as positive control. (C) Amaxa-transfected EXO1 construct to transformed MEFs, the same construct transfected to 293T cells is shown as positive control. (D) Doxycycline (dox) inducible EXO1 expression in 293T cells 16h and 24h after adding doxycycline. All the membranes were probed with antibody recognizing human EXO1.

All the tested vectors were under the control of the human cytomegalovirus (CMV) promoter, which has shown to be less effective in mouse fibroblasts compared to human cells (Qin et al. 2010). We therefore tried switching to a vector with a long terminal repeat (LTR) promoter that is more efficient in mouse fibroblasts. We chose the pBabe retroviral vector, which was effective in stably overexpressing FLAG-tagged DNA2 protein in wild type transformed MEFs

(Figure 34A). We replaced DNA2 with the mouse *Exo1* cDNA in the same vector, and created a stably expressing wild type cell line carrying an EXO1-FLAG construct, but we again could not detect EXO1 expression with the FLAG antibody (Figure 34A). We then cloned the mouse cDNA of *Exo1* into empty pBabe vectors with either puromycin or hygromycin resistance. We were able to create stable cell lines with these constructs in wild type and *Exo1* deficient cells (we could not use hygromycin cassette in *Exo1* deficient cells as they are resistant to hygromycin), but we could not detect EXO1 by Western blot (Figure 34B). We assessed the mRNA levels of *Exo1* to test whether the gene was transcribed, and surprisingly, high amount of *Exo1* mRNA was transcribed in transformed MEFs (Figure 34C). This indicated that EXO1 levels might be controlled post-translationally. We therefore added a protease inhibitor MG-132 to the cells to test whether this could prevent EXO1 degradation, but we could not detect EXO1 expression by Western blot even in the presence of MG-132 (Figure 34D).

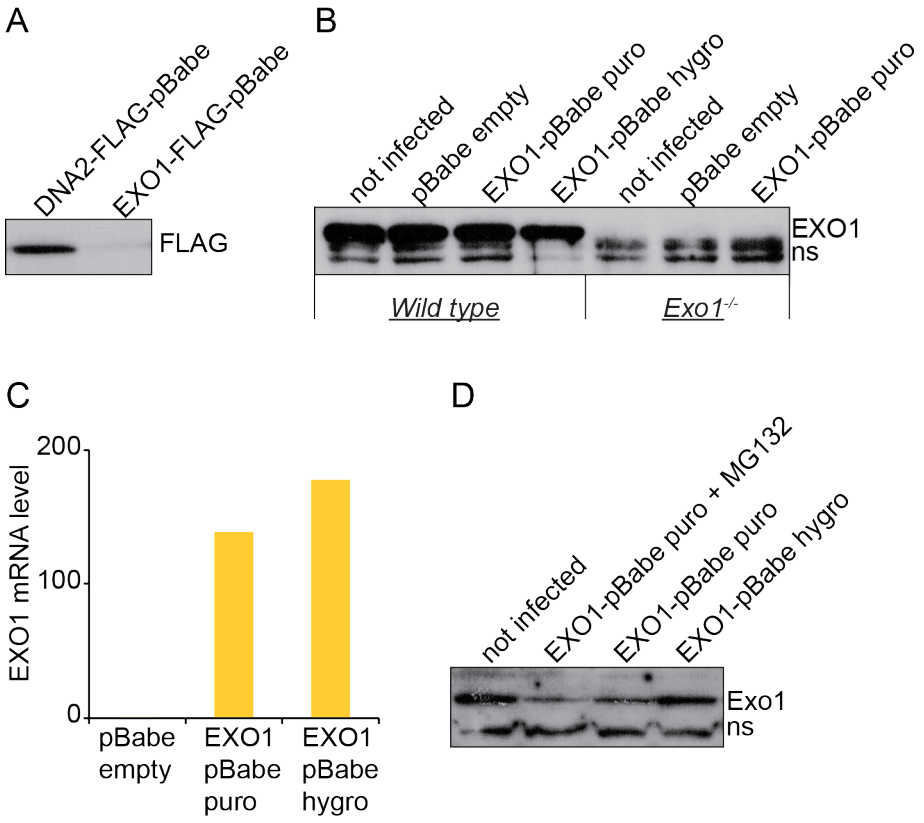

Figure 34. The expression of Exo1-pBabe constructs by Western blot. (A) Wild type transformed MEFs stably expressing DNA2-FLAG and EXO1-FLAG constructs. Membrane was probed with FLAG antibody. (B) Stable transformed MEF cells lines carrying EXO1 constructs. Membrane was probed with antibody recognizing mouse EXO1. (C) Real time PCR showing relative mRNA levels of *Exo1* in wild type transformed MEFs, normalized to empty vector transfected cells. (D) Wild type transformed MEF carrying EXO1 constructs, with the addition of protease inhibitor (MG132).

Since we could detect mRNA expression of *Exo1*, we decided to perform a functional assay using the EXO1-pBabe expressing wild type and double mutant cells. We assessed the G2-M checkpoint defect, which should be rescued in double mutant cells expressing functional EXO1. We observed no difference in wild type or double mutant cells expressing empty pBabe vector or EXO1-pBabe (Figure 35), indicating that EXO1 protein is either not made in those cells or that it is not functional.

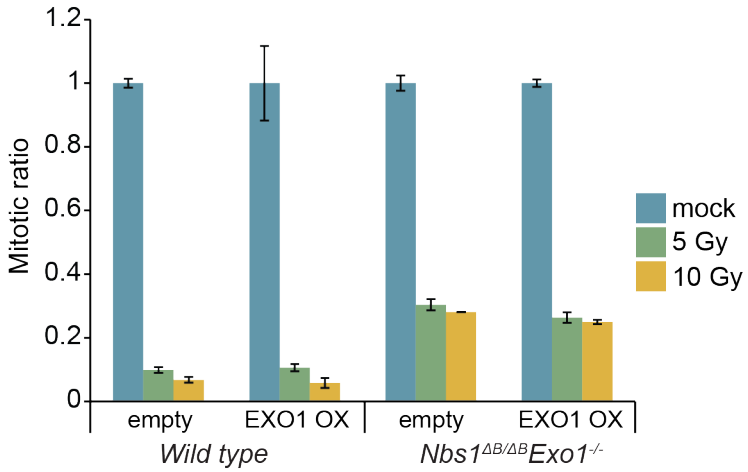

Figure 35. G2-M checkpoint with EXO1-pBabe expressing (EXO1 OX) transformed MEFs. The mitotic ratios of transformed MEFs are presented at 1h post-irradiation. The mitotic ratio of irradiated cells is normalized to mock-treated cells. Error bars indicate standard deviation.

Because we could not overexpress EXO1 to perform complementation experiments, we instead employed siRNA to downregulate it and verify some key results. We downregulated EXO1 in wild type, *Exo1*$^{-/-}$ and *Nbs1*$^{\Delta B/\Delta B}$ cell lines (Figure 36A). We then performed clonogenic survival assay to determine if Exo1 downregulation in *Nbs1* mutant cells rescued the cellular sensitivity to CPT. We confirmed to that downregulating EXO1 in *Nbs1*$^{\Delta B/\Delta B}$ cells rescued the sensitivity to CPT (Figure 36B), and also improved wild type cellular sensitivity, but did not affect the sensitivity of *Exo1* deficient cells (Figure 36B). We also performed the G2-M checkpoint assay and observed that EXO1 downregulation increased the checkpoint defect in *Nbs1*$^{\Delta B/\Delta B}$ cells to levels similar to what we observed in double mutant cells (Figure 36C). As expected, it did not alter the checkpoint defect of wild type or double mutant cells (Figure 36C).

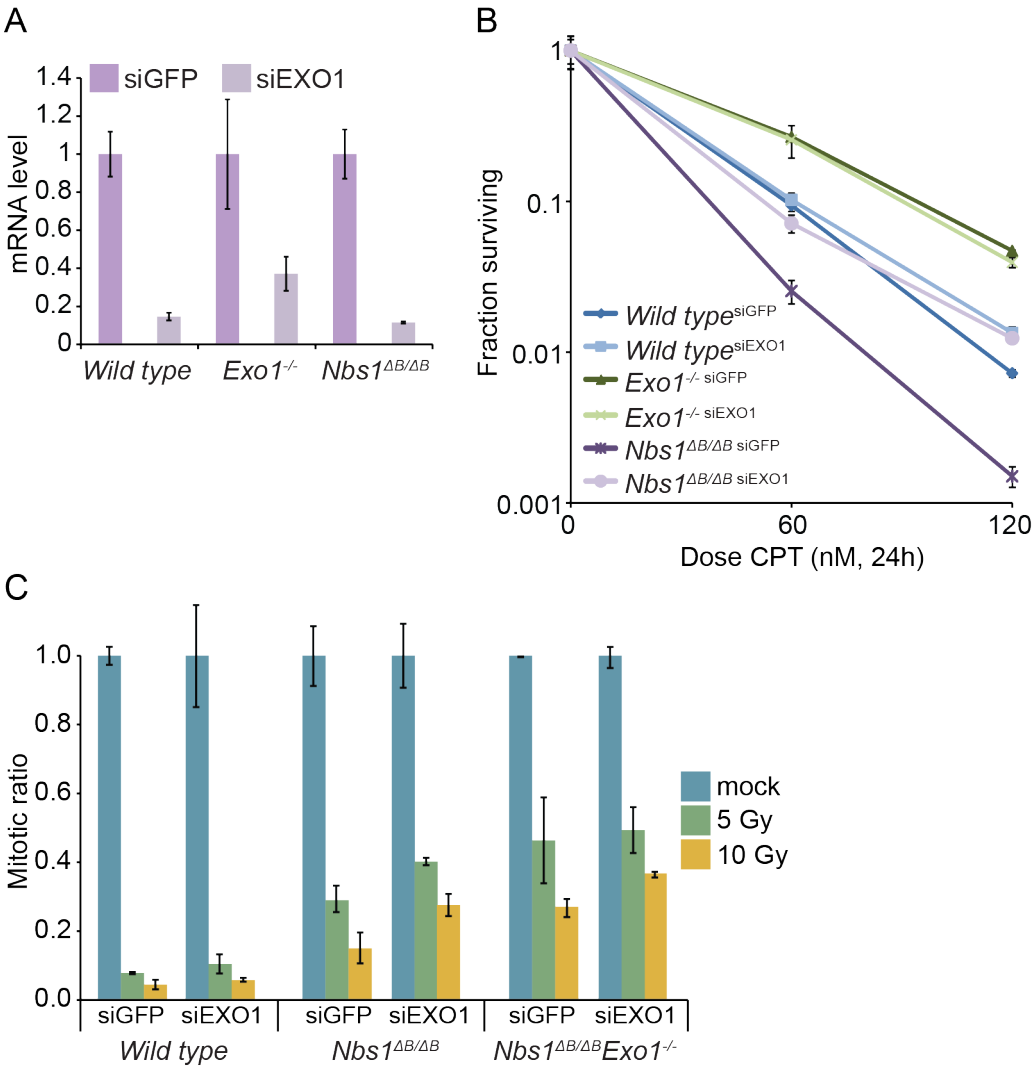

Figure 36. G2-M checkpoint and cellular sensitivity to CPT in *Exo1* downregulated cells by siRNA. (A) Real time PCR showing relative mRNA levels of EXO1 normalized to mock (siRNA against GFP) transfected cells. (B) Cellular sensitivity to CPT in mock (siGFP) and EXO1 downregulated cells (siEXO1) of the indicated genotypes. Error bars indicate standard deviation. (C) G2-M checkpoint of mock (siGFP) and EXO1 downregulated cells (siEXO1) of the indicated genotypes. Mitotic ratios are presented at 1h post-irradiation. The mitotic ratio of irradiated cells is normalized to mock-treated cells. Error bars indicate standard deviation.

8. Alternative model systems to examine the role of EXO1 in MRE11 complex defective cells

As an alternative approach to address the role of EXO1, we used human NBS patient cells. In NBS patients, two different fragments of NBS1 can be expressed: a C-terminal 70 kDa product (NBS^{p70}) containing the MRE11 interaction domain and ATM phosphorylation sites (this product is similar to that expressed in $Nbs1^{\Delta B/\Delta B}$ mice) and an N-terminal 26 kDa product (NBS^{p26}) containing the FHA and BRCT domains (Maser et al. 2001). We used transformed NBS patient fibroblasts (termed NBST), where only NBS^{p26} could be detected (Figure 37).

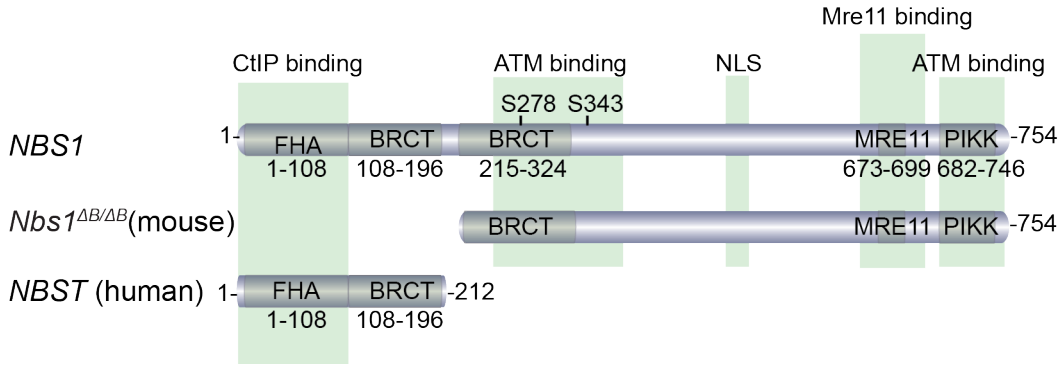

Figure 37. The comparison of mouse and human fibroblasts expressing mutant forms of NBS1. The diagram illustrates the fragments of NBS1 protein that is expressed either in $Nbs1^{\Delta B/\Delta B}$ mice or in NBS patient (NBST) fibroblasts.

We downregulated EXO1 using short hairpin RNA (shRNA) against EXO1 in NBST cells and confirmed the downregulation of EXO1 by real time PCR (Figure 38A). In order to address whether EXO1 downregulation affected the G2-M checkpoint response in NBST cells, we performed the G2-M checkpoint assay. We observed that EXO1 downregulation did not affect the G2-M checkpoint defect of NBST cells (Figure 38B). Next, we examined the cellular sensitivities to IR and CPT by clonogenic survival assays. However, the downregulation of EXO1 did not affect the cellular sensitivities of NBST cells to either IR (Figure 38C) or CPT (Figure 38D).

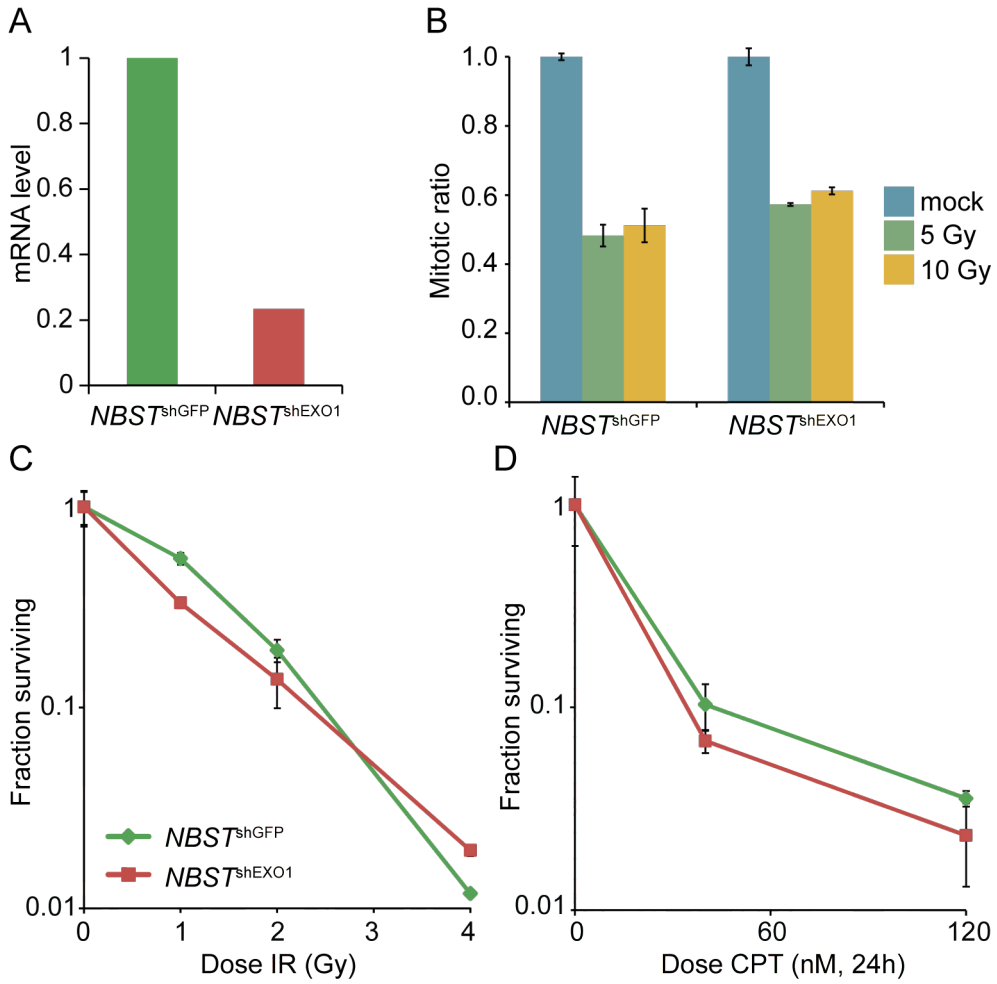

Figure 38. NBST cells with EXO1 downregulation do not recapitulate the mouse system. (A) Real time PCR showing relative mRNA levels of EXO1 normalized to mock (shRNA against GFP) transfected cells. (B) G2-M checkpoint of mock (shGFP) and EXO1 downregulated NBST cells (shEXO1) of the indicated genotypes. Mitotic ratios are presented at 1h post-irradiation. The mitotic ratio of irradiated cells is normalized to mock-treated cells. (C) Cellular sensitivity to IR in mock (shGFP) and EXO1 downregulated cells (shEXO1) NBST cells. (D) Cellular sensitivity to CPT in mock (shGFP) and EXO1 downregulated cells (shEXO1) NBST cells. Error bars indicate standard deviation.

It has been shown that in NBST cells, the MRE11 complex is predominantly cytoplasmic, as NBS^{p26} protein is not physically associated with the MRE11 complex (Maser et al. 2001), opposed to the $Nbs1^{\Delta B/\Delta B}$ mouse fibroblasts where NBS^{p70}-like protein retains its physical association with MRE11 complex and the nuclear localization of the complex (Williams et al. 2002). The lack of nuclear MRE11 complex in NBST cells probably eliminates the initiation of resection and therefore EXO1 downregulation does not affect the G2-M checkpoint responses or cellular sensitivity to DNA-damaging agents.

We also employed *S. cerevisiae* as model system to simultaneously delete Xrs2 (mammalian NBS1) and Exo1. We generated *exo1Δ, xrs2Δ, exo1Δ xrs2Δ and exo1Δ xrs2-R32G-S47A* haploid mutants by crossing isogenic strains. The *xrs2-R32G-S47A* mutant carries mutations in the FHA domain. We monitored the sensitivity to CPT in all the strains. In agreement with the previous studies, we observed that *xrs2Δ* mutant are highly sensitive to CPT and Exo1 deletion in did not rescue the *xrs2Δ* mutant sensitivity to CPT (Figure 39). The *xrs2-R32G-S47A* mutant, opposed to mouse NBS1 where the FHA domain has been mutated, was not sensitive to CPT. Exo1 deletion in *xrs2-R32G-S47A* background resulted in mildly increased sensitivity compared to *exo1Δ* mutant (Figure 39). Similar to human patient cells, complete elimination of Xrs2 in *S. cerevisiae* also results in the destabilization of the whole MRE11 complex, therefore it would be interesting to address whether expressing a hypomorphic form of Nbs1 similar to NBS^{p70} in *S. cerevisiae* results in the same outcome as we see in mouse cells.

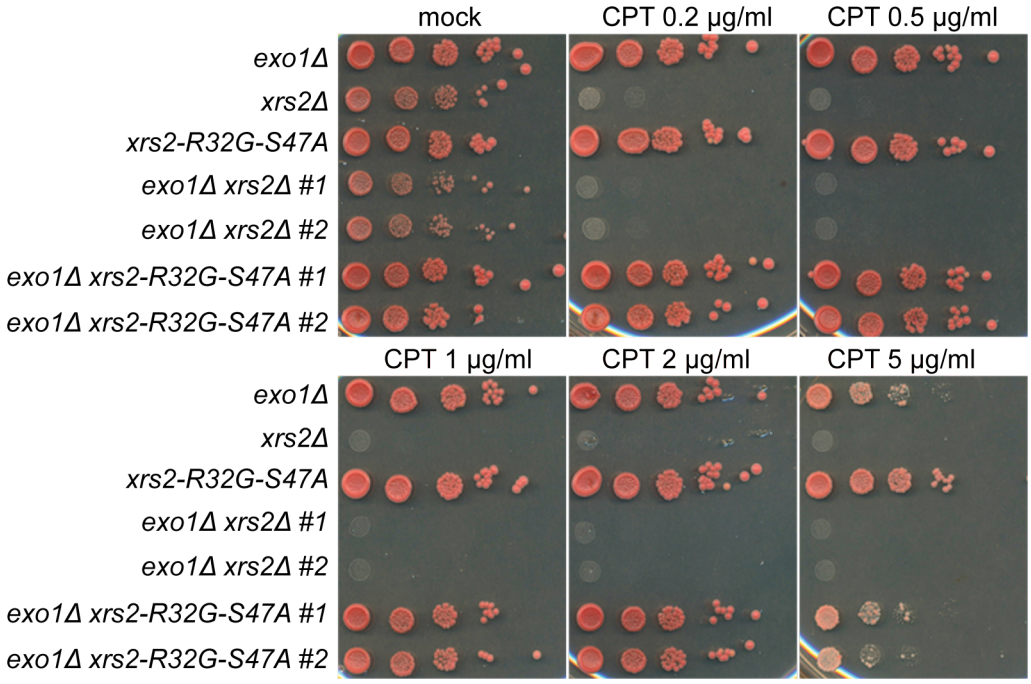

Figure 39. Exo1 deletion does not rescue the Xrs2 sensitivity to CPT in *S. Cerevisiae*. Exponentially growing cells of the indicated genotypes were 1:10 serially diluted and spotted onto selective plates containing increasing doses of CPT.

DISCUSSION

Discussion

The main aim of this project was to examine the genetic interaction between mammalian EXO1 and hypomorphic mutations in the MRE11 complex. The MRE11 complex has an essential role in replication fork progression and the cellular responses to DSBs (Stracker & Petrini 2011), and deletion of any of its members leads to embryonic lethality (Buis et al. 2008; Zhu et al. 2001; Luo et al. 1999). EXO1 is proposed to act downstream of the MRE11 complex following DSB detection by promoting DNA resection and HDR (Zhu et al. 2008; Mimitou & Symington 2008) and processing stalled replication forks in checkpoint-defective cells (Cotta-Ramusino et al. 2005; Froget et al. 2008; Segurado & Diffley 2008). The choice to examine the interaction of the MRE11 complex with EXO1 was based largely on work from *S. cerevisiae* studies. In *S. cerevisiae*, mutations of Mre11-Rad50-Xrs2 (MRX complex; mammalian MRE11 complex) members combined with those in Exo1 led to synthetic phenotypes such as impaired growth, reduced DSB resection and homologous recombination events, and elevated cellular sensitivity to DNA damaging agents (Moreau et al. 2001; Lewis et al. 2002; Tsubouchi & Ogawa 2000). Exo1 overexpression in *S. cerevisiae* was also found to bypass the requirement for the MRX complex in resection-related events but did not suppress defects in NHEJ (Tsubouchi & Ogawa 2000). The same genetic interactions are not observed between the MRE11 complex and other MMR proteins, suggesting that the phenotypes are independent from the role of EXO1 in MMR (Collins et al. 2007). This led to the speculation that EXO1 might bypass the requirement for fully functional MRE11 complex in mammalian cells to promote HDR and cell viability. As deletions in MRE11 complex genes are lethal, we used $Nbs1^{\Delta B/\Delta B}$ mice, which display similar cellular phenotypes to NBS patients, such as increased sensitivity to DNA damaging agents and mild G2-M checkpoint defect following IR. However, $Nbs1^{\Delta B/\Delta B}$ mice show very mild developmental defects and subfertility, but are not tumor-prone, and their survival is similar to wild type mice (Williams et al. 2002; Cherry et al. 2007). *Exo1* null mice show a modest reduction in survival (50% survival at the age of 17 months), increased

susceptibility to the development of lymphomas and are sterile due to meiotic failure (Schaetzlein et al. 2013; Wei et al. 2003), but their cellular responses to DSBs and replication defects have not been investigated thoroughly.

We observed a strong genetic interaction between EXO1 deficiency and the hypomorphic *Nbs1* mutation that resulted in embryonic lethality. Double mutant embryos at E14.5 were runted and had impaired nervous system development that included cranial malformation and neural tube closure defects. We are now in the process of characterizing the brain development of double mutant embryos as central nervous system (CNS) defects are the main pathology of human disease resulting from hypomorphic mutations in the MRE11 complex, such as in NBS and ATLD. Our preliminary results confirm CNS defects, as we observed smaller brains with a thinner cortical layer. In future work, we will examine the ventricular zone of the cortex in more detail to assess cell death and stem cell pools. We will also isolate neurosphere cultures to determine if they show similar defects as MEFs. Taken together, our results establish that the synthetic interaction between the MRE11 complex and EXO1 is evolutionarily conserved and indicates that EXO1 has many MRE11 complex independent roles that are required for organismal development when MRE11 complex functions are reduced. This could suggest that EXO1 mutations could be major modifiers of the pathological severity in ATLD and NBS. This could extend to A-T, the genomic instability syndrome resulting from mutations in ATM. We have initiated crosses between ATM and EXO1 deficient mice, but have not obtained any pups from at least 6 double heterozygous crosses. This is suggesting the possibility that EXO1 and ATM haploinsufficiency reduces fertility, a question we will examine more closely in future work.

At the cellular level, our data reveals a crucial role for EXO1 in DNA replication when MRE11 complex functions are compromised. The double mutant primary fibroblasts grow poorly, display a strong reduction in DNA synthesis and have decreased replication fork progression speed. Our data suggests that the double mutant cells enter mitosis without fully completing the S-phase, resulting in anaphase bridges, micronuclei and persistent DSBs. This leads to

chromosomal instability, as we observed highly elevated chromosomal aberrations in double mutant cells with a high incidence of chromatid breaks, confirming that the damage is arising from S-phase. This possibly leads to p53 activation and short term G1 checkpoint arrest followed by senescence. However, we believe that the deletion of p53 would not rescue the synthetic lethality as the SV40 transformed MEFs where p53 is inactivated grow poorly and retain highly elevated levels of chromosome aberrations. Similar to our data, yeast studies have revealed that that nearly all DSBs are converted to chromosome breaks in cells lacking both Exo1 and Rad50 (Nakai et al. 2011). This suggests the role of EXO1 in maintaining replication fork integrity and preventing replication-associated damage in MRE11 mutants, thereby maintaining chromosomal integrity of the cells. The MRE11 complex has a crucial role during replication, potentially by promoting ATR kinase activation in response to damage in S-phase (Stracker & Petrini 2011). We propose that EXO1 provides essential compensatory activities during S-phase if the MRE11 complex is not fully functional. EXO1 could process aberrant replication fork structures or promote resection at gaps or breaks, both of which would promote ATR activation in response to replication stress, ensuring that the incomplete S-phase does not proceed to mitosis (Figure 40).

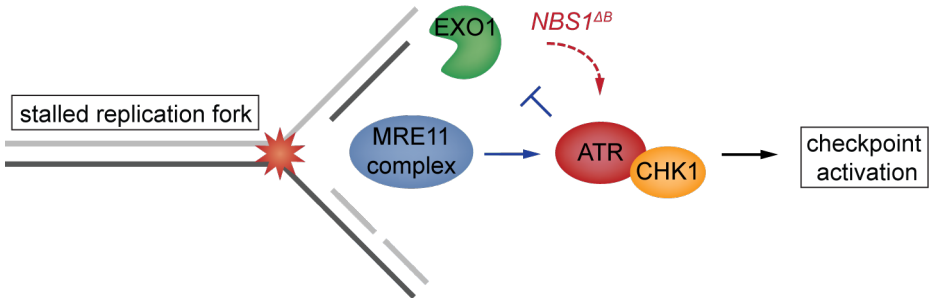

Figure 40. Proposed model for the role of EXO1 during DNA replication. In wild type cells, MRE11 complex promotes ATR kinase activation (blue arrow) if the replication fork is stalled. Normally, ATR inhibits EXO1, but its activity is increased in the defective *Nbs1*$^{\Delta B/\Delta B}$ background due to checkpoint defects (red arrow), enabling EXO1 to process gaps or replication structures that would promote ATR activation and partially compensate for the loss of MRE11 complex function.

Many studies revealed an important role for the MRE11 complex in promoting DNA resection that is necessary for HDR after DSBs, and EXO1 is proposed to act in tandem with MRE11 complex (Zhu et al. 2008; Mimitou & Symington 2008). The necessity for EXO1 in mammalian cells for resection is not very clear as some studies report that EXO1 is essential for promoting DSB resection (Bolderson et al. 2010; Tomimatsu et al. 2014; Tomimatsu et al. 2012) while others suggest very mild phenotypes, mainly due to the complementary or redundant functions of EXO1 in resection with BLM and DNA2 (Gravel et al. 2008; Zhu et al. 2008; Karanja et al. 2012). Our data confirmed that EXO1 deficiency alone does not detectably impair resection and that the NBS1 hypomorphic mutation results in resection defects, measured by SSA efficiency and RPA S4/S8 phosphorylation. Double mutant cells, however, display stronger defects in SSA along with impaired CHK1 phosphorylation, indicating that EXO1 becomes essential for the resection and ATR activation if MRE11 complex functions are defective. The lack of resection defect in EXO1 deficient cells likely reflects the ability of MRE11 complex to promote the recruitment of additional factors for resection, such as BLM and DNA2. Indeed, in yeast, MRX complex recruits Sgs1 (mammalian BLM) to DNA ends (Mimitou & Symington 2010; Chiolo et al. 2005). The MRE11 complex can also stimulate EXO1-mediated resection (Cannavo et al. 2013; Nimonkar et al. 2011), but EXO1 resection activity is also promoted by PCNA and the structurally related 9-1-1 complex (X. Chen et al. 2013; Ngo et al. 2014), potentially providing alternative recruitment options (Figure 41).

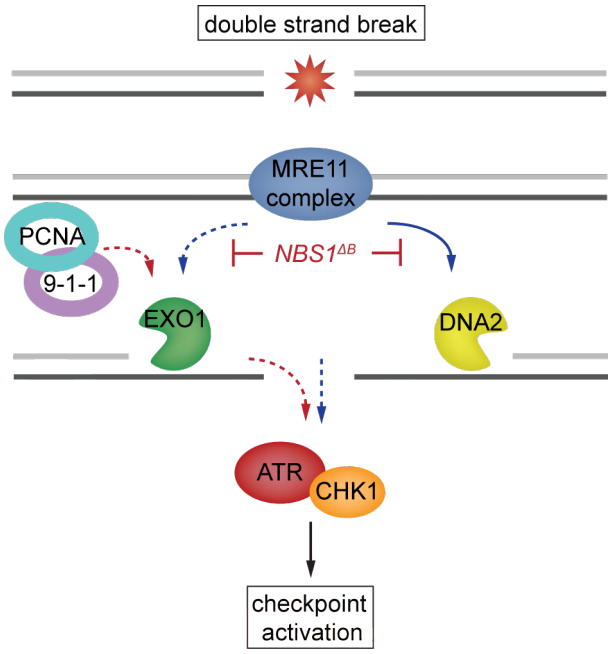

Figure 41. Proposed model for the role of EXO1 in DSB resection. In wild type cells, the resection is initiated by the MRE11 complex that promotes the longer-range resection by EXO1 and/or DNA2-BLM (blue arrows). In the defective *Nbs1*$^{\Delta B/\Delta B}$ background, EXO1 could be recruited independently from the MRE11 complex by PCNA and/or the 9-1-1 complex, enabling longer range resection to take place, which leads to ATR activation.

Another aspect to consider in explaining the resection data is the FHA domain of NBS1, which is deleted in the *Nbs1*$^{\Delta B}$ allele. This domain is implicated in the interaction with CtIP and its subsequent phosphorylation by ATM (Wang et al. 2013), which promotes resection, suggesting that this could underlie the resection defect in NBS1 hypomorphic cells. However, we did not observe defective CtIP phosphorylation following CPT or IR treatment in the single or double mutant cells. This could indicate that some specific phosphorylation events are impaired that we were not able to detect with the antibody used. Alternatively, that CtIP phosphorylation could occur in the absence of the NBS1 FHA and BRCT domains and full activation of ATM, which is consistent with a role of CDKs for CtIP phosphorylation that was found to be a prerequisite for ATM to phosphorylate CtIP (Wang et al. 2013).

Our results suggest a role for EXO1 in promoting G2-M checkpoint induction when the MRE11 complex is compromised. We observe that after high dose of IR, a large fraction of double mutant cells escape G2 arrest and enter mitosis,

compared to the mild checkpoint defect in NBS1 hypomorphic cells and no defect in EXO1 deficient cells. Consistent with the G2-M checkpoint defect, we observed reduced CHK2 phosphorylation in NBS1 hypomorphic and double mutant cells in response to IR. However, in addition to the CHK2 phosphorylation defect, double mutant cells also exhibited deficient ATM phosphorylation. This could indicate that other ATM activities, besides CHK2 phosphorylation, are contributing to the checkpoint arrest and depend on EXO1 when MRE11 functions are compromised. One possibility is that EXO1 activity through generating ssDNA enhances RAD17 recruitment, which has been shown to increase ATM activation (Q. Wang et al. 2014; Rein & Stracker 2014). Studies show that the G2-M checkpoint is essential for preventing tumor initiation (Kastan & Bartek 2004), thereby EXO1 activities could be important in suppressing malignancies in MRE11 mutant backgrounds. This is consistent with additional genetic studies that correlated G2-M checkpoint defects with tumor suppression in a variety of experimental settings involving different MRE11 complex alleles (Stracker et al. 2008; Stracker et al. 2007; Foster et al. 2012; Gupta et al. 2013).

We used several DNA damaging agents to determine the influence of EXO1 on cellular sensitivity. We found that the lack of EXO1 contributes to UV sensitivity independently of NBS1 status, consistent with the proposed role of EXO1 in processing NER intermediates (Giannattasio et al. 2010). Although the MRE11 complex has been also implicated in UV sensitivity (Brugmans et al. 2009; Yanagihara et al. 2011), we have not seen in previous experiments the sensitivity to UV in NBS1 hypomorphic cells from either mice or humans. However, the lack of EXO1 exacerbates the sensitivity to IR, MMC and cisplatin in NBS1 hypomorphic cells, while not causing any detectable sensitivity on its own. All of these DNA damaging agents induce DNA resection and/or G2-M checkpoint activation (Kottemann & Smogorzewska 2013; Xu et al. 2002) consistent with the proposed role of EXO1 in DNA resection and G2-M checkpoint induction in NBS1 hypomorphic cells. Strikingly, we discovered that EXO1 promotes cell death in response to CPT, as EXO1 deficiency results in enhanced survival after treatment with CPT and rescues the sensitivity of *Nbs1*

mutants, especially at low CPT doses where fewer DSBs are generated. This was a surprising and interesting result, leading us to investigate the basis for this rescue.

TOP1 inhibition with CPT at low concentration in yeast and human cells has been shown to induce replication fork slowing and promote aberrant replication fork structures, mainly reversed forks, which is uncoupled from DSB formation (Ray Chaudhuri et al. 2012). We do not observe initial replication fork slowing in response to low CPT dose, suggesting that in mouse fibroblasts the replication stress is subtle enough to escape surveillance pathways and allow cells to continue to G2-phase where we observe cells accumulating. For these reasons it was technically not possible to directly monitor the replication fork stability and restart. However, from the replication restart experiments with HU treatment we observed that EXO1 has negative influence on fork restart. We therefore speculated that EXO1 might have a role in processing regressed replication forks or other aberrant fork structures that could lead to the generation of replication intermediates that are toxic for the cells. Consistent with that, several yeast studies showed that Exo1 activities must be tightly controlled to prevent over-resection (Cotta-Ramusino et al. 2005; Segurado & Diffley 2008). The endonuclease MUS81 and DNA helicase FBH1 have both been implicated in processing abnormal replication structures (Fugger et al. 2013; Jeong et al. 2013; Mankouri et al. 2013). We therefore downregulated MUS81 and FBH1 in our mutants to verify whether they work in the same pathway as EXO1. Indeed, we observed that downregulating either MUS81 or FBH1 rescued the CPT sensitivity of *Nbs1* mutants but did not affect the sensitivity of EXO1 deficient cells to the same degree. Collectively, we propose that EXO1 can process CPT-induced lesions, such as regressed forks, and thereby generate toxic breakdown products either directly or indirectly through additional nucleases such as MUS81 or FBH1. Fork processing by EXO1 is normally prevented by the MRE11 complex that may act directly by stabilizing fork structures to prevent degradation and/or indirectly by promoting checkpoint activation to reduce EXO1 activity (Figure 42).

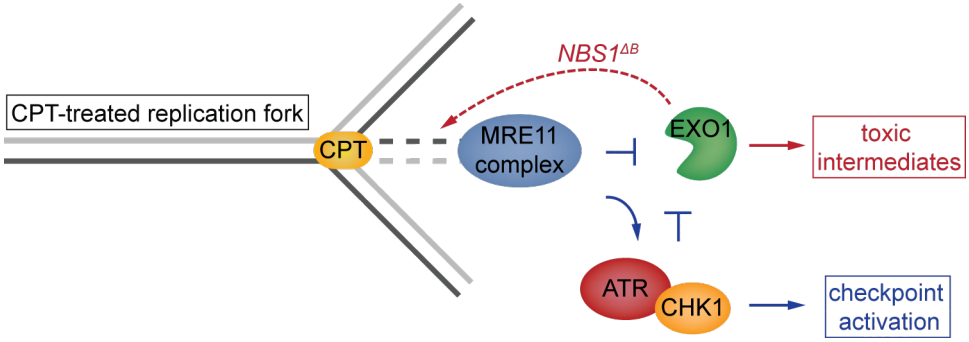

Figure 42. Proposed model for the role of EXO1 in promoting CPT sensitivity. In wild type cells, MRE11 is stabilizing regressed forks by prevent their degradation and/or activating ATR kinase (blue arrow). In the defective *Nbs1*$^{\Delta B/\Delta B}$ background, EXO1 can process the regressed forks and thereby generate toxic intermediates.

MUS81 activity is strictly limited to mitosis (Gallo-Fernández et al. 2012) in normal cells but checkpoint inhibition allows it to be active and promote replication fork degradation during S-phase. Our results suggest that MUS81 promotes the sensitivity of NBS1 mutants to CPT, suggesting that impaired intra-S and G2-M activation may allow excessive MUS81 activity. As MRE11 complex members and EXO1 are mutated in human cancers, these results could be applicable to mechanisms of clinical therapy resistance. This is especially relevant in cases of HNPCC and sporadic colorectal cancer where EXO1 mutations are found (Liberti & Rasmussen 2004) and a CPT derivate irinotecan is commonly used for the treatment (Vasen et al. 2007).

Little is known about EXO1 posttranscriptional regulation and we therefore wanted to perform complementation experiments with EXO1 phospho-mimic and phospho-mutants in EXO1 deficient and double mutant cells to reveal how these modifications impact EXO1 function. Yeast studies identified Exo1 as a target of the ATR pathway (Tsang et al. 2014) and studies with human cells show that EXO1 is phosphorylated by both ATM and ATR (Bolderson et al. 2010; El-Shemerly et al. 2008), both of which were proposed to inhibit EXO1 activity to prevent excessive degradation and control its stability. Recently, CDKs were reported to phosphorylate EXO1 to promote resection (Tomimatsu et al. 2014). Understanding the regulation of EXO1 could be beneficial to fully explain the mechanism by which EXO1 promotes the cellular responses to DNA damage in MRE11 complex mutants. Despite numerous attempts using

different expression systems and both the mouse and human cDNAs, we could not detectably express EXO1 protein in mouse fibroblasts. Currently, no other studies report EXO1 overexpression in mouse cells, although we and other groups were able to overexpress EXO1 in human cancer cell lines, such as 293T and U2OS (Karanja et al. 2012; Tomimatsu et al. 2012; Tomimatsu et al. 2014; Bolderson et al. 2010). This may reflect translational regulation and require the addition of untranslated region (UTR) sequence or the use of a BAC that contains the introns. As EXO1 expression can potentially destroy DNA structures that are essential for cell viability, its activity must be precisely regulated to avoid cellular toxicity. Similarly, unregulated DNA2 can cause over-resection, counteracting the correct repair of the lesion by HDR (Karanja et al. 2014). Our results indicate that EXO1 levels are controlled post-transcriptionally at many levels as we see highly elevated EXO1 mRNA with several constructs that were used to over-express EXO1 but no detectable protein.

In summary, our results demonstrate a genetic and functional relationship between the MRE11 complex and EXO1. We have shown that EXO1 becomes essential for mammalian development, S-phase progression and the cellular responses to DNA damage in the context of a relatively mild NBS1 mutation. As these defects are not apparent in normal cells, this clearly defines essential functions for EXO1 in DNA replication and DSB repair when the MRE11 complex is compromised. While consistent with EXO1 operating downstream of the MRE11 complex in some roles, it suggests that the crucial functions of EXO1 are likely to be largely independent of the MRE11 complex. Our results also indicate that EXO1, FBH1 and MUS81 may be important modifiers of phenotypic severity in NBS, ATLD and NBSLD, the hereditary diseases associated with hypomorphic mutations of MRE11 complex. Moreover, EXO1 could be an important modulator of the sensitivity or resistance to different DNA damaging agents and its status should be considered as a target in cancer therapy. Future work will be required to fully understand the complex genetic relationships of EXO1 as well as its regulation at the molecular level.

Conclusions

1. Loss of EXO1 in *Nbs1* hypomorphic mice leads to synthetic lethality.
2. EXO1 is essential for cell growth and chromosomal stability when MRE11 complex functions are compromised.
3. Loss of EXO1 impairs checkpoint response, signal transduction and resection in MRE11 defective cells after DNA damage.
4. Loss of EXO1 modifies the SSA defect in NBS1 mutants.
5. Loss of EXO1 differentially influences the sensitivity of MRE11 complex defective cells to DNA damaging agents.
6. EXO1 is necessary for replication fork stability when MRE11 complex functions are compromised.
7. EXO1 loss rescues the camptothecin sensitivity of MRE11 complex mutants.

References

Ahn, J., Urist, M. & Prives, C., 2004. The Chk2 protein kinase. *DNA repair*, 3(8-9), pp.1039–47.

Alam, N.A. et al., 2003. Germline deletions of EXO1 do not cause colorectal tumors and lesions which are null for EXO1 do not have microsatellite instability. *Cancer Genetics and Cytogenetics*, 147, pp.121–127.

Alani, E., Padmore, R. & Kleckner, N., 1990. Analysis of wild-type and rad50 mutants of yeast suggests an intimate relationship between meiotic chromosome synapsis and recombination. *Cell*, 61, pp.419–436.

Amin, N.S. et al., 2001. exo1-Dependent mutator mutations: model system for studying functional interactions in mismatch repair. *Molecular and cellular biology*, 21(15), pp.5142–55.

Bak, S.T., Sakellariou, D. & Pena-Diaz, J., 2014. The dual nature of mismatch repair as antimutator and mutator: for better or for worse. *Frontiers in genetics*, 5(August), p.287.

Bakkenist, C.J. & Kastan, M.B., 2003. DNA damage activates ATM through intermolecular autophosphorylation and dimer dissociation. *Nature*, 421(6922), pp.499–506.

Balmaña, J. et al., 2011. Stumbling blocks on the path to personalized medicine in breast cancer: the case of PARP inhibitors for BRCA1/2-associated cancers. *Cancer discovery*, 1(1), pp.29–34.

Bardwell, P.D. et al., 2004. Altered somatic hypermutation and reduced class-switch recombination in exonuclease 1-mutant mice. *Nature immunology*, 5(2), pp.224–9.

Barlow, C. et al., 1996. Atm-deficient mice: a paradigm of ataxia telangiectasia. *Cell*, 86(1), pp.159–71.

Bartek, J., Bartkova, J. & Lukas, J., 2007. DNA damage signalling guards against activated oncogenes and tumour progression. *Oncogene*, 26(56), pp.7773–9.

Bartek, J., Lukas, C. & Lukas, J., 2004. Checking on DNA damage in S phase. *Nature reviews. Molecular cell biology*, 5(10), pp.792–804.

Bender, C.F. et al., 2002. Cancer predisposition and hematopoietic failure in Rad50(S/S) mice. *Genes & development*, 16(17), pp.2237–51.

Bennardo, N. et al., 2009. Limiting the persistence of a chromosome break diminishes its mutagenic potential. *PLoS genetics*, 5(10), p.e1000683.

Berger, J.M. & Wang, J.C., 1996. Recent developments in DNA topoisomerase II structure and mechanism. *Current opinion in structural biology*, 6(1), pp.84–90.

Bolderson, E. et al., 2010. Phosphorylation of Exo1 modulates homologous recombination repair of DNA double-strand breaks. *Nucleic acids research*, 38(6), pp.1821–31.

Bouwman, P. & Jonkers, J., 2012. The effects of deregulated DNA damage signalling on cancer chemotherapy response and resistance. *Nature reviews. Cancer*, 12(9), pp.587–98.

Branzei, D. & Foiani, M., 2010. Maintaining genome stability at the replication fork. *Nature reviews. Molecular cell biology*, 11(3), pp.208–19.

Bregenhorn, S. & Jiricny, J., 2014. Biochemical characterization of a cancer-associated E109K missense variant of human exonuclease 1. *Nucleic acids research*, 42(11), pp.7096–103.

Brem, R. & Hall, J., 2005. XRCC1 is required for DNA single-strand break repair in human cells. *Nucleic acids research*, 33(8), pp.2512–20.

Brown, E.J. & Baltimore, D., 2000. ATR disruption leads to chromosomal fragmentation and early embryonic lethality. *Genes & development*, 14(4), pp.397–402.

Brugmans, L. et al., 2009. NBS1 cooperates with homologous recombination to counteract chromosome breakage during replication. *DNA repair*, 8(12), pp.1363–70.

Bruhn, C. et al., 2014. The essential function of the MRN complex in the resolution of endogenous replication intermediates. *Cell reports*, 6(1), pp.182–95.

Buis, J. et al., 2008. Mre11 nuclease activity has essential roles in DNA repair and genomic stability distinct from ATM activation. *Cell*, 135(1), pp.85–96.

Bunting, S.F. et al., 2010. 53BP1 inhibits homologous recombination in Brca1-deficient cells by blocking resection of DNA breaks. *Cell*, 141(2), pp.243–54.

Bunting, S.F. et al., 2012. BRCA1 functions independently of homologous recombination in DNA interstrand crosslink repair. *Molecular cell*, 46(2), pp.125–35.

Van der Burgt, I. et al., 1996. Nijmegen breakage syndrome. *Journal of medical genetics*, 33(2), pp.153–6.

Buscemi, G. et al., 2001. Chk2 activation dependence on Nbs1 after DNA damage. *Molecular and cellular biology*, 21, pp.5214–5222.

Caldecott, K.W., 2014. DNA single-strand break repair. *Experimental cell research*, 329(1), pp.2–8.

Caldecott, K.W., 2014. Protein ADP-ribosylation and the cellular response to DNA strand breaks. *DNA repair*, 19, pp.108–13.

Callén, E. et al., 2009. Essential Role for DNA-PKcs in DNA Double-Strand Break Repair and Apoptosis in ATM-Deficient Lymphocytes. *Molecular Cell*, 34, pp.285–297.

Campbell, K. et al., 2011. Specific GATA Factors Act as Conserved Inducers of an Endodermal-EMT. *Developmental Cell*, 21, pp.1051–1061.

Canman, C.E. et al., 1998. Activation of the ATM kinase by ionizing radiation and phosphorylation of p53. *Science (New York, N.Y.)*, 281(5383), pp.1677–9.

Cannavo, E., Cejka, P. & Kowalczykowski, S.C., 2013. Relationship of DNA degradation by Saccharomyces cerevisiae exonuclease 1 and its stimulation by RPA and Mre11-Rad50-Xrs2 to DNA end resection. *Proceedings of the National Academy of Sciences of the United States of America*, 110(18), pp.E1661–8.

Cannon, B. et al., 2013. Visualization of local DNA unwinding by Mre11/Rad50/Nbs1 using single-molecule FRET. *Proceedings of the National Academy of Sciences of the United States of America*, 110(47), pp.18868–73.

Carr, A.M. & Lambert, S., 2013. Replication stress-induced genome instability: the dark side of replication maintenance by homologous recombination. *Journal of molecular biology*, 425(23), pp.4733–44.

Chapman, J.R. & Jackson, S.P., 2008. Phospho-dependent interactions between NBS1 and MDC1 mediate chromatin retention of the MRN complex at sites of DNA damage. *EMBO reports*, 9(8), pp.795–801.

Chapman, J.R., Taylor, M.R.G. & Boulton, S.J., 2012. Playing the end game: DNA double-strand break repair pathway choice. *Molecular cell*, 47(4), pp.497–510.

Chaudhuri, J. et al., 2007. Evolution of the immunoglobulin heavy chain class switch recombination mechanism. *Advances in immunology*, 94(06), pp.157–214.

Chen, H., Lisby, M. & Symington, L.S., 2013. RPA coordinates DNA end resection and prevents formation of DNA hairpins. *Molecular cell*, 50(4), pp.589–600.

Chen, P.-L. et al., 2005. Inactivation of CtIP leads to early embryonic lethality mediated by G1 restraint and to tumorigenesis by haploid insufficiency. *Molecular and cellular biology*, 25(9), pp.3535–42.

Chen, X. et al., 2013. PCNA promotes processive DNA end resection by Exo1. *Nucleic acids research*, 41(20), pp.9325–38.

Cherry, S.M. et al., 2007. The Mre11 complex influences DNA repair, synapsis, and crossing over in murine meiosis. *Current biology : CB*, 17(4), pp.373–8.

Cheung-Ong, K., Giaever, G. & Nislow, C., 2013. DNA-damaging agents in cancer chemotherapy: serendipity and chemical biology. *Chemistry & biology*, 20(5), pp.648–59.

Chiolo, I. et al., 2005. Srs2 and Sgs1 DNA helicases associate with Mre11 in different subcomplexes following checkpoint activation and CDK1-mediated Srs2 phosphorylation. *Molecular and cellular biology*, 25(13), pp.5738–51.

Ciccia, A. & Elledge, S.J., 2010. The DNA damage response: making it safe to play with knives. *Molecular cell*, 40(2), pp.179–204.

Cimprich, K. a & Cortez, D., 2008. ATR: an essential regulator of genome integrity. *Nature reviews. Molecular cell biology*, 9(8), pp.616–27.

Cleaver, J.E., Lam, E.T. & Revet, I., 2009. Disorders of nucleotide excision repair: the genetic and molecular basis of heterogeneity. *Nature reviews. Genetics*, 10(11), pp.756–68.

Collins, S.R. et al., 2007. Functional dissection of protein complexes involved in yeast chromosome biology using a genetic interaction map. *Nature*, 446, pp.806–810.

Cooper, G.M. & Hausman, R.E., 2007. *The Cell: A Molecular Approach 2nd Edition*,

Cotta-Ramusino, C. et al., 2005. Exo1 processes stalled replication forks and counteracts fork reversal in checkpoint-defective cells. *Molecular cell*, 17(1), pp.153–9.

Critchlow, S.E., Bowater, R.P. & Jackson, S.P., 1997. Mammalian DNA double-strand break repair protein XRCC4 interacts with DNA ligase IV. *Current biology : CB*, 7, pp.588–598.

Daley, J.M. & Sung, P., 2014. 53BP1, BRCA1, and the choice between recombination and end joining at DNA double-strand breaks. *Molecular and cellular biology*, 34(8), pp.1380–8.

David, S.S., O'Shea, V.L. & Kundu, S., 2007. Base-excision repair of oxidative DNA damage. *Nature*, 447(7147), pp.941–50.

Davidson, D. et al., 2013. Small Molecules, Inhibitors of DNA-PK, Targeting DNA Repair, and Beyond. *Frontiers in pharmacology*, 4(January), p.5.

Demuth, I. et al., 2004. An inducible null mutant murine model of Nijmegen breakage syndrome proves the essential function of NBS1 in chromosomal stability and cell viability. *Human molecular genetics*, 13(20), pp.2385–97.

Deshpande, R. a et al., 2014. ATP-driven Rad50 conformations regulate DNA tethering, end resection, and ATM checkpoint signaling. *The EMBO journal*, 33(5), pp.482–500.

Dherin, C. et al., 2009. Characterization of a highly conserved binding site of Mlh1 required for exonuclease I-dependent mismatch repair. *Molecular and cellular biology*, 29(3), pp.907–18.

Difilippantonio, S. et al., 2007. Distinct domains in Nbs1 regulate irradiation-induced checkpoints and apoptosis. *The Journal of experimental medicine*, 204(5), pp.1003–11.

Difilippantonio, S. et al., 2005. Role of Nbs1 in the activation of the Atm kinase revealed in humanized mouse models. *Nature cell biology*, 7(7), pp.675–85.

Donzelli, M. & Draetta, G.F., 2003. Regulating mammalian checkpoints through Cdc25 inactivation. *EMBO reports*, 4(7), pp.671–7.

Dudley, D.D. et al., 2005. Mechanism and control of V(D)J recombination versus class switch recombination: similarities and differences. *Advances in immunology*, 86(D), pp.43–112.

Dueva, R. & Iliakis, G., 2013. Alternative pathways of non-homologous end joining (NHEJ) in genomic instability and cancer. , 2(3), pp.163–177.

Dupré, A. et al., 2008. A forward chemical genetic screen reveals an inhibitor of the Mre11-Rad50-Nbs1 complex. *Nature chemical biology*, 4(2), pp.119–25. h

Duursma, A.M. et al., 2013. A role for the MRN complex in ATR activation via TOPBP1 recruitment. *Molecular cell*, 50(1), pp.116–22.

Edwards, S.L. et al., 2008. Resistance to therapy caused by intragenic deletion in BRCA2. *Nature*, 451(7182), pp.1111–5.

El-Shemerly, M. et al., 2008. ATR-dependent pathways control hEXO1 stability in response to stalled forks. *Nucleic acids research*, 36(2), pp.511–9.

Falck, J. et al., 2002. The DNA damage-dependent intra-S phase checkpoint is regulated by parallel pathways. *Nature genetics*, 30(3), pp.290–4.

Falck, J., Coates, J. & Jackson, S.P., 2005. Conserved modes of recruitment of ATM, ATR and DNA-PKcs to sites of DNA damage. *Nature*, 434(7033), pp.605–11.

Fiorentini, P. et al., 1997. Exonuclease I of Saccharomyces cerevisiae functions in mitotic recombination in vivo and in vitro. *Molecular and cellular biology*, 17(5), pp.2764–73.

Fong, P.C. et al., 2009. Inhibition of poly(ADP-ribose) polymerase in tumors from BRCA mutation carriers. *The New England journal of medicine*, 361(2), pp.123–34.

Forment, J. V et al., 2011. Structure-specific DNA endonuclease Mus81/Eme1 generates DNA damage caused by Chk1 inactivation. *PloS one*, 6(8), p.e23517.

Foster, S.S. et al., 2012. Cell cycle- and DNA repair pathway-specific effects of apoptosis on tumor suppression. *Proceedings of the National Academy of Sciences of the United States of America*, 109(25), pp.9953–8.

Frappart, P.-O. et al., 2005. An essential function for NBS1 in the prevention of ataxia and cerebellar defects. *Nature medicine*, 11(5), pp.538–44.

Froget, B. et al., 2008. Cleavage of stalled forks by fission yeast Mus81/Eme1 in absence of DNA replication checkpoint. *Molecular biology of the cell*, 19(2), pp.445–56.

Fugger, K. et al., 2013. FBH1 co-operates with MUS81 in inducing DNA double-strand breaks and cell death following replication stress. *Nature communications*, 4, p.1423.

Furgason, J.M. & Bahassi, E.M., 2013. Targeting DNA repair mechanisms in cancer. *Pharmacology & therapeutics*, 137(3), pp.298–308.

Gallo-Fernández, M. et al., 2012. Cell cycle-dependent regulation of the nuclease activity of Mus81-Eme1/Mms4. *Nucleic acids research*, 40(17), pp.8325–35.

Garaycoechea, J.I. et al., 2012. Genotoxic consequences of endogenous aldehydes on mouse haematopoietic stem cell function. *Nature*, 489(7417), pp.571–5.

Garcia, V. et al., 2011. Bidirectional resection of DNA double-strand breaks by Mre11 and Exo1. *Nature*, 479(7372), pp.241–4.

Genschel, J., Bazemore, L.R. & Modrich, P., 2002. Human exonuclease I is required for 5' and 3' mismatch repair. *The Journal of biological chemistry*, 277(15), pp.13302–11.

Genschel, J. & Modrich, P., 2003. Mechanism of 5'-directed excision in human mismatch repair. *Molecular cell*, 12(5), pp.1077–86.

Giannattasio, M. et al., 2010. Exo1 competes with repair synthesis, converts NER intermediates to long ssDNA gaps, and promotes checkpoint activation. *Molecular cell*, 40(1), pp.50–62.

Gloeckner, C.J., Boldt, K. & Ueffing, M., 2009. Strep/FLAG tandem affinity purification (SF-TAP) to study protein interactions. *Current Protocols in Protein Science*.

Golding, S.E. et al., 2012. Dynamic inhibition of ATM kinase provides a strategy for glioblastoma multiforme radiosensitization and growth control. *Cell cycle (Georgetown, Tex.)*, 11(6), pp.1167–73.

Gottlieb, T.M. & Jackson, S.P., 1993. The DNA-dependent protein kinase: Requirement for DNA ends and association with Ku antigen. *Cell*, 72, pp.131–142.

Grabarz, A. et al., 2013. A role for BLM in double-strand break repair pathway choice: prevention of CtIP/Mre11-mediated alternative nonhomologous end-joining. *Cell reports*, 5(1), pp.21–8.

Gravel, S. et al., 2008. DNA helicases Sgs1 and BLM promote DNA double-strand break resection. *Genes & development*, 22(20), pp.2767–72.

Guo, Z. et al., 2010. ATM activation by oxidative stress. *Science (New York, N.Y.)*, 330, pp.517–521.

Gupta, G.P. et al., 2013. The Mre11 complex suppresses oncogene-driven breast tumorigenesis and metastasis. *Molecular cell*, 52(3), pp.353–65.

Halazonetis, T.D., Gorgoulis, V.G. & Bartek, J., 2008. An oncogene-induced DNA damage model for cancer development. *Science (New York, N.Y.)*, 319(5868), pp.1352–5.

Hanahan, D. & Weinberg, R.A., 2011. Hallmarks of cancer: the next generation. *Cell*, 144(5), pp.646–74.

Harper, J.W. & Elledge, S.J., 2007. The DNA damage response: ten years after. *Molecular cell*, 28(5), pp.739–45.

Hartwell, L.H. & Weinert, T.A., 1989. Checkpoints: controls that ensure the order of cell cycle events. *Science (New York, N.Y.)*, 246(4930), pp.629–34.

Hashimoto, Y. et al., 2010. Rad51 protects nascent DNA from Mre11-dependent degradation and promotes continuous DNA synthesis. *Nature structural & molecular biology*, 17(11), pp.1305–11.

Henry-Mowatt, J. et al., 2003. XRCC3 and Rad51 modulate replication fork progression on damaged vertebrate chromosomes. *Molecular Cell*, 11, pp.1109–1117.

Hickson, I. et al., 2004. Identification and characterization of a novel and specific inhibitor of the ataxia-telangiectasia mutated kinase ATM. *Cancer research*, 64(24), pp.9152–9.

Hirao, A. et al., 2002. Chk2 is a tumor suppressor that regulates apoptosis in both an ataxia telangiectasia mutated (ATM)-dependent and an ATM-independent manner. *Molecular and cellular biology*, 22(18), pp.6521–32.

Ho, C.K. et al., 2010. Mus81 and Yen1 promote reciprocal exchange during mitotic recombination to maintain genome integrity in budding yeast. *Molecular cell*, 40(6), pp.988–1000.

Hopfner, K. et al., 2002. The Rad50 zinc-hook is a structure joining Mre11 complexes in DNA recombination and repair. *Nature*, 418(6897), pp.562–6.

Hosoya, N. & Miyagawa, K., 2014. Targeting DNA damage response in cancer therapy. *Cancer science*, 105(4), pp.370–88.

Hosseini, M. et al., 2014. Oxidative and Energy Metabolism as Potential Clues for Clinical Heterogeneity in Nucleotide Excision Repair Disorders. *The Journal of investigative dermatology*, pp.1–11.

Hsiang, Y.H. et al., 1989. DNA topoisomerase I-mediated DNA cleavage and cytotoxicity of camptothecin analogues. *Cancer research*, 49(16), pp.4385–9.

Hu, J. et al., 2012. The intra-S phase checkpoint targets Dna2 to prevent stalled replication forks from reversing. *Cell*, 149(6), pp.1221–32.

Huang, K.N. & Symington, L.S., 1993. A 5'-3' exonuclease from Saccharomyces cerevisiae is required for in vitro recombination between linear DNA molecules with overlapping homology. *Molecular and cellular biology*, 13(6), pp.3125–34.

Jackson, D. a & Pombo, A., 1998. Replicon clusters are stable units of chromosome structure: evidence that nuclear organization contributes to the efficient activation and propagation of S phase in human cells. *The Journal of cell biology*, 140(6), pp.1285–95.

Jackson, S.P. & Bartek, J., 2009. The DNA-damage response in human biology and disease. *Nature*, 461(7267), pp.1071–8.

Jagmohan-Changur, S. et al., 2003. EXO1 variants occur commonly in normal population: evidence against a role in hereditary nonpolyposis colorectal cancer. *Cancer research*, 63(1), pp.154–8.

Jasin, M. & Rothstein, R., 2013. Repair of strand breaks by homologous recombination. *Cold Spring Harbor perspectives in biology*, 5(11), p.a012740.

Jaspers, J.E. et al., 2013. Loss of 53BP1 causes PARP inhibitor resistance in Brca1-mutated mouse mammary tumors. *Cancer discovery*, 3(1), pp.68–81.

Jeong, Y.-T. et al., 2013. FBH1 promotes DNA double-strand breakage and apoptosis in response to DNA replication stress. *The Journal of cell biology*, 200(2), pp.141–9.

Jiricny, J., 2006. The multifaceted mismatch-repair system. *Nature reviews. Molecular cell biology*, 7(5), pp.335–46.

Kaelin, W.G., 2005. The concept of synthetic lethality in the context of anticancer therapy. *Nature reviews. Cancer*, 5(9), pp.689–98.

Kamath-Loeb, a. S. et al., 1998. Werner syndrome protein. II. Characterization of the integral 3' --> 5' DNA exonuclease. *The Journal of biological chemistry*, 273(51), pp.34145–50.

Kang, J., Bronson, R.T. & Xu, Y., 2002. Targeted disruption of NBS1 reveals its roles in mouse development and DNA repair. *The EMBO journal*, 21(6), pp.1447–55.

Kang, Y.-H., Lee, C.-H. & Seo, Y.-S., 2010. Dna2 on the road to Okazaki fragment processing and genome stability in eukaryotes. *Critical reviews in biochemistry and molecular biology*, 45(2), pp.71–96.

Kanu, N. & Behrens, A., 2007. ATMIN defines an NBS1-independent pathway of ATM signalling. *The EMBO journal*, 26, pp.2933–2941.

Karanja, K.K. et al., 2012. DNA2 and EXO1 in replication-coupled, homology-directed repair and in the interplay between HDR and the FA/BRCA network. *Cell cycle (Georgetown, Tex.)*, 11(21), pp.3983–96.

Karanja, K.K. et al., 2014. Preventing over-resection by DNA2 helicase/nuclease suppresses repair defects in Fanconi anemia cells. *Cell cycle (Georgetown, Tex.)*, 13(10), pp.1540–50.

Kastan, M.B. & Bartek, J., 2004. Cell-cycle checkpoints and cancer. *Nature*, 432(7015), pp.316–23.

Kauppi, L., Jasin, M. & Keeney, S., 2013. How much is enough? Control of DNA double-strand break numbers in mouse meiosis. *Cell cycle (Georgetown, Tex.)*, 12(17), pp.2719–20.

Kelland, L., 2007. The resurgence of platinum-based cancer chemotherapy. *Nature reviews. Cancer*, 7(8), pp.573–84.

King, C. et al., 2014. Characterization and preclinical development of LY2603618: a selective and potent Chk1 inhibitor. *Investigational new drugs*, 32(2), pp.213–26.

Kirkpatrick, D.T. et al., 2000. Decreased meiotic intergenic recombination and increased meiosis I nondisjunction in exo1 mutants of Saccharomyces cerevisiae. *Genetics*, 156(4), pp.1549–57.

De Klein, A. et al., 2000. Targeted disruption of the cell-cycle checkpoint gene ATR leads to early embryonic lethality in mice. *Current biology : CB*, 10(8), pp.479–82.

Kottemann, M.C. & Smogorzewska, A., 2013. Fanconi anaemia and the repair of Watson and Crick DNA crosslinks. *Nature*, 493(7432), pp.356–63.

Koundrioukoff, S. et al., 2013. Stepwise activation of the ATR signaling pathway upon increasing replication stress impacts fragile site integrity. S. E. Plon, ed. *PLoS genetics*, 9(7), p.e1003643.

Lam, A.F., Krogh, B.O. & Symington, L.S., 2008. Unique and overlapping functions of the Exo1, Mre11 and Pso2 nucleases in DNA repair. *DNA repair*, 7(4), pp.655–62.

De Lange, T., 2009. How telomeres solve the end-protection problem. *Science (New York, N.Y.)*, 326(5955), pp.948–52.

Lavin, M.F. & Kozlov, S., 2007. ATM activation and DNA damage response. *Cell cycle (Georgetown, Tex.)*, 6(8), pp.931–42.

Lee, B.I. & Wilson, D.M., 1999. The RAD2 domain of human exonuclease 1 exhibits 5' to 3' exonuclease and flap structure-specific endonuclease activities. *The Journal of biological chemistry*, 274(53), pp.37763–9.

Lee, J. & Dunphy, W.G., 2013. The Mre11-Rad50-Nbs1 (MRN) complex has a specific role in the activation of Chk1 in response to stalled replication forks. *Molecular biology of the cell*, 24(9), pp.1343–53.

Lee, J.-H. et al., 2013. Ataxia telangiectasia-mutated (ATM) kinase activity is regulated by ATP-driven conformational changes in the Mre11/Rad50/Nbs1 (MRN) complex. *The Journal of biological chemistry*, 288(18), pp.12840–51.

Lee, J.-H. & Paull, T.T., 2004. Direct activation of the ATM protein kinase by the Mre11/Rad50/Nbs1 complex. *Science (New York, N.Y.)*, 304(5667), pp.93–6.

Lee, J.H. et al., 2003. Distinct functions of Nijmegen breakage syndrome in ataxia telangiectasia mutated-dependent responses to DNA damage. *Molecular cancer research : MCR*, 1(9), pp.674–81.

Lee, S.D. & Alani, E., 2006. Analysis of interactions between mismatch repair initiation factors and the replication processivity factor PCNA. *Journal of molecular biology*, 355(2), pp.175–84.

Lewis, L.K. et al., 2002. Differential suppression of DNA repair deficiencies of Yeast rad50, mre11 and xrs2 mutants by EXO1 and TLC1 (the RNA component of telomerase). *Genetics*, 160(1), pp.49–62.

Li, M. et al., 2013. The FHA and BRCT domains recognize ADP-ribosylation during DNA damage response. *Genes & development*, 27(16), pp.1752–68.

Li, M. & Yu, X., 2014. The role of poly(ADP-ribosyl)ation in DNA damage response and cancer chemotherapy. *Oncogene*, (August), pp.1–8.

Li, Z. et al., 1995. The XRCC4 gene encodes a novel protein involved in DNA double-strand break repair and V(D)J recombination. *Cell*, 83, pp.1079–1089.

Liberti, S.E. & Rasmussen, L.J., 2004. Is hEXO1 a cancer predisposing gene? *Molecular cancer research : MCR*, 2(8), pp.427–32.

Lin, W. et al., 2013. Mammalian DNA2 helicase/nuclease cleaves G-quadruplex DNA and is required for telomere integrity. *The EMBO journal*, 32(10), pp.1425–39.

Lindahl, T. & Barnes, D.E., 2000. Repair of Endogenous DNA Damage. *Cold Spring Harbor Symposia on Quantitative Biology*, 65, pp.127–134.

Lisby, M. et al., 2004. Choreography of the DNA damage response: Spatiotemporal relationships among checkpoint and repair proteins. *Cell*, 118, pp.699–713.

Liu, J. & Kipreos, E.T., 2000. Evolution of cyclin-dependent kinases (CDKs) and CDK-activating kinases (CAKs): differential conservation of CAKs in yeast and metazoa. *Molecular biology and evolution*, 17(7), pp.1061–74.

Liu, Q. et al., 2000. Chk1 is an essential kinase that is regulated by Atr and required for the G(2)/M DNA damage checkpoint. *Genes & development*, 14(12), pp.1448–59.

Lord, C.J. & Ashworth, A., 2013. Mechanisms of resistance to therapies targeting BRCA-mutant cancers. *Nature medicine*, 19(11), pp.1381–8.

Lord, C.J. & Ashworth, A., 2008. Targeted therapy for cancer using PARP inhibitors. *Current opinion in pharmacology*, 8(4), pp.363–9.

Lord, C.J. & Ashworth, A., 2012. The DNA damage response and cancer therapy. *Nature*, 481(7381), pp.287–94.

Lukas, C. et al., 2003. Distinct spatiotemporal dynamics of mammalian checkpoint regulators induced by DNA damage. *Nature cell biology*, 5(3), pp.255–60.

Lukas, C. et al., 2004. Mdc1 couples DNA double-strand break recognition by Nbs1 with its H2AX-dependent chromatin retention. *The EMBO journal*, 23(13), pp.2674–83.

Lukas, J., Lukas, C. & Bartek, J., 2011. More than just a focus: The chromatin response to DNA damage and its role in genome integrity maintenance. *Nature cell biology*, 13(10), pp.1161–9.

Luo, G. et al., 1999. Disruption of mRad50 causes embryonic stem cell lethality, abnormal embryonic development, and sensitivity to ionizing radiation. *Proceedings of the National Academy of Sciences of the United States of America*, 96(13), pp.7376–81.

Ma, C.X., Janetka, J.W. & Piwnica-Worms, H., 2011. Death by releasing the breaks: CHK1 inhibitors as cancer therapeutics. *Trends in molecular medicine*, 17(2), pp.88–96.

Mahaney, B.L., Meek, K. & Lees-Miller, S.P., 2009. Repair of ionizing radiation-induced DNA double-strand breaks by non-homologous end-joining. *The Biochemical journal*, 417(3), pp.639–50.

Mailand, N. et al., 2000. Rapid destruction of human Cdc25A in response to DNA damage. *Science (New York, N.Y.)*, 288(5470), pp.1425–9.

Makharashvili, N. et al., 2014. Catalytic and noncatalytic roles of the CtIP endonuclease in double-strand break end resection. *Molecular cell*, 54(6), pp.1022–33.

Mankouri, H.W., Huttner, D. & Hickson, I.D., 2013. How unfinished business from S-phase affects mitosis and beyond. *The EMBO journal*, 32(20), pp.2661–71.

Marnett, L.J. & Plastaras, J.P., 2001. Endogenous DNA damage and mutation. *Trends in genetics : TIG*, 17(4), pp.214–21.

Marteijn, J. a et al., 2014. Understanding nucleotide excision repair and its roles in cancer and ageing. *Nature reviews. Molecular cell biology*, 15(7), pp.465–81.

Maser, R.S., Zinkel, R. & Petrini, J.H., 2001. An alternative mode of translation permits production of a variant NBS1 protein from the common Nijmegen breakage syndrome allele. *Nature genetics*, 27(4), pp.417–21.

Matsuoka, S. et al., 2007. ATM and ATR substrate analysis reveals extensive protein networks responsive to DNA damage. *Science (New York, N.Y.)*, 316(5828), pp.1160–6.

Matsuoka, S., Huang, M. & Elledge, S.J., 1998. Linkage of ATM to cell cycle regulation by the Chk2 protein kinase. *Science (New York, N.Y.)*, 282, pp.1893–1897.

McKinnon, P.J., 2004. ATM and ataxia telangiectasia. *EMBO reports*, 5(8), pp.772–6.

McVey, M. & Lee, S.E., 2008. MMEJ repair of double-strand breaks (director's cut): deleted sequences and alternative endings. *Trends in genetics : TIG*, 24(11), pp.529–38.

Merkle, D. et al., 2002. The DNA-dependent protein kinase interacts with DNA to form a protein-DNA complex that is disrupted by phosphorylation. *Biochemistry*, 41(42), pp.12706–14.

Mimitou, E.P. & Symington, L.S., 2009. DNA end resection: many nucleases make light work. *DNA repair*, 8(9), pp.983–95.

Mimitou, E.P. & Symington, L.S., 2010. Ku prevents Exo1 and Sgs1-dependent resection of DNA ends in the absence of a functional MRX complex or Sae2. *The EMBO journal*, 29(19), pp.3358–69.

Mimitou, E.P. & Symington, L.S., 2008. Sae2, Exo1 and Sgs1 collaborate in DNA double-strand break processing. *Nature*, 455(7214), pp.770–4.

Mir, S.E. et al., 2010. In silico analysis of kinase expression identifies WEE1 as a gatekeeper against mitotic catastrophe in glioblastoma. *Cancer cell*, 18(3), pp.244–57.

Mirzoeva, O.K. & Petrini, J.H., 2001. DNA damage-dependent nuclear dynamics of the Mre11 complex. *Molecular and cellular biology*, 21(1), pp.281–8.

Mohaghegh, P. & Hickson, I.D., 2002. Premature aging in RecQ helicase-deficient human syndromes. *The international journal of biochemistry & cell biology*, 34(11), pp.1496–501.

Morales, M. et al., 2005. The Rad50S allele promotes ATM-dependent DNA damage responses and suppresses ATM deficiency: implications for the Mre11 complex as a DNA damage sensor. *Genes & development*, 19(24), pp.3043–54.

Moreau, S., Morgan, E.A. & Symington, L.S., 2001. Overlapping functions of the Saccharomyces cerevisiae Mre11, Exo1 and Rad27 nucleases in DNA metabolism. *Genetics*, 159(4), pp.1423–33.

Morin, I. et al., 2008. Checkpoint-dependent phosphorylation of Exo1 modulates the DNA damage response. *The EMBO journal*, 27(18), pp.2400–10.

Moynahan, M.E. & Jasin, M., 2010. Mitotic homologous recombination maintains genomic stability and suppresses tumorigenesis. *Nature reviews. Molecular cell biology*, 11(3), pp.196–207.

Moynahan, M.E., Pierce, A.J. & Jasin, M., 2001. BRCA2 is required for homology-directed repair of chromosomal breaks. *Molecular cell*, 7(2), pp.263–72.

Mueller, J. et al., 2009. Comprehensive molecular analysis of mismatch repair gene defects in suspected Lynch syndrome (hereditary nonpolyposis colorectal cancer) cases. *Cancer research*, 69(17), pp.7053–61.

Munck, J.M. et al., 2012. Chemosensitization of cancer cells by KU-0060648, a dual inhibitor of DNA-PK and PI-3K. *Molecular cancer therapeutics*, 11(8), pp.1789–98.

Muñoz-Galván, S. et al., 2013. Competing roles of DNA end resection and non-homologous end joining functions in the repair of replication-born double-strand breaks by sister-chromatid recombination. *Nucleic acids research*, 41(3), pp.1669–83.

Murga, M. et al., 2009. A mouse model of ATR-Seckel shows embryonic replicative stress and accelerated aging. *Nature genetics*, 41(8), pp.891–8.

Nakada, D., Hirano, Y. & Sugimoto, K., 2004. Requirement of the Mre11 complex and exonuclease 1 for activation of the Mec1 signaling pathway. *Molecular and cellular biology*, 24(22), pp.10016–25.

Nakai, W. et al., 2011. Chromosome integrity at a double-strand break requires exonuclease 1 and MRX. *DNA repair*, 10(1), pp.102–10.

Negrini, S., Gorgoulis, V.G. & Halazonetis, T.D., 2010. Genomic instability--an evolving hallmark of cancer. *Nature reviews. Molecular cell biology*, 11(3), pp.220–8.

Nelms, B.E. et al., 1998. In situ visualization of DNA double-strand break repair in human fibroblasts. *Science*, 280, pp.590–2.

Ngo, G.H.P. et al., 2014. The 9-1-1 checkpoint clamp stimulates DNA resection by Dna2-Sgs1 and Exo1. *Nucleic acids research*, 42(16), pp.10516–28.

Nicolette, M.L. et al., 2010. Mre11-Rad50-Xrs2 and Sae2 promote 5' strand resection of DNA double-strand breaks. *Nature structural & molecular biology*, 17(12), pp.1478–85.

Nimonkar, A. V et al., 2011. BLM-DNA2-RPA-MRN and EXO1-BLM-RPA-MRN constitute two DNA end resection machineries for human DNA break repair. *Genes & development*, 25(4), pp.350–62.

Nishida, H. et al., 2009. Inhibition of ATR protein kinase activity by schisandrin B in DNA damage response. *Nucleic acids research*, 37(17), pp.5678–89.

O'Driscoll, M. et al., 2003. A splicing mutation affecting expression of ataxia-telangiectasia and Rad3-related protein (ATR) results in Seckel syndrome. *Nature genetics*, 33(4), pp.497–501.

Oberbeck, N. et al., 2014. Maternal aldehyde elimination during pregnancy preserves the fetal genome. *Molecular cell*, 55(6), pp.807–17.

Peasland, a et al., 2011. Identification and evaluation of a potent novel ATR inhibitor, NU6027, in breast and ovarian cancer cell lines. *British journal of cancer*, 105(3), pp.372–81.

Peltomäki, P., 2003. Role of DNA mismatch repair defects in the pathogenesis of human cancer. *Journal of clinical oncology : official journal of the American Society of Clinical Oncology*, 21(6), pp.1174–9.

Polato, F. et al., 2014. CtIP-mediated resection is essential for viability and can operate independently of BRCA1. *The Journal of experimental medicine*, 211(6), pp.1027–36.

Polo, S.E. & Jackson, S.P., 2011. Dynamics of DNA damage response proteins at DNA breaks: a focus on protein modifications. *Genes & development*, 25(5), pp.409–33.

Polyak, K. & Garber, J., 2011. Targeting the missing links for cancer therapy. *Nature medicine*, 17(3), pp.283–4.

Prevo, R. et al., 2012. The novel ATR inhibitor VE-821 increases sensitivity of pancreatic cancer cells to radiation and chemotherapy. *Cancer biology & therapy*, 13(11), pp.1072–81.

Qin, J.Y. et al., 2010. Systematic comparison of constitutive promoters and the doxycycline-inducible promoter. *PloS one*, 5(5), p.e10611.

Qvist, P. et al., 2011. CtIP Mutations Cause Seckel and Jawad Syndromes. *PLoS genetics*, 7(10), p.e1002310.

Rainey, M.D. et al., 2008. Transient inhibition of ATM kinase is sufficient to enhance cellular sensitivity to ionizing radiation. *Cancer research*, 68(18), pp.7466–74.

Rasheed, Z. a & Rubin, E.H., 2003. Mechanisms of resistance to topoisomerase I-targeting drugs. *Oncogene*, 22(47), pp.7296–304.

Ray Chaudhuri, A. et al., 2012. Topoisomerase I poisoning results in PARP-mediated replication fork reversal. *Nature structural & molecular biology*, 19(4), pp.417–23.

Rein, K. & Stracker, T.H., 2014. The MRE11 complex: An important source of stress relief. *Experimental cell research*, 329(1), pp.162–169.

Reinhardt, H.C. et al., 2007. p53-deficient cells rely on ATM- and ATR-mediated checkpoint signaling through the p38MAPK/MK2 pathway for survival after DNA damage. *Cancer cell*, 11(2), pp.175–89.

Richardson, C., Horikoshi, N. & Pandita, T.K., 2004. The role of the DNA double-strand break response network in meiosis. *DNA repair*, 3(8-9), pp.1149–64.

Robinson, D., 2002. Cancer clusters: findings vs feelings. *MedGenMed : Medscape general medicine*, 4, p.16.

Roset, R. et al., 2014. The Rad50 hook domain regulates DNA damage signaling and tumorigenesis. *Genes & development*, 28(5), pp.451–62.

Ruzankina, Y. et al., 2007. Deletion of the developmentally essential gene ATR in adult mice leads to age-related phenotypes and stem cell loss. *Cell stem cell*, 1(1), pp.113–26.

San Filippo, J., Sung, P. & Klein, H., 2008. Mechanism of eukaryotic homologous recombination. *Annual review of biochemistry*, 77, pp.229–57.

Sartori, A.A. et al., 2007. Human CtIP promotes DNA end resection. *Nature*, 450(7169), pp.509–14.

Schaetzlein, S. et al., 2013. Mammalian Exo1 encodes both structural and catalytic functions that play distinct roles in essential biological processes. *Proceedings of the National Academy of Sciences of the United States of America*, 110(27), pp.E2470–9.

Schlacher, K. et al., 2011. Double-strand break repair-independent role for BRCA2 in blocking stalled replication fork degradation by MRE11. *Cell*, 145(4), pp.529–42.

Schmutte, C. et al., 2001. The interaction of DNA mismatch repair proteins with human exonuclease I. *The Journal of biological chemistry*, 276(35), pp.33011–8.

Schoppy, D.W. et al., 2012. Oncogenic stress sensitizes murine cancers to hypomorphic suppression of ATR. *The Journal of clinical investigation*, 122(1), pp.241–52.

Schreiber, V. et al., 2006. Poly(ADP-ribose): novel functions for an old molecule. *Nature reviews. Molecular cell biology*, 7(7), pp.517–28.

Sedelnikova, O. a et al., 2004. Senescing human cells and ageing mice accumulate DNA lesions with unrepairable double-strand breaks. *Nature cell biology*, 6(2), pp.168–70.

Segurado, M. & Diffley, J.F.X., 2008. Separate roles for the DNA damage checkpoint protein kinases in stabilizing DNA replication forks. *Genes & development*, 22(13), pp.1816–27.

Shao, H. et al., 2014. Hydrolytic function of Exo1 in mammalian mismatch repair. *Nucleic acids research*, 42(11), pp.7104–12.

Shen, J.C. et al., 1998. Werner syndrome protein. I. DNA helicase and dna exonuclease reside on the same polypeptide. *The Journal of biological chemistry*, 273(51), pp.34139–44.

Shibata, A. et al., 2014. DNA double-strand break repair pathway choice is directed by distinct MRE11 nuclease activities. *Molecular cell*, 53(1), pp.7–18.

Shiloh, Y. & Ziv, Y., 2012. The ATM protein: the importance of being active. *The Journal of cell biology*, 198(3), pp.273–5.

Shim, E.Y. et al., 2010. Saccharomyces cerevisiae Mre11/Rad50/Xrs2 and Ku proteins regulate association of Exo1 and Dna2 with DNA breaks. *The EMBO journal*, 29(19), pp.3370–80.

Shull, E.R.P. et al., 2009. Differential DNA damage signaling accounts for distinct neural apoptotic responses in ATLD and NBS. *Genes & development*, 23(2), pp.171–80.

Siddik, Z.H., 2003. Cisplatin: mode of cytotoxic action and molecular basis of resistance. *Oncogene*, 22(47), pp.7265–79.

Simsek, D. & Jasin, M., 2010. Alternative end-joining is suppressed by the canonical NHEJ component Xrcc4-ligase IV during chromosomal translocation formation. *Nature structural & molecular biology*, 17(4), pp.410–6.

Spillare, E.A. et al., 1999. p53-mediated apoptosis is attenuated in Werner syndrome cells. *Genes & development*, 13(11), pp.1355–60.

Srivastava, M. et al., 2012. An inhibitor of nonhomologous end-joining abrogates double-strand break repair and impedes cancer progression. *Cell*, 151(7), pp.1474–87.

Stracker, T.H. et al., 2009. Artemis and nonhomologous end joining-independent influence of DNA-dependent protein kinase catalytic subunit on chromosome stability. *Molecular and cellular biology*, 29(2), pp.503–14.

Stracker, T.H. et al., 2008. Chk2 suppresses the oncogenic potential of DNA replication-associated DNA damage. *Molecular cell*, 31(1), pp.21–32.

Stracker, T.H. et al., 2013. The ATM signaling network in development and disease. *Frontiers in genetics*, 4, p.37.

Stracker, T.H. et al., 2007. The carboxy terminus of NBS1 is required for induction of apoptosis by the MRE11 complex. *Nature*, 447(7141), pp.218–21.

Stracker, T.H. et al., 2004. The Mre11 complex and the metabolism of chromosome breaks: the importance of communicating and holding things together. *DNA repair*, 3(8-9), pp.845–54.

Stracker, T.H. & Petrini, J.H.J., 2011. The MRE11 complex: starting from the ends. *Nature reviews. Molecular cell biology*, 12(2), pp.90–103.

Stracker, T.H. & Petrini, J.H.J., 2008. Working together and apart: the twisted relationship of the Mre11 complex and Chk2 in apoptosis and tumor suppression. *Cell cycle (Georgetown, Tex.)*, 7(23), pp.3618–21.

Stucki, M. & Jackson, S.P., 2006. gammaH2AX and MDC1: anchoring the DNA-damage-response machinery to broken chromosomes. *DNA repair*, 5(5), pp.534–43.

Sun, J. et al., 2012. Human Ku70/80 protein blocks exonuclease 1-mediated DNA resection in the presence of human Mre11 or Mre11/Rad50 protein complex. *The Journal of biological chemistry*, 287(7), pp.4936–45.

Syljuåsen, R.G. et al., 2005. Inhibition of human Chk1 causes increased initiation of DNA replication, phosphorylation of ATR targets, and DNA breakage. *Molecular and cellular biology*, 25(9), pp.3553–62.

Symington, L.S. & Gautier, J., 2011. Double-strand break end resection and repair pathway choice. *Annual review of genetics*, 45, pp.247–71.

Szankasi, P. & Smith, G.R., 1992. A DNA exonuclease induced during meiosis of Schizosaccharomyces pombe. *The Journal of biological chemistry*, 267(5), pp.3014–23.

Takai, H. et al., 2000. Aberrant cell cycle checkpoint function and early embryonic death in Chk1$^{-/-}$ mice. *Genes & Development*, pp.1439–1447.

Takai, H. et al., 2002. Chk2-deficient mice exhibit radioresistance and defective p53-mediated transcription. *The EMBO journal*, 21(19), pp.5195–205.

Taylor, a M.R., Groom, a & Byrd, P.J., 2004. Ataxia-telangiectasia-like disorder (ATLD)-its clinical presentation and molecular basis. *DNA repair*, 3(8-9), pp.1219–25.

Taylor, A., 2001. Chromosome instability syndromes. *Best practice & research. Clinical haematology*, 14(3), pp.631–44.

Thangavel, S. et al., 2010. Human RECQ1 and RECQ4 helicases play distinct roles in DNA replication initiation. *Molecular and cellular biology*, 30(6), pp.1382–96.

Theunissen, J.F. et al., 2003. Checkpoint failure and chromosomal instability without lymphomagenesis in Mre11(ATLD1/ATLD1) mice. *Molecular cell*, 12(6), pp.1511–23.

Tishkoff, D.X. et al., 1997. Identification and characterization of Saccharomyces cerevisiae EXO1, a gene encoding an exonuclease that interacts with MSH2. *Proceedings of the National Academy of Sciences of the United States of America*, 94(14), pp.7487–92.

Tishkoff, D.X. et al., 1998. Identification of a human gene encoding a homologue of Saccharomyces cerevisiae EXO1, an exonuclease implicated in mismatch repair and recombination. *Cancer research*, 58(22), pp.5027–31.

Toledo, L.I. et al., 2008. ATR signaling can drive cells into senescence in the absence of DNA breaks. *Genes & development*, 22(3), pp.297–302.

Tomimatsu, N. et al., 2012. Exo1 plays a major role in DNA end resection in humans and influences double-strand break repair and damage signaling decisions. *DNA repair*, 11(4), pp.441–8.

Tomimatsu, N. et al., 2014. Phosphorylation of EXO1 by CDKs 1 and 2 regulates DNA end resection and repair pathway choice. *Nature communications*, 5, p.3561.

Tran, P.T., Simon, J. a & Liskay, R.M., 2001. Interactions of Exo1p with components of MutLalpha in Saccharomyces cerevisiae. *Proceedings of the National Academy of Sciences of the United States of America*, 98(17), pp.9760–5.

Tsang, E. et al., 2014. The extent of error-prone replication restart by homologous recombination is controlled by Exo1 and checkpoint proteins. *Journal of cell science*, 127(Pt 13), pp.2983–94.

Tsubouchi, H. & Ogawa, H., 2000. Exo1 roles for repair of DNA double-strand breaks and meiotic crossing over in Saccharomyces cerevisiae. *Molecular biology of the cell*, 11(7), pp.2221–33.

Uchisaka, N. et al., 2009. Two brothers with ataxia-telangiectasia-like disorder with lung adenocarcinoma. *The Journal of pediatrics*, 155(3), pp.435–8.

Uziel, T. et al., 2003. Requirement of the MRN complex for ATM activation by DNA damage. *The EMBO journal*, 22(20), pp.5612–21.

Vallur, A.C. & Maizels, N., 2010. Distinct activities of exonuclease 1 and flap endonuclease 1 at telomeric g4 DNA. *PloS one*, 5(1), p.e8908.

Vasen, H.F. a et al., 2007. Guidelines for the clinical management of Lynch syndrome (hereditary non-polyposis cancer). *Journal of medical genetics*, 44(6), pp.353–62.

Verdun, R.E. & Karlseder, J., 2007. Replication and protection of telomeres. *Nature*, 447(7147), pp.924–31.

De Villartay, J.P., 2009. V(D)J recombination deficiencies. *Advances in Experimental Medicine and Biology*, 650, pp.46–58.

Walden, H. & Deans, A.J., 2014. The Fanconi anemia DNA repair pathway: structural and functional insights into a complex disorder. *Annual review of biophysics*, 43, pp.257–78.

Waltes, R. et al., 2009. Human RAD50 deficiency in a Nijmegen breakage syndrome-like disorder. *American journal of human genetics*, 84(5), pp.605–16.

Wang, H. et al., 2014. CtIP maintains stability at common fragile sites and inverted repeats by end resection-independent endonuclease activity. *Molecular cell*, 54(6), pp.1012–21.

Wang, H. et al., 2013. The interaction of CtIP and Nbs1 connects CDK and ATM to regulate HR-mediated double-strand break repair. *PLoS genetics*, 9(2), p.e1003277.

Wang, J.H. et al., 2009. Mechanisms promoting translocations in editing and switching peripheral B cells. *Nature*, 460(7252), pp.231–6.

Wang, Q. et al., 2014. Rad17 recruits the MRE11-RAD50-NBS1 complex to regulate the cellular response to DNA double-strand breaks. *The EMBO journal*, 33(8), pp.862–77.

Wang, X.W. et al., 2001. Functional interaction of p53 and BLM DNA helicase in apoptosis. *The Journal of biological chemistry*, 276(35), pp.32948–55.

Ward, I.M. & Chen, J., 2001. Histone H2AX is phosphorylated in an ATR-dependent manner in response to replicational stress. *The Journal of biological chemistry*, 276(51), pp.47759–62.

Wei, K. et al., 2003. Inactivation of Exonuclease 1 in mice results in DNA mismatch repair defects, increased cancer susceptibility, and male and female sterility. *Genes & development*, 17(5), pp.603–14.

Williams, B.R. et al., 2002. A murine model of Nijmegen breakage syndrome. *Current biology : CB*, 12(8), pp.648–53.

Williams, R.S. et al., 2009. Nbs1 flexibly tethers Ctp1 and Mre11-Rad50 to coordinate DNA double-strand break processing and repair. *Cell*, 139(1), pp.87–99.

Wiltzius, J.J.W. et al., 2005. The Rad50 hook domain is a critical determinant of Mre11 complex functions. *Nature structural & molecular biology*, 12(5), pp.403–7.

Woods, D. & Turchi, J.J., 2013. Chemotherapy induced DNA damage response: convergence of drugs and pathways. *Cancer biology & therapy*, 14(5), pp.379–89.

Wu, L. & Hickson, I.D., 2003. The Bloom's syndrome helicase suppresses crossing over during homologous recombination. *Nature*, 426(6968), pp.870–4.

Xu, B. et al., 2002. Two molecularly distinct G(2)/M checkpoints are induced by ionizing irradiation. *Molecular and cellular biology*, 22(4), pp.1049–59.

Xu, Y., 2006. DNA damage: a trigger of innate immunity but a requirement for adaptive immune homeostasis. *Nature reviews. Immunology*, 6(4), pp.261–70.

Xu, Y. et al., 1996. Targeted disruption of ATM leads to growth retardation, chromosomal fragmentation during meiosis, immune defects, and thymic lymphoma. *Genes & development*, 10(19), pp.2411–22.

Yanagihara, H. et al., 2011. NBS1 recruits RAD18 via a RAD6-like domain and regulates Pol η-dependent translesion DNA synthesis. *Molecular cell*, 43(5), pp.788–97.

Ying, S., Hamdy, F.C. & Helleday, T., 2012. Mre11-dependent degradation of stalled DNA replication forks is prevented by BRCA2 and PARP1. *Cancer research*, 72(11), pp.2814–21.

You, Z. et al., 2005. ATM activation and its recruitment to damaged DNA require binding to the C terminus of Nbs1. *Molecular and cellular biology*, 25(13), pp.5363–79.

Zakharyevich, K. et al., 2012. Delineation of joint molecule resolution pathways in meiosis identifies a crossover-specific resolvase. *Cell*, 149(2), pp.334–47.

Zhang, T. et al., 2012. Competition between NBS1 and ATMIN controls ATM signaling pathway choice. *Cell reports*, 2(6), pp.1498–504.

Zhao, S. et al., 2000. Functional link between ataxia-telangiectasia and Nijmegen breakage syndrome gene products. *Nature*, 405(6785), pp.473–7.

Zhao, S., Renthal, W. & Lee, E.Y.-H.P., 2002. Functional analysis of FHA and BRCT domains of NBS1 in chromatin association and DNA damage responses. *Nucleic acids research*, 30(22), pp.4815–22.

Zhou, Y. & Paull, T.T., 2013. DNA-dependent protein kinase regulates DNA end resection in concert with Mre11-Rad50-Nbs1 (MRN) and ataxia telangiectasia-mutated (ATM). *The Journal of biological chemistry*, 288(52), pp.37112–25.

Zhu, J. et al., 2001. Targeted disruption of the Nijmegen breakage syndrome gene NBS1 leads to early embryonic lethality in mice. *Current biology : CB*, 11(2), pp.105–9.

Zhu, J.Y. et al., 1991. The ability of simian virus 40 large T antigen to immortalize primary mouse embryo fibroblasts cosegregates with its ability to bind to p53. *Journal of virology*, 65(12), pp.6872–80.

Zhu, Z. et al., 2008. Sgs1 helicase and two nucleases Dna2 and Exo1 resect DNA double-strand break ends. *Cell*, 134(6), pp.981–94.